THEORY OF THE MEASUREMENT AND STANDARDIZATION OF IN-FLIGHT PERFORMANCE OF AIRCRAFT

EVERETT W. DUNLAP
Supervisory Aerospace Engineer

MILTON B. PORTER
Captain, USAF
Aerospace Engineer

TECHNOLOGY DOCUMENT No. 71-1

APRIL 1971

AIR FORCE FLIGHT TEST CENTER
EDWARDS AIR FORCE BASE, CALIFORNIA
AIR FORCE SYSTEMS COMMAND
UNITED STATES AIR FORCE

278

UNCLASSIFIED

Security Classification

DOCUMENT CONTROL DATA - R & D

(Security classification of title, body of abstract and indexing annotation must be entered when the overall report is classified)

1. ORIGINATING ACTIVITY *(Corporate author)* Air Force Flight Test Center Edwards Air Force Base, California	2a. REPORT SECURITY CLASSIFICATION Unclassified 2b. GROUP N/A

3. REPORT TITLE

Theory of the Measurement and Standardization of In-flight Performance of Aircraft

4. DESCRIPTIVE NOTES *(Type of report and inclusive dates)*

Final

5. AUTHOR(S) *(First name, middle initial, last name)*

Everett W. Dunlap
Milton B. Porter

6. REPORT DATE	7a. TOTAL NO. OF PAGES	7b. NO. OF REFS
April 1971	284	28

8a. CONTRACT OR GRANT NO.	9a. ORIGINATOR'S REPORT NUMBER(S)
b. PROJECT NO.	FTC-TD-71-1
c.	9b. OTHER REPORT NO(S) *(Any other numbers that may be assigned this report)*
d.	N/A

10. DISTRIBUTION STATEMENT

This document has been approved for public release and resale; its distribution is unlimited.

11. SUPPLEMENTARY NOTES	12. SPONSORING MILITARY ACTIVITY
N/A	6510th Test Wing Edwards AFB, California

13. ABSTRACT

The contents of this report were prepared to give those engaged in aircraft flight test an understanding of the analysis required to arrive at standardized flight data. Toward that end, considerable attention was given to the derivation of equations. In contrast to earlier reports, simplifying assumptions were not made; rather, efforts were made to keep the derivations of all equations as nearly exact as possible. Emphasis has been placed on climbs and level accelerations since these tests, particularly for supersonic aircraft, consume a large part of a test program and require calculations which are much more lengthy than for other tests. The information in this document was the basis for the development of uniform digital computer programs which are being constructed for use in processing flight data and correcting it to standard conditions. These programs have been given the name Uniform Flight Test Analysis System (UFTAS). ( )

DD FORM 1 NOV 65 1473

UNCLASSIFIED

Security Classification

14. KEY WORDS	LINK A		LINK B		LINK C	
	ROLE	WT	ROLE	WT	ROLE	WT
aircraft performance flight test data standardized data climb performance level accelerations supersonic aircraft excess thrust						

FTC-TD-71-1

THEORY OF THE MEASUREMENT AND STANDARDIZATION OF IN-FLIGHT PERFORMANCE OF AIRCRAFT

EVERETT W. DUNLAP
Supervisory Aerospace Engineer

MILTON B. PORTER
Captain, USAF
Aerospace Engineer

FOREWORD

This document is a comprehensive collection of equations, data, and supporting information for use in processing aircraft flight data and correcting it to standard conditions. It does not represent a final effort; as new material comes into being, new sections and revisions to existing sections will be issued.

The authors are indebted to Mr. William R. Turley, Aerospace Engineer, who prepared the equations on the dynamic response of vanes which appear in section V, and to Mrs. Barbara L. Smith, Engineering Technician, for typing all of the equations.

Prepared by:

Everett W. Dunlap
EVERETT W. DUNLAP
Supervisory Aerospace Engineer

Milton B. Porter Jr.
MILTON B. PORTER
Captain, USAF
Aerospace Engineer

Reviewed and approved by
17 April 1971

Thomas J. Cecil
THOMAS J. CECIL
Colonel, USAF
Commander, 6510th Test Wing

Robert M. White
ROBERT M. WHITE
Brigadier General, USAF
Commander

ABSTRACT

The contents of this report were prepared to give those engaged in aircraft flight test an understanding of the analysis required to arrive at standardized flight data. Toward that end, considerable attention was given to the derivation of equations. In contrast to earlier reports, simplifying assumptions were not made; rather, efforts were made to keep the derivations of all equations as nearly exact as possible. Emphasis has been placed on climbs and level accelerations since these tests, particularly for supersonic aircraft, consume a large part of a test program and require calculations which are much more lengthy than for other tests. The information in this document was the basis for the development of uniform digital computer programs which are being constructed for use in processing flight data and correcting it to standard conditions. These programs have been given the name Uniform Flight Test Analysis System (UFTAS).

table of contents

INTRODUCTION

This document is an outgrowth of the development of uniform digital computer programs which have been constructed for use in processing aircraft flight test data and in correcting it to a set of standard conditions. These programs have been given the name Uniform Flight Test Analysis Systems (UFTAS) and have as their basis the equations developed herein.

In contrast to earlier reports (e.g., Flight Test Engineering Handbook, AF Technical Report No. 6273, by Russel M. Herrington, et al.) simplifying assumptions were not made; rather efforts were made to keep the derivations of all equations as nearly exact as possible. This was done so that the equations would remain valid as airplane speeds and altitudes increase and/or the accuracy of instrumentation systems is improved. In general, correction terms in the final equations may be deleted when it is found that their magnitudes are small compared to the accuracy desired in the end results.

Considerable attention was given to detailing the derivations and to presenting information to give the reader an understanding of the analysis required to arrive at standardized flight data rather than incorporating "cookbook" procedures. Although most of the topics covered are not dependent on the type of power plant, performance parameters and corrections to standard conditions have been included for jet powered aircraft only. Emphasis has been placed on climbs and level accelerations since these tests consume the major portion of a test program, particularly for

supersonic aircraft. Further, calculation of test parameters and standardization procedures are much more lengthy than for other tests (e.g., cruise control, turning performance, etc.) and, hence, the difficulty in computing standard performance for climbs and level accelerations is much greater. The basic approach is quite simple, however, and is illustrated in figure 1.

Briefly, the method is as follows: first, the performance parameter, excess thrust, is computed from the aircraft's measured performance via the equations of motion. Next, the excess thrust computed from test conditions is corrected to standard conditions. Finally, standardized climb or acceleration parameters are computed from the standardized excess thrust by means of equations of motion.

The section titled Determination of Excess Thrust discusses in detail the diverse aircraft flight parameters which may be used in these calculations. For many years readings of airspeed and altitude from conventional airspeed indicators and altimeters have been a basis for measuring test performance. The accuracy of excess thrust computed from such readings could be described as, at best, adequate. Data obtained at low altitudes and speeds are satisfactory; however, as altitudes and especially speeds are increased, the use of airspeed indicators and altimeters as the sole sources of performance data becomes much inferior to sensitive accelerometer installations. A precision of less than $\pm 0.01g$ in measured flightpath acceleration has been obtained during flight tests at the Air Force Flight Test Center and improvements are

expected. Although not in general use, procedures for calculating excess thrust from aircraft position measurements (radar, Askania camera, etc.) have been developed. Accuracy of excess thrust computed with data from these systems is superior to that from the airspeed-altitude method.

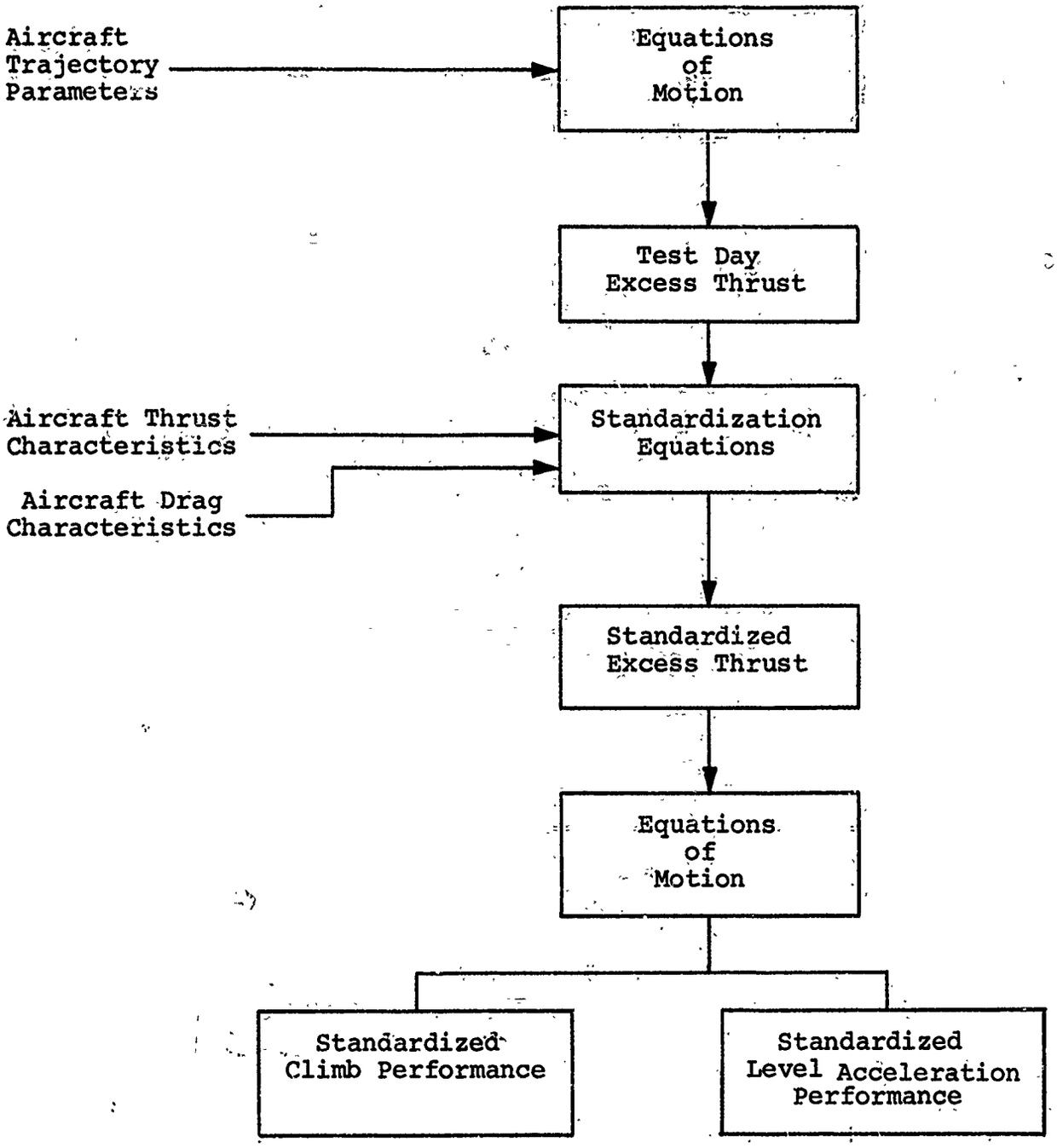

Figure 1: Outline of Method for Standardization of Climbs and Level Accelerations.

The most convenient parameter with which to work in standardizing airplane performance data is excess thrust. Corrections, in terms of excess thrust, are most easily derived from equations of motion. If accelerometers are used, excess thrust can be computed from measured acceleration, and it can be related easily to rate of climb, turning performance, and other performance parameters.

In writing the equations of motion to deduce test excess thrust, (or other performance parameters) the assumption of a flat, non-rotating earth with a constant gravity field has historically been made. (See for example, AF Technical Report 6273, Flight Test Engineering Handbook.) To ensure that test performance data are not degraded, exact equations of motion have been written which account for effects from the earth's rotation and for variation in its gravity field. General equations in terms of test excess thrust are derived in the section, Determination of Excess Thrust, for various flight parameters. In preparation for the derivation of these equations, the coordinate systems employed are described in the following section, Coordinate Systems and Transformations, and the properties of the earth used in the derivations are contained in the section, Geophysical Properties. In the next two sections, information may be found on standard atmospheres and on the basic measurements needed to determine airspeed, altitude, Mach number, and temperature.

As in the calculation of test excess thrust, formulation of excess thrust at standard conditions has been carried out in a more nearly exact fashion than is found in AF Technical Report

6273, Flight Test Engineering Handbook. This has been done to make certain that accuracy inherent in the test data is not degraded in the standardization process. A detailed derivation of the equations for extrapolating test excess thrust to standard conditions appears in the section, Standardization of Excess Thrust.

Once excess thrust for standard conditions has been determined, other parameters (e.g., time to climb, standard weight, etc.) follow quite easily for either climbs or level accelerations. Equations for computing these parameters appear in the section, Standardization of Performance Parameters.

SECTION I

COORDINATE SYSTEMS AND TRANSFORMATIONS

SUMMARY

General information about coordinate systems is presented; this is followed by descriptions of the various coordinate systems used in the calculation of excess thrust. Matrices to make transformations from one axis system to another are developed. This is done by first treating the general case and then the specific cases which are needed in section V, Determination of Excess Thrust.

TABLE OF CONTENTS

LIST OF ILLUSTRATIONS

SYMBOLS USED IN THIS SECTION

Symbol	Definition	Units
B	aircraft roll angle about the wind x_w-axis (airspeed vector)	rad
cg	center of gravity	pct MAC
h_r	geometric altitude of the radar coordinate origin	ft
i,j,k	unit vectors along the x,y,z axes, respectively	--
$[M_x(\theta)]$	axes transformation matrix for the rotation through the angle θ about the x-axis	--
$[M(\theta_1,\theta_2,\theta_3)]$	multiple axis transformation matrix	--
x,y,z	axes labels or components of a vector in a rectangular Cartesian coordinate system (appropriate subscripts denote the particular axes system)	--
α	angle of attack	rad
β	sideslip angle	rad
γ	flightpath climb angle measured from the geocentric horizontal plane	rad
δ_{D_r}	geodetic latitude of the radar coordinate origin	rad
δ_L	aircraft geocentric latitude	rad
δ_{L_r}	geocentric latitude of the radar coordinate origin	rad
$\Delta\delta_{L_r}$	meridian tilt angle of the radar axes horizontal plane ($=\delta_{D_r}-\delta_{L_r}$)	rad
δ_r	$=\delta_{L_r}-\Delta\delta_{L_r}$, the angle between the radar z_r-axis and the equatorial plane	rad

$\theta_1, \theta_2, \theta_3$	rotation angles for the general axes transformation	rad
λ_{L_r}	longitude of the radar coordinate origin	rad
$\Delta\lambda_L$	difference between the aircraft longitude and the longitude of the radar coordinate origin	rad
ϕ_r	the angle between the radar x_r-axis and true north	rad
π	the angle 3.14159.... radians	rad
σ	flightpath heading angle measured from true north	rad
$[\ ]$	matrix	--
$[\ ]^T$	transpose matrix	--
$[\ ]^{-1}$	inverse matrix	--

Subscripts

b	aircraft body axes	--
e	geocentric axes	--
g	north-, geocentrically-directed horizon axes (local geocentric)	--
r	radar axes	--
w	aircraft wind axes	--
1, 2, 3, 4	general axes systems	--

INTRODUCTION

In general, aircraft test data are sensed in a translating and rotating coordinate system. In this case, to compute the forces which produce the motion, the acceleration data must be transformed to an inertial coordinate system to correct for such factors as centripetal and Coriolis acceleration. This section describes the basic coordinate (or axes) systems required for the expressions and equations in the other sections of the document. In addition, the necessary coordinate transformation matrices are developed.

COORDINATE SYSTEMS

The axes systems used are right-handed rectangular Cartesian coordinate systems with axes denoted respectively by the symbols x, y, and z with appropriate subscripts (See figure 1). The three axes are mutually perpendicular, and the direction of positive rotation about each axis is indicated by the curled fingers if the axis is grasped by the right hand with the thumb pointing in the positive linear direction of the axis. For example, rotation about the z-axis would carry the x-axis toward the y-axis. The axes system is uniquely specified if the position of the origin and the directions of two of the three axes are given. The third axis is then chosen to complete the right hand system.

Associated with the axes system is a set of three unit vectors, i, j, and k, with the same subscript as x, y, and z, colinear respectively with x, y, and z, and with the same positive directions. A vector can be expressed in component form

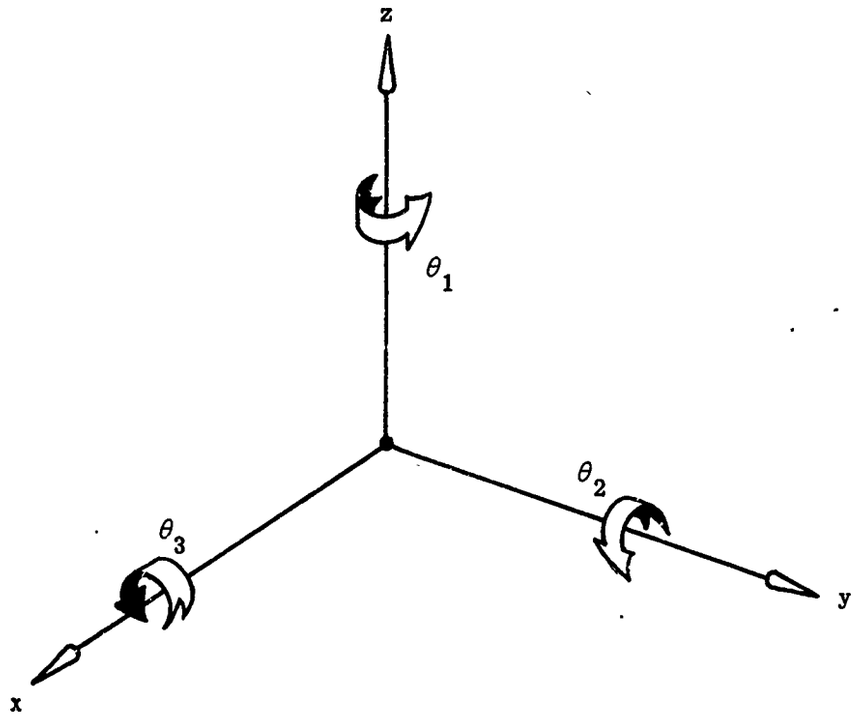

Figure 1 General Coordinates

as three scalars multiplied respectively by the unit vectors.

GEOCENTRIC COORDINATE SYSTEM

For the purpose of this document aircraft trajectories will be considered to be relatively near the earth's surface, and the center of the earth will be considered an inertial point. The geocentric axes system (x_e, y_e, z_e) (shown in figure 2) will then be fixed in the earth with its origin at the geocenter, the z_e-axis pointing toward the south pole, and the x_e-axis in the equatorial plane pointing toward the earth's surface at a specified longitude. For development of the radar reduction equations this longitude will be chosen as the longitude of the radar coordinate origin. The geocentric axes system is then inertial except that it rotates with the earth.

LOCAL GEOCENTRIC COORDINATE SYSTEMS

The second coordinate system to be defined is the north-, geocentrically-directed horizon axes system (x_g, y_g, z_g) or local geocentric-axes system for short (See figure 3). Its origin can be located at either the surface of the earth (geoid) on the radius line from the geocenter to the aircraft cg or at the aircraft cg. The x_g-axis is directed north and the z_g-axis toward the geocenter. The y_g-axis is then pointing east. These local geocentric axes are oriented with respect to the geocentric axes by two angles: δ_L, the aircraft geocentric latitude, and $\Delta\lambda_L$, the difference between the aircraft and radar coordinate origin longitudes.

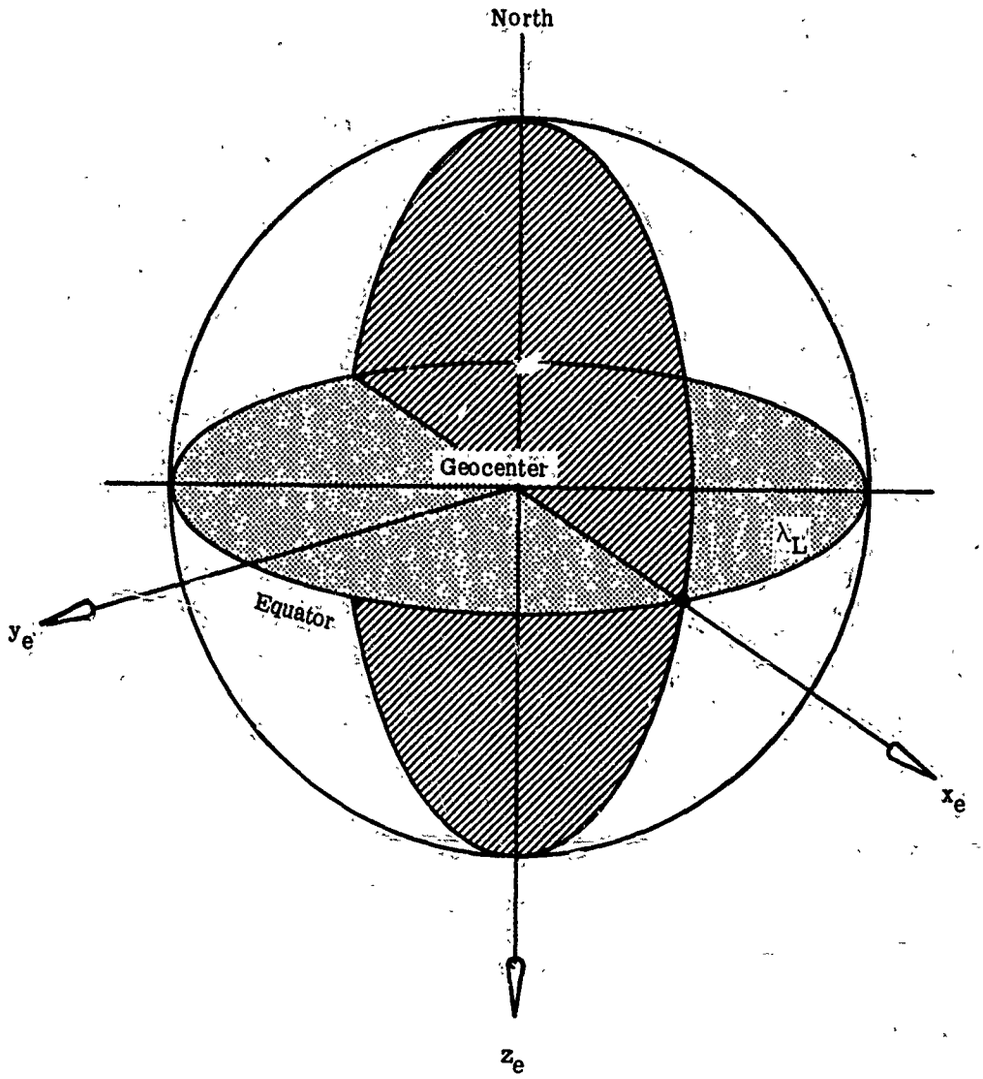

Figure 2 Geocentric Coordinates

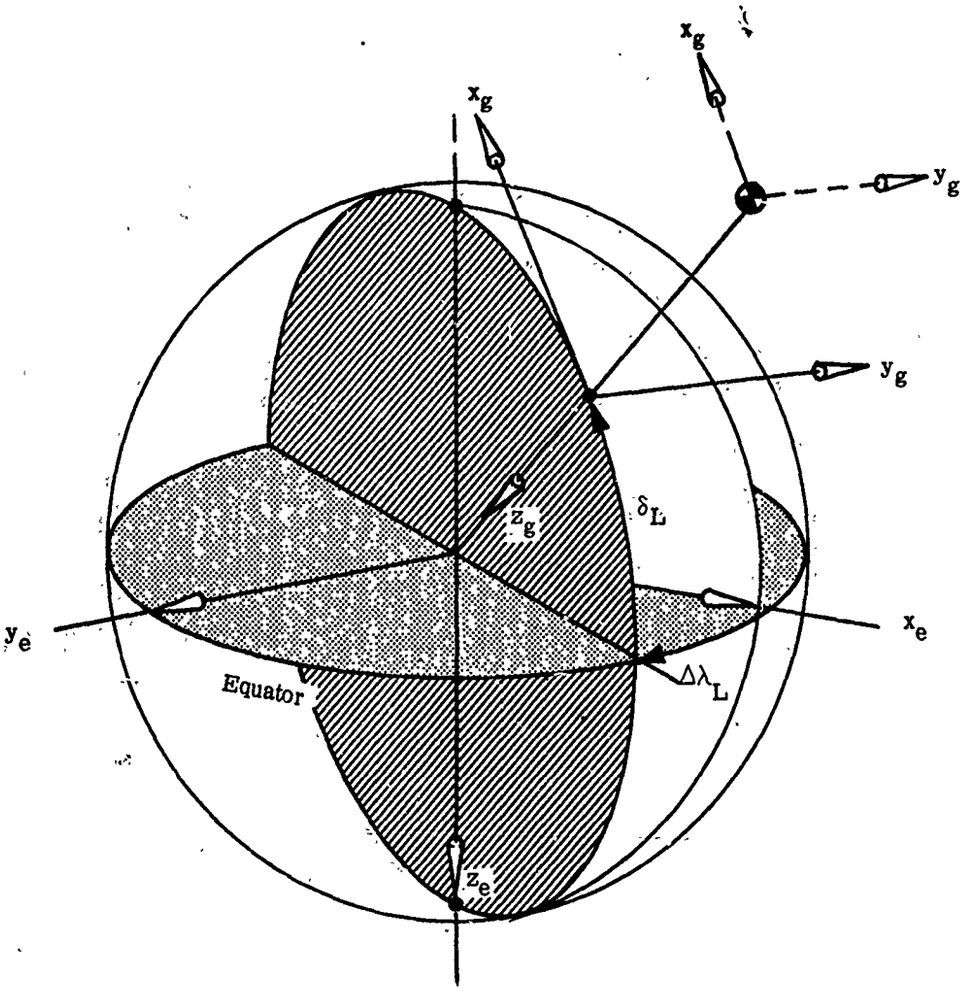

Figure 3 Local Geocentric Coordinates

AIRCRAFT WIND COORDINATE SYSTEM

The third coordinate system to be defined is the aircraft wind-axes system (x_w, y_w, z_w) (shown in figure 4). Its origin is located at the aircraft cg with the x_w-axis oriented in the direction of the aircraft airspeed vector and the z_w-axis directed downward in the vertical plane of symmetry of the aircraft. The y_w-axis is then directed out of the right side of the aircraft. The wind axes are oriented with respect to the local geocentric axes by three angles: the flightpath heading angle, σ, measured from true north to the geocentric horizontal projection of the airspeed vector; the flightpath climb angle, γ, measured from the geocentric horizontal ($x_g y_g$-plane) to the airspeed vector; and the roll angle about the airspeed vector, B. The first two of these angles represents the aircraft flightpath orientation with respect to the airmass. The angles are not the same as the angles of the flightpath with respect to the ground if the wind is blowing.

AIRCRAFT BODY COORDINATE SYSTEM

The fourth coordinate system to be defined is the aircraft body-axes system (x_b, y_b, z_b) (shown in figure 5). Its origin is also located at the aircraft cg with the x_b-axis directed forward along the longitudinal axis of the aircraft and the z_b-axis directed downward in the vertical plane of symmetry of the body. The body axes are oriented with respect to the wind axes by the sideslip angle and angle

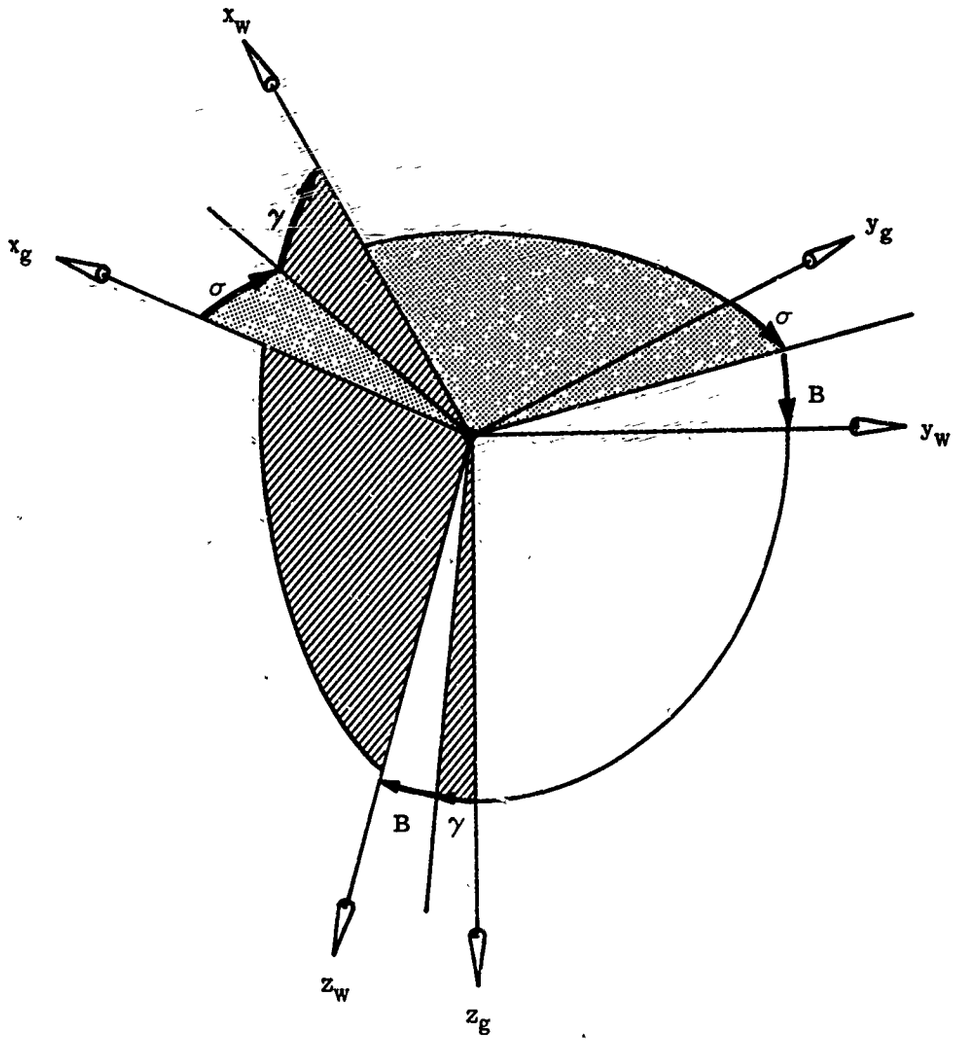

Figure 4 Aircraft Wind Coordinates

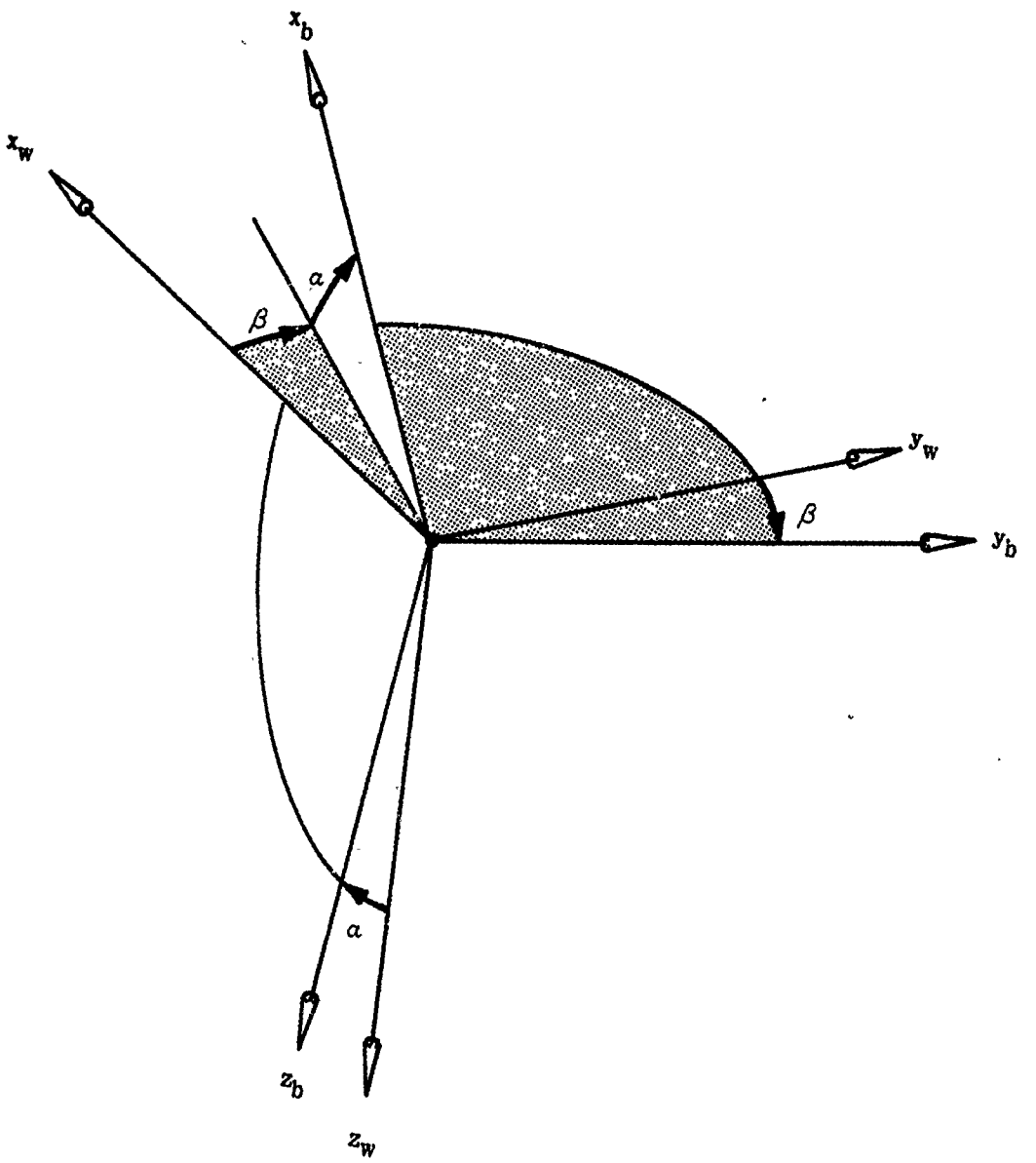

Figure 5 Body Coordinates

of attack. The sideslip angle, β, is measured from the airspeed vector (x_w-axis) to its projection on the $x_b z_b$-plane. The angle of attack, α, is measured from the projection of the x_b-axis on the $x_w y_w$-plane to the x_b-axis itself.

RADAR COORDINATE SYSTEM

The final axes system to be described is the radar coordinate system (x_r, y_r, z_r) (shown in the two views of figure 6). Its origin is located at the radar site at an altitude h_r, a longitude λ_{L_r} and a geodetic latitude δ_{D_r}. The $x_r y_r$-plane is oriented with respect to the geocentric horizontal by a tilt angle $\Delta\delta_{L_r}$ in the meridian plane. Usually the tilt angle has a negative value such that the $x_r y_r$-plane is parallel to the geodetic horizontal. However, in general, the radar plane may not be exactly geodetically horizontal due to local anomolies in the earth's gravitational field. Also, if there is any error in the alinement of the radar axes with respect to true north, the angle ϕ_r between the x_r-axis and the meridan plane will be non-zero. If the radar plane is geodetically horizontal $\Delta\delta_{L_r}$ can be calculated for a given latitude using the geodetic to geocentric latitude transformation equation in Section III.

COORDINATE TRANSFORMATION MATRICES

To illustrate the method by which a transformation matrix is derived a general three axis rotation will be demonstrated, and the associated transformation matrices will be developed for this rotation. Succeeding matrices will then be obtained by analogy with the general matrices.

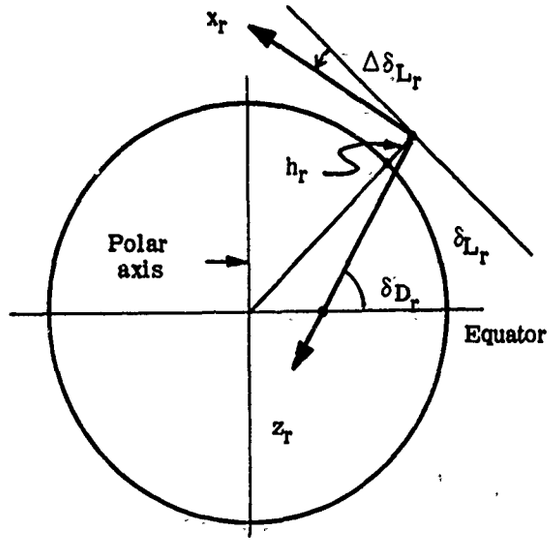

Figure 6a Radar Coordinates Tilt Angle

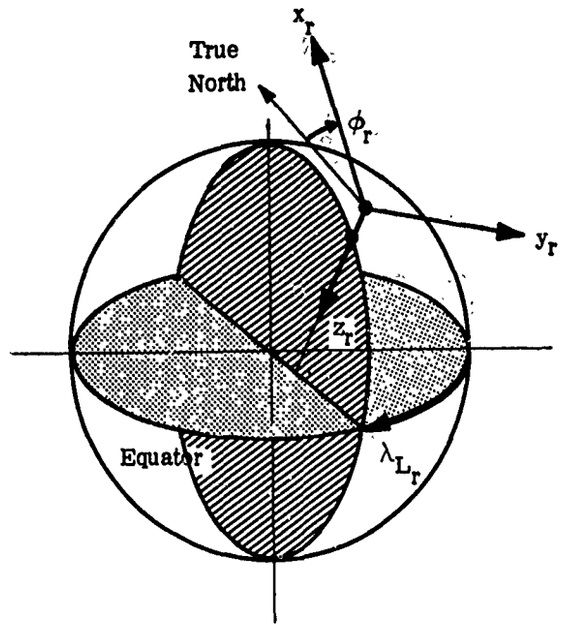

Figure 6b Radar Coordinates Bearing Angle

GENERAL AXES TRANSFORMATIONS

From the geometry of figure 7, which shows a positive rotation about the z-axis, the following equations for the coordinates (x_2, y_2, z_2) in terms of (x_1, y_1, z_1) can be derived

$$x_2 = (\cos\theta_1)x_1 + (\sin\theta_1)y_1 + (0)z_1 \qquad (1)a$$

$$y_2 = (-\sin\theta_1)x_1 + (\cos\theta_1)y_1 + (0)z_1 \qquad (1)b$$

$$z_2 = (0)x_1 + (0)y_1 + (1)z_1 \qquad (1)c$$

This set of equations is alternately expressed as the matrix equation $X_2 = MX_1$, or in component form

$$\begin{bmatrix} x_2 \\ y_2 \\ z_2 \end{bmatrix} = \begin{bmatrix} \cos\theta_1 & \sin\theta_1 & 0 \\ -\sin\theta_1 & \cos\theta_1 & 0 \\ 0 & 0 & 1 \end{bmatrix} \begin{bmatrix} x_1 \\ y_1 \\ z_1 \end{bmatrix} = \left[M_{z_1}(\theta_1)\right] \begin{bmatrix} x_1 \\ y_1 \\ z_1 \end{bmatrix} \qquad (2)$$

where the subscript z_1 on M denotes the axis of rotation, and θ_1 denotes the angle of rotation. If the rotation were in the opposite direction (through a negative angle θ_1 which is similar to the rotation of (x_2, y_2, z_2) to (x_1, y_1, z_1) the signs of the two (sin θ) terms in $[M_{z_1}(\theta_1)]$ would be switched, but the other terms in the matrix would be unchanged. From matrix theory the rotation matrix from (x_2, y_2, z_2) to

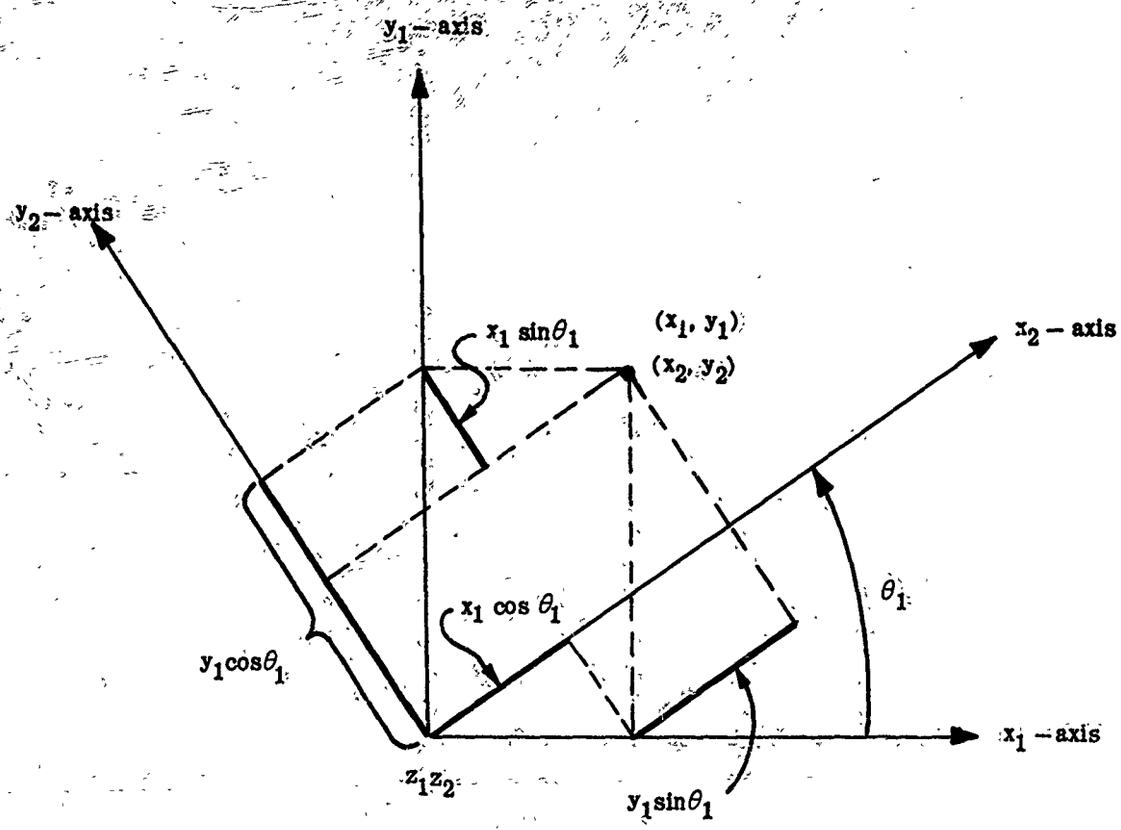

Figure 7 General Axes Rotation

(x_1, y_1, z_1) is known to be the inverse of $[M_{z_1}(\theta_1)]$ or $[M_{z_1}(\theta_1)]^{-1}$. Also, these transformation matrices can be shown to be orthogonal, which by definition means that the inverse is equal to the transpose: $[M_{z_1}(\theta_1)]^{-1}=[M_{z_1}(\theta_1)]^T$. (The orthogonality property further means that the cofactors of each matrix element must equal the element. This property provides a convenient method of checking any matrix for errors among its elements.) If the new axes (x_2, y_2, z_2) are now rotated through an angle θ_2 about the y_2-axis to form the axes system (x_3, y_3, z_3), then $y_3=y_2$, and z would replace x in figure 7, and x would replace y; so, by inspection we write the second transformation matrix

$$\begin{bmatrix} x_3 \\ y_3 \\ z_3 \end{bmatrix} = \begin{bmatrix} \cos\theta_2 & 0 & -\sin\theta_2 \\ 0 & 1 & 0 \\ \sin\theta_2 & 0 & \cos\theta_2 \end{bmatrix} \begin{bmatrix} x_2 \\ y_2 \\ z_2 \end{bmatrix} = [M_{y_2}(\theta_2)] \begin{bmatrix} x_2 \\ y_2 \\ z_2 \end{bmatrix} \tag{3}$$

Similarly, if a transformation is made to (x_4, y_4, z_4) by rotation through θ_3 about the x_3-axis, then y replaces x and z replaces y in figure 7, so that again the transformation written by inspection is

$$\begin{bmatrix} x_4 \\ y_4 \\ z_4 \end{bmatrix} = \begin{bmatrix} 1 & 0 & 0 \\ 0 & \cos\theta_3 & \sin\theta_3 \\ 0 & -\sin\theta_3 & \cos\theta_3 \end{bmatrix} \begin{bmatrix} x_3 \\ y_3 \\ z_3 \end{bmatrix} = [M_{x_3}(\theta_3)] \begin{bmatrix} x_3 \\ y_3 \\ z_3 \end{bmatrix} \tag{4}$$

The total transformation from (x_1, y_1, z_1) to (x_4, y_4, z_4)

is then

$$\begin{bmatrix} x_4 \\ y_4 \\ z_4 \end{bmatrix} = \left[M_{x_3}(\theta_3)\right]\left[M_{y_2}(\theta_2)\right]\left[M_{z_1}(\theta_1)\right]\begin{bmatrix} x_1 \\ y_1 \\ z_1 \end{bmatrix} = \left[M(\theta_1, \theta_2, \theta_3)\right]\begin{bmatrix} x_1 \\ y_1 \\ z_1 \end{bmatrix} \tag{5}$$

To make the reverse transformation from (x_4, y_4, z_4) to (x_1, y_1, z_1) the transpose (inverse) of $M(\theta_1, \theta_2, \theta_3)$ is required. The transpose is obtained by use of the reversal law for the transpose of a product of matrices

$$\left[M(\theta_1,\theta_2,\theta_3)\right]^T = \left[M_{z_1}(\theta_1)\right]^T\left[M_{y_2}(\theta_2)\right]^T\left[M_{x_3}(\theta_3)\right]^T \tag{6}$$

TRANSFORMATIONS FROM GEOCENTRIC TO LOCAL GEOCENTRIC

By analysis of figure 3 it can be determined that two rotations are required to transform the geocentric axes (x_e, y_e, z_e) to the local geocentric axes (x_g, y_g, z_g). First, a rotation about the z_e-axis through the angle $(\pi+\Delta\lambda_L)$ yields the transformation matrix which by analogy with $[M_{z_1}(\theta_1)]$ is

$$\left[M_{z_e}(\pi+\Delta\lambda_L)\right] = \begin{bmatrix} \cos(\pi+\Delta\lambda_L) & \sin(\pi+\Delta\lambda_L) & 0 \\ -\sin(\pi+\Delta\lambda_L) & \cos(\pi+\Delta\lambda_L) & 0 \\ 0 & 0 & 1 \end{bmatrix} \tag{7}$$

This is simplified by trigonometric identities to the following

$$\left[M_{z_e}(\Delta\lambda_L)\right] = \begin{bmatrix} -\cos\Delta\lambda_L & -\sin\Delta\lambda_L & 0 \\ \sin\Delta\lambda_L & -\cos\Delta\lambda_L & 0 \\ 0 & 0 & 1 \end{bmatrix} \tag{8}$$

Second, a rotation about the y_g-axis through the angle $(\pi/2-\delta_L)$ yields the transformation matrix which by analogy with $[M_{y_2}(\theta_2)]$ is

$$\left[M_{y_g}(\tfrac{\pi}{2}-\delta_L)\right] = \begin{bmatrix} \cos(\tfrac{\pi}{2}-\delta_L) & 0 & -\sin(\tfrac{\pi}{2}-\delta_L) \\ 0 & 1 & 0 \\ \sin(\tfrac{\pi}{2}-\delta_L) & 0 & \cos(\tfrac{\pi}{2}-\delta_L) \end{bmatrix} \tag{9}$$

which simplifies to

$$\left[M_{y_g}(\delta_L)\right] = \begin{bmatrix} \sin\delta_L & 0 & -\cos\delta_L \\ 0 & 1 & 0 \\ \cos\delta_L & 0 & \sin\delta_L \end{bmatrix} \tag{10}$$

Expanding the matrix product we obtain the matrix of the transformation from geocentric axes to local geocentric axes

$$\left[M(\Delta\lambda_L,\delta_L)\right] = \begin{bmatrix} -\cos\Delta\lambda_L\sin\delta_L & -\sin\Delta\lambda_L\sin\delta_L & -\cos\delta_L \\ \sin\Delta\lambda_L & -\cos\Delta\lambda_L & 0 \\ -\cos\Delta\lambda_L\cos\delta_L & -\sin\Delta\lambda_L\cos\delta_L & \sin\delta_L \end{bmatrix} \tag{11}$$

The inverse of this transformation matrix for the reverse trans-

formation from local geocentric to geocentric coordinates is

$$\left[M(\delta_L,\Delta\lambda_L)\right] = \begin{bmatrix} -\cos\Delta\lambda_L\sin\delta_L & \sin\Delta\lambda_L & -\cos\Delta\lambda_L\cos\delta_L \\ -\sin\Delta\lambda_L\sin\delta_L & -\cos\Delta\lambda_L & -\sin\Delta\lambda_L\cos\delta_L \\ -\cos\delta_L & 0 & \sin\delta_L \end{bmatrix} \tag{12}$$

TRANSFORMATIONS FROM LOCAL GEOCENTRIC TO WIND COORDINATES

The transformation from the local geocentric coordinates to the aircraft wind coordinates consists of rotations through the flightpath heading angle, σ, the climb angle, γ, and the roll angle, B, in the same sequence and about the same axes as the rotations illustrated through the angles θ_1, θ_2, and θ_3 in the general three axes transformation. Consequently, the resulting transformation matrix is

$$\left[M(\sigma,\gamma,B)\right] = \begin{bmatrix} 1 & 0 & 0 \\ 0 & \cos B & \sin B \\ 0 & -\sin B & \cos B \end{bmatrix} \begin{bmatrix} \cos\gamma & 0 & -\sin\gamma \\ 0 & 1 & 0 \\ \sin\gamma & 0 & \cos\gamma \end{bmatrix} \begin{bmatrix} \cos\sigma & \sin\sigma & 0 \\ -\sin\sigma & \cos\sigma & 0 \\ 0 & 0 & 1 \end{bmatrix} \tag{13}$$

For one application in the section describing the radar reduction equations only the portion involving the first two transformations through σ and γ to an unbanked wind axes system are required. Expanding this product first we obtain

$$\left[M(\sigma,\gamma)\right] = \begin{bmatrix} \cos\gamma\cos\sigma & \cos\gamma\sin\sigma & -\sin\gamma \\ -\sin\sigma & \cos\sigma & 0 \\ \sin\gamma\cos\sigma & \sin\gamma\sin\sigma & \cos\gamma \end{bmatrix} \tag{14}$$

Next, forming the product to rotate to the banked wind axes we obtain the total transform matrix

$$\left[M(\sigma,\gamma,B)\right] = \begin{bmatrix} \cos\gamma\cos\sigma & \cos\gamma\sin\sigma & -\sin\gamma \\ -\cos B\sin\sigma + \sin B\sin\gamma\cos\sigma & \cos B\cos\sigma + \sin B\sin\gamma\sin\sigma & \sin B\cos\gamma \\ \sin B\sin\sigma + \cos B\sin\gamma\cos\sigma & -\sin B\cos\sigma + \cos B\sin\gamma\sin\sigma & \cos B\cos\gamma \end{bmatrix} \tag{15}$$

TRANSFORMATIONS FROM BODY COORDINATES TO WIND COORDINATES

The transformation from body coordinates to wind coordinates requires two rotations in the negative directions first through α and then β about the y_b- and z_w-axes, respectively. The transformation matrix is then

$$\left[M(\alpha,\beta)\right] = \begin{bmatrix} \cos\beta & -\sin\beta & 0 \\ \sin\beta & \cos\beta & 0 \\ 0 & 0 & 1 \end{bmatrix} \begin{bmatrix} \cos\alpha & 0 & \sin\alpha \\ 0 & 1 & 0 \\ -\sin\alpha & 0 & \cos\alpha \end{bmatrix} \tag{16}$$

When the sideslip is neglected the total matrix reduces to the second one involving α only. When β is included the total matrix is

$$\left[M(\alpha,\beta)\right] = \begin{bmatrix} \cos\beta\cos\alpha & -\sin\beta & \cos\beta\sin\alpha \\ \sin\beta\cos\alpha & \cos\beta & \sin\beta\sin\alpha \\ -\sin\alpha & 0 & \cos\alpha \end{bmatrix} \tag{17}$$

TRANSFORMATIONS FROM RADAR TO GEOCENTRIC COORDINATES

To transform the radar measurements to geocentric coordinates, transformations through the two orientation angles $(\pi-\phi_r)$ about the radar z_r-axis and $(\pi/2-\delta_r)$ (where $\delta_r=\delta_{L_r}-\Delta\delta_{L_r}$) about the y_e-axis are required. The resulting matrix is then

$$\left[M\left(\pi-\phi_r,\frac{\pi}{2}-\delta_r\right)\right]=\begin{bmatrix}\cos\left(\frac{\pi}{2}-\delta_r\right) & 0 & -\sin\left(\frac{\pi}{2}-\delta_r\right)\\ 0 & 1 & 0\\ \sin\left(\frac{\pi}{2}-\delta_r\right) & 0 & \cos\left(\frac{\pi}{2}-\delta_r\right)\end{bmatrix}\begin{bmatrix}\cos(\pi-\phi_r) & \sin(\pi-\phi_r) & 0\\ -\sin(\pi-\phi_r) & \cos(\pi-\phi_r) & 0\\ 0 & 0 & 1\end{bmatrix} \tag{18}$$

Performing appropriate trigonometric substitutions

$$\left[M(\phi_r,\delta_r)\right]=\begin{bmatrix}\sin\delta_r & 0 & -\cos\delta_r\\ 0 & 1 & 0\\ \cos\delta_r & 0 & \sin\delta_r\end{bmatrix}\begin{bmatrix}-\cos\phi_r & \sin\phi_r & 0\\ -\sin\phi_r & -\cos\phi_r & 0\\ 0 & 0 & 1\end{bmatrix} \tag{19}$$

Multiplying the two matrices together

$$\left[M(\phi_r,\delta_r)\right]=\begin{bmatrix}-\cos\phi_r\sin\delta_r & \sin\phi_r\sin\delta_r & -\cos\delta_r\\ -\sin\phi_r & -\cos\phi_r & 0\\ -\cos\phi_r\cos\delta_r & \sin\phi_r\cos\delta_r & \sin\delta_r\end{bmatrix} \tag{20}$$

SECTION II

GEOPHYSICAL PROPERTIES

SUMMARY

The usual assumptions that have been made in the past (a flat, non-rotating earth with a constant gravity field) lead to significant errors when performance data are acquired with inertial navigation systems or with accelerometers (such as two-axis flightpath accelerometer systems). Accelerations brought about by the earth's rotation, for example, can be readily sensed by current installations in test aircraft. Further, the magnitude of the errors caused by these assumptions becomes larger as speeds and altitudes are increased. The more nearly exact equations derived in section V, Determination of Excess Thrust, make use of the model of the shape of the earth, its gravitational field, etc., set down in this section.

TABLE OF CONTENTS

SYMBOLS USED IN THIS SECTION

Symbol	Definition	Units
f	earth's flattening $(f = \frac{r_o - r_p}{r_o})$	dimensionless
g_L	local effective acceleration due to gravity	ft per sec^2
$g_{Lx_g}, g_{Ly_g}, g_{Lz_g}$	geocentric components of local acceleration due to gravity	ft per sec^2
g_r	reference acceleration of gravity	ft per sec^2
g_{SL}	sea level acceleration of gravity	ft per sec^2
$g_{x_g}, g_{y_g}, g_{z_g}$	geocentric components of acceleration due to gravitational attraction alone	ft per sec^2
H	geopotential altitude in geopotential units	ft
h	geometric (tapeline) altitude	ft
h_1	geocentric altitude as shown in figure 2	ft
h_2	geodetic altitude as shown in figure 2	ft
h_3	geometric altitude as shown in figure 2	ft
J_2, J_3, J_4	coefficients of the zonal harmonics of the earth's gravitational potential	dimensionless
r	local radius of the earth	ft
r_p	polar radius of the earth	ft
r_o	equatorial radius of the earth	ft
R_e	effective earth radius	ft
t	time	sec

Symbol	Definition	Units
x,y	Cartesian coordinates	---
x_g, y_g, z_g	geocentric position coordinates	ft
δ_D	geodetic latitude	rad
δ_L	geocentric latitude	rad
λ	longitude	rad
$\mu_\oplus$	product of universal gravitational constant and the mass of the earth	ft^3 per sec^2
Φ	gravitational potential function	ft^2 per sec^2
$\omega_\oplus$	angular rotation rate of the earth	rad per sec

INTRODUCTION

In this section equations for the earth's geophysical properties are presented. The geophysical parameters which are necessary for atmospheric trajectory calculations are those which describe the earth's mean sea level surface, the aircraft's position relative to that surface, the gravitational attraction between the earth and the aircraft, and the earth's rotation rate, which provides centrifugal relief from the force of gravity. An attempt has been made to present equations which have precision comparable to the general aircraft equations of motion presented in the section, Determination of Excess Thrust.

Various approximations to the earth's shape and gravitational field have been made to simplify the equations of motion. However, with the introduction of high performance aircraft into the Air Force inventory, improved equations have become desirable. High accuracy accelerometers and precise inertial navigation systems can sense accelerations such as those induced by the earth's rotation, and they can sense forces caused by variation in gravity with altitude and latitude. These navigation systems must also account for the oblate shape of the earth in order to provide accurate position data. The old assumptions of a flat earth and constant gravity are no longer adequate in most cases.

Since the advent of artificial earth satellites a number of refinements in the measurements of the earth's geophysical properties have been made. These precise equations with slight simplifications have been used in this section. An attempt has been made to state the important assumptions and describe the simplifications to allow for future analysis of the adequacy of the equations.

DIMENSIONAL PROPERTIES

The strength of the earth's crust is low enough when compared to total earth mass and rotational energy that its surface shape has been forced to assume the approximate form of a ball of fluid in hydrodynamic equilibrium. Such a ball of fluid in space (in the absence of surrounding bodies) would assume a spherical shape under the action of internal gravity; however, when given a specific rotational rate about a "polar" axis it would develop a bulge about its equator and assume the shape of an ellipsoid of revolution.

In actual fact the earth does not have a circular equator and its density is not uniform. However, for reference purposes an ellipsoidal surface is defined which approximates mean sea level. Mean sea level is also approximately the geoid surface of dynamical balance between gravitational force and the inertia of the rotating mass (see figure 1).

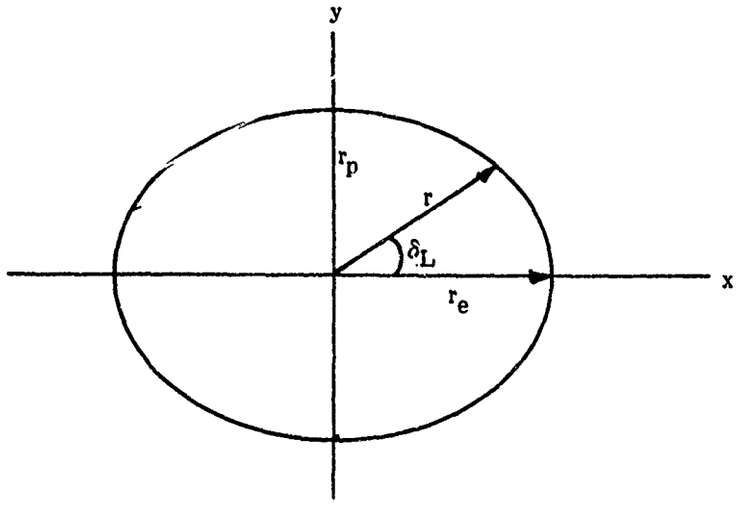

Figure 1 The Reference Ellipsoid

EQUATORIAL AND POLAR RADII

The dimensions of the reference ellipsoid are generally given by stating an equatorial radius, r_o, and a flattening, f, defined to be the quotient formed by dividing the equatorial radius into the difference between the equatorial and polar radii:

$$f = \frac{r_o - r_p}{r_o} \tag{1}$$

This equation can be solved to yield an expression for the polar radius in terms of the equatorial radius and earth flattening:

$$r_p = r_o(1 - f) \tag{2}$$

Substitution of these radii into the polar coordinate equation for an ellipse yields a general equation for the radius of the ellipsoidal surface as a function of the geocentric latitude, δ_L, which is the angle between the radius vector and the equatorial plane:

$$r^2 = \frac{r_o^2(1-f)^2}{(1-f)^2\cos^2\delta_L + \sin^2\delta_L} \tag{3}$$

One alternate form of this equation is obtained by use of the trigonometric half-angle formulas and by dividing by $(1-f)^2$:

$$r^2 = \frac{2r_o^2}{[1+(\frac{1}{1-f})^2] + [1-(\frac{1}{1-f})^2]\cos 2\delta_L} \tag{4}$$

Another computationally convenient form of this equation can be obtained by expansion using a Maclaurin series and appropriate trigonometric substitutions. For example, for $1/f = 298.30$ the following expansion yields the same radius as equation (4) to the nearest foot or better:

$$r = r_o(.99832172 + .00167616\cos 2\delta_L + .00000211\cos 4\delta_L) \tag{5}$$

GEODETIC AND GEOCENTRIC LATITUDES AND ALTITUDES

Having defined the reference ellipsoidal surface of the earth, we can turn to the problem of measuring an aircraft's altitude with respect to that surface. Four altitudes will be defined. An exaggerated illustration of these altitudes is shown in figure 2. The first is the geocentric altitude which is merely the distance measured along an extension of the radius vector from the ellipsoid surface up to the aircraft. This distance when added to the earth radius at that point gives the straight line distance between the earth's center and the aircraft. The geocentric altitude is required in the general equations which describe accelerations in the geocentric reference system.

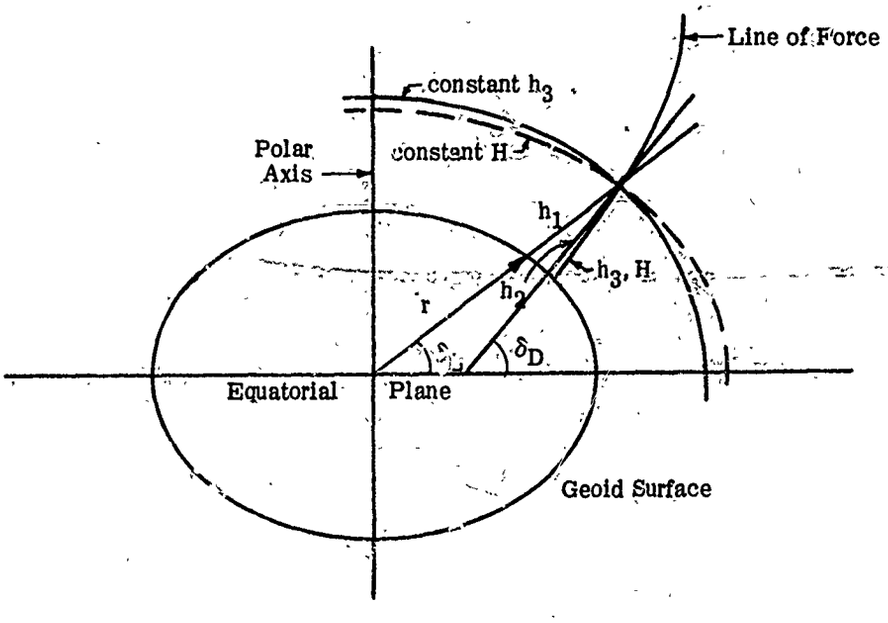

Figure 2 Altitudes Related to the Geoid

The second altitude to be defined is the geodetic altitude. This is the straight line distance from the aircraft to the nearest point on the geoid (sea level) surface. The angle between this line and the equatorial plane is defined to be the geodetic latitude, δ_D. The geodetic altitude is the true altitude or straight line height of a point above the earth's surface. By observation of figure 2 one can see that the differences between the geocentric and geodetic latitudes and altitudes vary and are a maximum near a latitude of 45 degrees. These differences also vary with altitude.

A precise equation for transforming between geodetic and geocentric latitudes is presented in reference 1, pp. 96 ff. However, for aircraft trajectories which generally lie below 150,000 feet, the precise equations can be approximated with little error by the sea level expression.

This relation between the two latitudes at sea level is easily derived. The slope of the ellipsoid surface is obtained by differentiation of its rectangular coordinate equation:

$$\frac{dy}{dx} = -\frac{r_p^2 x}{r_o^2 y} \tag{6}$$

Then since a geodetic latitude line is by definition everywhere normal to the surface, its slope is the negative

reciprocal of the surface slope:

$$\tan\delta_D = \left(\frac{r_o}{r_p}\right)^2 \frac{y}{x} = \left(\frac{r_o}{r_p}\right)^2 \tan\delta_L \qquad (7)$$

Substituting for the radii ratio from equation (2) and rearranging we obtain the simple exact relation between the latitudes of a point at sea level:

$$\tan\delta_L = (1-f)^2 \tan\delta_D \qquad (8)$$

The maximum difference between the two latitudes is about eleven and one-half minutes of arc or eleven and one-half nautical miles error in position on the earth's surface if the incorrect latitude were to be used.

The relation of equation (8) can be approximated by the first term of a series (reference 2, p. 485):

$$\delta_L - \delta_D = -(.19323889)\sin 2\delta_D \qquad (9)$$

Equations could also be presented relating the geocentric and geodetic altitudes, but little error results from assuming that they are equal. The difference is one foot or less below 150,000 feet altitude and less than 60 feet at an altitude of about one earth radius (reference 1, p. 102). The remaining two altitudes as shown in figure 2 are described later.

GRAVITATIONAL FIELD

By definition the gravitational potential function of the earth, Φ, is a scalar quantity such that the partial derivative of Φ in a given direction yields the acceleration due to gravity (reference 3, p. 173). For example in the x direction by definition ($\equiv$)

$$\frac{\partial \Phi}{\partial x} \equiv \frac{d^2x}{dt^2} \tag{10}$$

If the earth were a homogeneous sphere, it would have a central force field with a gravitational potential function given by

$$\Phi = \frac{\mu_\oplus}{r + h} \tag{11}$$

where (r+h) is the distance from the geocenter to a given point. Differentiation of this function in the (r+h) direction yields

$$\frac{\partial \Phi}{\partial (r+h)} = \frac{\partial}{\partial (r+h)} \left(\frac{\mu_\oplus}{r+h}\right) = -\frac{\mu_\oplus}{(r+h)^2}$$

or

$$\frac{d^2(r+h)}{dt^2} = -\frac{\mu_\oplus}{(r+h)^2} \tag{12}$$

which is the inverse square law gravity equation.

Since the earth is not a homogeneous sphere nor even an ellipsoid of revolution, its true potential function must be obtained by an integration over its entire volume or alternately as a series solution to the differential equation of Laplace (reference 4, p. 141). Neglecting the earth's asphericity with longitude (assuming the shape is an ellipsoid of revolution) and only presenting the first four terms, the series for the earth's potential is (reference 5, p. 2)

$$\Phi = \frac{\mu_\oplus}{(r+h)}\left[1 + \frac{J_2}{2}\left(\frac{r_o}{r+h}\right)^2\left(1 - 3\sin^2\delta_L\right) + \frac{J_3}{2}\left(\frac{r_o}{r+h}\right)^3\left(3 - 5\sin^2\delta_L\right)\sin\delta_L - \frac{J_4}{8}\left(\frac{r_o}{r+h}\right)^4\left(3 - 30\sin^2\delta_L + 35\sin^4\delta_L\right)\right]$$

The components of gravitational acceleration in the local geocentric coordinate system can be obtained by partial differentiation of the potential function in the three coordinate directions x_g, y_g, and z_g. To perform this differentiation the following relations are required:

$$g_{x_g} = \frac{\partial\Phi}{\partial x_g} = \frac{1}{r+h}\frac{\partial\Phi}{\partial\delta_L} \tag{14a}$$

$$g_{y_g} = \frac{\partial\Phi}{\partial y_g} = -\frac{1}{(r+h)\sin\delta_L}\frac{\partial\Phi}{\partial\lambda} \tag{14b}$$

$$g_{z_g} = \frac{\partial \Phi}{\partial z_g} = -\frac{\partial \Phi}{\partial (r+h)} \qquad (14c)$$

Performing the differentiation indicated by equation (14a) we obtain the north component of gravitational acceleration:

$$g_{x_g} = -\left(\frac{\mu_\oplus}{r_o^2}\right)\left(\frac{r_o}{r+h}\right)^4 \left[3J_2 \sin\delta_L - \frac{3}{2}J_3\left(\frac{r_o}{r+h}\right)(1-5\sin^2\delta_L) - \frac{5}{2}J_4\left(\frac{r_o}{r+h}\right)^2(3-7\sin^2\delta_L)\sin\delta_L\right]\cos\delta_L \qquad (13)$$

Since the variation of the potential function with longitude has been neglected the eastward component of the gravitational acceleration is zero:

$$g_{y_g} = 0 \qquad (15b)$$

Finally, evaluating equation (14c), we obtain the geocentric vertical component of the gravitational acceleration:

$$g_{z_g} = \left(\frac{\mu_\oplus}{r_o^2}\right)\left(\frac{r_o}{r+h}\right)^2 \left[1 + \frac{3}{2}J_2\left(\frac{r_o}{r+h}\right)(1-3\sin^2\delta_L)\right. \qquad (15a)$$

$$+ 2J_3\left(\frac{r_o}{r+h}\right)^3(3-5\sin^2\delta_L)\sin\delta_L$$

$$\left. - \frac{5}{8}J_4\left(\frac{r_o}{r+h}\right)^4(3-30\sin^2\delta_L + 35\sin^4\delta_L)\right] \qquad (15c)$$

These components yield the acceleration due to gravitational attraction alone. To determine the apparent acceleration of a particle at a fixed point with respect to the

earth's surface the so called "centrifugal relief," which is contributed to the particle by the earth's rotation, must be included. The components of the "centrifugal relief" actually arise as a result of the particle's motion with respect to inertial space, and the derivation of these components appears in the section, Determination of Excess Thrust. For the present purpose the "centrifugal relief" components will be added to the gravitational attraction acceleration components without further comment. The resulting centrifugally relieved geocentric components of the acceleration are then

$$g_{L_{x_g}} = -\left(\frac{\mu_\oplus}{r_o^2}\right)\left(\frac{r_o}{r+h}\right)^4\left[3J_2\sin\delta_L - \frac{3}{2}J_3\left(\frac{r_o}{r+h}\right)(1-5\sin^2\delta_L) - \frac{5}{2}J_4\left(\frac{r_o}{r+h}\right)^2(3-7\sin^2\delta_L)\sin\delta_L\right]\cos\delta_L - \omega_\oplus^2(r+h)\cos\delta_L\sin\delta_L \qquad (16a)$$

$$g_{L_{y_g}} = 0 \qquad (16b)$$

$$g_{L_{z_g}} = \left(\frac{\mu_\oplus}{r_o^2}\right)\left(\frac{r_o}{r+h}\right)^2\left[1+\frac{3}{2}J_2\left(\frac{r_o}{r+h}\right)^2(1-3\sin^2\delta_L) + 2J_3\left(\frac{r_o}{r+h}\right)^3(3-5\sin^2\delta_L)\sin\delta_L - \frac{5}{8}J_4\left(\frac{r_o}{r+h}\right)^4(3-30\sin^2\delta_L+35\sin^4\delta_L)\right] - \omega_\oplus^2(r+h)\cos^2\delta_L \qquad (16c)$$

The magnitude of the resultant acceleration due to gravity at a point above the earth is then

$$g_L = [(g_{L_{x_g}})^2 + (g_{L_{z_g}})^2]^{1/2} \qquad (17)$$

GEOMETRIC AND GEOPOTENTIAL ALTITUDES

The total gravity components of equation (16) have been obtained by summing the final acceleration contributions from gravitational attraction and "centrifugal relief." A different approach is taken in reference 6, p. 5. The total potential or geopotential at a point is defined as the sum of the gravitational potential and the fictitious "centrifugal force" potential. The lines of gravity force which result from this potential are by definition everywhere perpendicular to the surfaces of constant potential, and since the potential surfaces are ellisoids the lines of force are curved (reference 6, figure I.2.4(a)). The curvature is such that latitude increases with altitude along the line of force.

Geometric altitude is defined to be the curved distance measured along a line of force from the zero potential level (approximately sea level) to the given altitude point.

It is convenient to define another altitude parameter which is especially useful in the model atmosphere equations of the section, Atmospheric Environment. This parameter is

physically equivalent to the geopotential but has the units of length and is called the geopotential altitude. It is defined by the equation

$$H = \int_0^h \frac{g_L}{g_r} dh \qquad (18)$$

where g_r is the standard value of the reference sea level acceleration due to gravity. In accordance with its definition the geopotential altitude is also measured along the curved lines of force; however, the physical or geometric length of a geopotential foot is not constant. The length is a function of the local gravity and consequently increases with altitude because of the reduction in gravity.

The most precise technique for calculating geopotential altitude requires a simultaneous numerical integration of the differential equations relating the acceleration of gravity and the latitude and radius of each point along the curved line of force to the geometric altitude of that point (reference 6, pp. 6, 7).

The curvature of the line of force is exaggerated in reference 6, and for the range of altitudes considered in this document the geometric and geopotential altitudes can be considered to be measured along straight lines coinciding with the geodetic altitude lines. The error associated with this assumption is negligible. Consequently, the three

different altitudes, geocentric, geodetic and geometric, can all be considered equal, and we can speak of the geometric altitude as being representative of all three.

By an appropriate assumption an equation can be derived which allows direct calculation of geopotential altitude from geometric altitude and vice versa without the necessity of the numerical integration from sea level up to the given altitude (reference 7, pp. 217, 218 and 488). The assumption which is necessary is that the centrifugal relief is not a function of altitude. By analysis of equation (16) it can be determined that this assumption amounts to less than one percent error in magnitude of the centrifugal relief term for altitudes below 200,000 feet. Since the term is a small fraction of the total gravitational acceleration the assumption introduces negligible error.

To develop the conversion equation an inverse square law gravity field is assumed, but the earth's effective radius, R_e, and sea level acceleration due to gravity are expressed as a function of latitude to make the resulting equation fit the actual gravity field more closely. For an inverse square gravity field the acceleration due to gravity is

$$g_L = g_{SL}\left(\frac{R_e}{R_e + h}\right)^2 \qquad (19)$$

Substituting this gravity expression into equation (18) and integrating, we obtain the conversion equation:

$$H = \frac{g_{SL}}{g_r}\left(\frac{R_e h}{R_e + h}\right) \tag{20}$$

Equation (20) can easily be solved to obtain the inverse equation for h as a function of H.

To obtain the expression for R_e, we first differentiate equation (19).

$$\frac{\partial g_L}{\partial h} = -2 g_{SL} \frac{R_e^2}{(R_e + h)^3}$$

Evaluated at sea level (h = 0), this becomes

$$\left.\frac{\partial g_L}{\partial h}\right|_{h=0} = -\frac{2 g_{SL}}{R_e}$$

and solving for R_e

$$R_e = -\frac{2 g_{SL}}{\left.\frac{\partial g_L}{\partial h}\right|_{h=0}} \tag{21}$$

Equations for the sea level gravity and the partial derivative at sea level are presented in reference (7). Similar equations can also be derived by appropriate substitution and differentiation of equation (16).

The value of geopotential altitude at each geometric altitude as given by the more nearly exact numerical integration of reference 6 and as given by equation (20) are identical to the nearest foot up through 188,000 feet.

GEOPHYSICAL CONSTANTS

In order to select a consistent set of geophysical constants a brief study was made to compare the values of acceleration of gravity as computed by equations (17) and (19). Equation (19) was evaluated by using the following equation for the effective earth radius obtained from reference 7:

$$R_e = \frac{64.344882(1 - .0026373\cos 2\delta_D + .0000059\cos^2 2\delta_D)}{3.085462\times10^{-6} + 2.27\times10^{-9}\cos 2\delta_D - 2\times10^{-12}\cos 4\delta_D} \qquad (22)$$

In order to evaluate equation (17) the constants in equations (4) and (16) had to be supplied. The values of these constants as shown in references 3, 6, and 9 were substituted, and the accelerations from equation (17) produced by each set of constants were compared with those from equation (19). The set of constants from reference

9 produced the closest agreement between equations (17) and (19). These values were the ones "most used" for orbital calculations.

The values from reference 6 and those from reference 3 which are more recent, produce accelerations which differ from those of equation (19). If the values from reference 3 or later values are to be used in equation (4) and (16), then a new expression for the effective earth radius should be derived by evaluation and differentiation of equation (17) in accordance with equation (21). However, it is believed that the constants from reference 9 are adequate for aircraft trajectory analysis. These constants are presented in the following table.

Constant	Value	Units
r_o	6,378,165	meters
	20,925,738	feet
$\mu_\oplus$	3.986032×10^{14}	meters^3 per sec^2
	1.4077768×10^{16}	ft^3 per sec^2
1/f	298.30	nondimensional
J_2	1082.30×10^{-6}	nondimensional
J_3	-2.3×10^{-6}	nondimensional
J_4	-1.8×10^{-6}	nondimensional
$\omega_\oplus$	7.2921×10^{-5}	radians per sec

REFERENCES

1. Combs, A.L., et al., Six-Degree-of-Freedom Flight Path Study Gereralized Computer Program, Problem Formulation, FDL-TDR-64-1, Part I, Volume I, Air Force Flight Dynamics Laboratory, Wright-Patterson AFB, Ohio, October 1964.
2. Anon, The American Ephemeris and Nautical Almanac, 1967, U.S. Government Printing Office, Washington D.C., 1964
3. Baker, R.M.L., and Makemson, M.W., An Introduction to Astrodynamics, (second edition), Academic Press Inc., New York, 1967.
4. Baker, R.M.L., Astrodynamics Applications and Advanced Topics, Academic Press Inc., New York, 1967.
5. Makemson, M.W., Baker, R.M.L., and Westrom, G.B., "Analysis and Standardization of Astrodynamic Constants," The Journal of the Astronautical Sciences, Volume VIII, Number 1, Spring 1961.
6. Anon, U.S. Standard Atmosphere, 1962, U.S. Government Printing Office, Washington D.C., December 1962.
7. List, R.J., Smithsonian Meteorological Tables, (sixth revised edition, first reprint), Smithsonian Institution, Washington D.C., 1958. (Smithsonian Miscellaneous Collections, Vol 114, also Publication 4014)

8. Minzner, R.A., et. al., The ARDC Model Atmosphere, 1959, AFCRC-TR-59-267, Air Force Cambridge Research Center, Bedford, Massachussets, August 1959.

9. Kaula, W.M., A Review of Geodetic Parameters, NASA-TND-1847, Goddard Space Flight Center, Maryland, May 1963.

SECTION III

ATMOSPHERIC ENVIRONMENT

SUMMARY

The basic assumptions, definitions, and constants which have been used in generating model atmospheres are presented. Such an atmosphere provides the norm to which all test data are corrected. Information about the various models is also presented, together with the concepts of geometric and geopotential altitudes.

TABLE OF CONTENTS

SYMBOLS USED IN THIS SECTION

Symbol	Definition	Units
g	acceleration due to gravity	ft/sec^2
g_L	local effective acceleration due to gravity	ft/sec^2
g_r	reference acceleration of gravity	ft/sec^2
g_{SL}	sea level acceleration of gravity	ft/sec^2
h	geometric altitude	ft
H	geopotential altitude	ft
L_M	temperature gradient, dT_a/dH	°K/ft
M	molecular weight of air or	dimensionless
M	Mach number	dimensionless
M_o	molecular weight of air at sea level	dimensionless
P_a	ambient pressure	lb/ft^2
r	local radius of the earth	ft
R	universal gas constant	$ft^2/sec^2°K$
T_a	ambient temperature	deg K
T_i	temperature of the ice point (273.15°K)	deg K
T_M	molecular scale temperature	deg K
ρ	air density	$slugs/ft^3$
σ	air density ratio, ρ/ρ_{SL}	dimensionless
Φ	geopotential	ft^2/sec^2
Subscripts		
b	base of atmospheric layer	-
SL	sea level	-

ATMOSPHERIC ENVIRONMENT

INTRODUCTION

The physical characteristics of the earth's atmosphere vary greatly, changing from day to day and with seasons of the year. The performance of an aircraft is dependent on the nature of the airmass through which it flies. For example, the thrust of a turbojet engine increases appreciably with a decrease in air temperature. Therefore some set of standard conditions must be established in order for performance data to have some meaning when correlating data from one flight to another or comparing the performance of one aircraft to that of another. When flight test results are reduced to standard conditions, ideally the corrections applied ought to be as small as possible to minimize errors due to linear approximations. (Reference the section, Standardization of Excess Thrust.) This might imply the use of a reference atmosphere which accurately represented the mean atmospheric properties at the test site except for the fact that reduction of test data acquired elsewhere in the world for purposes of comparison could then entail large corrections. A compromise between small corrections and universal applicability requires the use of an idealized middle-latitude, year-round mean atmospheric model.

MODEL ENVIRONMENT

BASIC ASSUMPTIONS

Since the earliest models of the atmosphere were published (circa 1920) the same assumptions, with minor variations, have been made in the range of 0 to 20,000 meters (≈65,600 feet). These have included:

(1) Sea level temperature is 15°C

(2) A constant temperature gradient from sea level to about 11,000 meters (36,089 feet), and then

(3) A constant temperature from 11,000 to 20,000 meters

Additionally, it has been assumed that

(4) The air is dry

(5) The atmosphere is a perfect gas so that the equation of state

$$P_a = \rho R T_a \tag{1}$$

applies

(6) Hydrostatic equilibrium exists, assuming that the atmosphere is static with respect to the earth:

$$dP_a = -\rho g\, dh \tag{2}$$

By combining equations (1) and (2) the usual differential form of the barometric equation is obtained

$$\frac{dP_a}{P_a} = -\frac{g}{RT_a}dh \tag{3}$$

If g is taken to be constant and T_a is replaced by a linear function of h, equation (3) can be integrated quite simply to calculate pressures. This procedure was followed in tabulating the older atmospheres; however, the assumption of constant g becomes inadequate as altitudes are extended and new techniques (discussed in following paragraphs) were devised.

PRIMARY CONSTANTS

In order to compute properties of a model atmosphere, it is necessary to establish values for basic constants appropriate to the earth's atmosphere. To illustrate, constants which have been used to form tabular values of concern in aircraft flight test have been extracted from reference 4 and appear in table 1. For a more complete list of constants together with a discussion of their origin, see reference 4, pages 4 and 5.

Table 1 - Primary Constants

Symbol		Units
$P_{a_{SL}}$	29.92126	in. Hg
ρ_{SL}	0.076474	lb ft^{-3}
$t_{a_{SL}}$	15	°C
g_r *	32.1741	ft sec^{-2}
T_i	273.15	°K
γ	1.40	dimensionless
R	3089.80	$ft^2 sec^{-2} °K^{-1}$

UNIVERSAL GAS CONSTANT

The universal gas constant in the perfect gas law has the dimensions of energy $mole^{-1}$ (degree absolute)$^{-1}$. When divided by the mass of one mole, the gas constant of air has dimensions of energy (unit mass)$^{-1}$ (degree absolute)$^{-1}$. In the English system of units used in flight test work, the energy is expressed in ft-lb_f, the mass in lb_m and temperature unit in °K so that the gas constant becomes ft-$lb_f lb_m^{-1} °K^{-1}$ or ft ft-$sec^{-2} °K^{-1}$. If the gas law is written

$$P_a = \rho g R T_a$$

R has the dimensions ft $°K^{-1}$. If the law is written

* The adopted value of g_r is 9.80665 meters sec^{-2} which converted to the English system of units is 32.174049 feet sec^{-2}. The above value from the U.S. 1962 Atmosphere, reference 4, has been rounded incorrectly.

$$P_a \propto \rho R T_a$$

as was done in this report in equation (1) then R has the dimensions $ft^2 sec^{-2} {}^\circ K^{-1}$.

SPEED OF SOUND

The speed of sound is by definition the speed of propagation of the wave formed by an infinitesimal pressure disturbance. Such a disturbance very closely approximates an adiabatic reversible (isentropic) process. Considering this, the conservation equations for mass and momentum can be combined to give

$$a^2 = \left(\frac{\partial P}{\partial \rho}\right)_s$$

and for an ideal gas

$$a^2 = \gamma R T_a \qquad (4)$$

In the ARDC 1959 and the U.S. 1962 atmospheres (references 4 and 6) γ has been taken to be 1.40 exact (to an altitude of 90 kilometers).

RELATIONSHIPS USED TO DEFINE MODEL ATMOSPHERES

As was previously pointed out, the barometric equation (equation 3) can be integrated easily provided that a constant value of g is assumed. This was done in the older

atmospheres, and data were tabulated as a function of tape-line altitude, h. At the high altitudes to which more recent models have been computed this assumption is no longer valid. Further, variation in molecular weight, M, has been accounted for by writing the perfect gas law in the form

$$\rho = \frac{P_a M}{R T_a} \tag{5}$$

See, for example, reference 4, page 5, and reference 6, page 4. Integration of the resulting barometric equation becomes quite complex, even when g and M are replaced by very simple functions of h. To retain the mathematical simplicity of the equations used for low altitude calculations, two transformations of variables have been made. The two new parameters are: geopotential altitude, H, from combining g and h, and molecular-scale temperature, T_M, from combining T_a and M. By defining T_M as a series of linear functions of H, integration may be carried out exactly as for equations using geometric altitude and constant g.

Molecular-Scale Temperature

By definition the molecular-scale temperature is

$$T_M = \frac{M_o}{M} T_a \tag{6}$$

At extreme altitudes T_M is widely different from the kinetic temperature (reference 4, page 8); however, since $T_M = T_a$ in the altitude range of interest in aircraft flight test, no further consideration is given to this parameter.

Geopotential Altitude*

The geopotential at an altitude h is the potential energy of a unit mass at that altitude relative to the potential energy of the same mass at mean sea level. In differential form geopotential, Φ, is related to geometric (tapeline) altitude by

$$d\Phi = g_L \, dh \tag{7}$$

The force of gravity in equation (7) is the resultant of two forces: (1) the gravitational attraction which derives from Newton's universal law of gravitation, and (2) the centrifugal force (commonly called centrifugal relief) in

* The following information on geopotential altitude pertains to model atmospheres. Additional information may be found in the section, Geophysical Properties.

a reference frame attached to the earth, assuming that the atmosphere rotates with the earth. Hence, a local value of g is a function of both vertical displacement* above the earth's surface and latitude.

Integrating equation (7) the geopotential at an altitude of h is

$$\Phi = \int_0^h g_L \, dh \tag{8}$$

In accordance with equation (8) the geopotential altitude is defined as

$$H = \frac{\Phi}{g_r} = \int_0^h \frac{g_L}{g_r} \, dh \tag{9}$$

By introducing the reference gravity, g_r, geopotential altitude has the dimensions of length (geopotential feet in the English system), and is equivalent to Φ, which is the amount of work done in raising a unit mass from

* In the U.S. 1962 Atmosphere a refinement is made in that h is measured along the line of force through the point, from the equipotential surface for which $\Phi = 0$ to the point in question, causing the lines of force to curve toward the poles. The difference in distance according to this definition and a straight line distance is negligible within the sensible atmosphere and is, therefore, of no consequence in aircraft flight testing.

mean sea level to a geometric altitude of h. A value of 9.80665 meters sec^{-2} (32.17405 feet sec^{-2}) was adopted for the ICAO Standard Atmosphere and for the ARDC 1959 Atmosphere. The same value was also adopted for the U.S. Standard Atmosphere, 1962 for a geographic latitude of exactly 45°. It should be noted that physical displacements between equipotential surfaces separated by a constant amount in terms of geopotential is not constant. Rather, the physical displacement increases with altitude because of the decreasing values of g.

In differential form equation (9) is

$$g_r \, dH = g_L \, dh \tag{10}$$

Substituting equation (10), equation (3) may be written as

$$d(\ln P_a) = -\frac{g_r}{R T_a} dH \tag{11}$$

In order to integrate this equation to find geopotential altitude as a function of pressure, $H(T_a)$ is substituted. To simplify the procedure, it is assumed that the atmosphere is made up of layers in which the temperature varies linearly with geopotential altitude (constant temperature gradient).

The general temperature-altitude relationship is then

$$T_a = (T_a)_b + L_M(H - H_b) \tag{12}$$

Substituting equation (12) in equation (11) and integrating produces the following equation:

$$\ln P_a = -\frac{g_r}{RL_M} \ln[(T_a)_b + L_M(H - H_b)] \tag{13}$$

Taking $(P_a)_b$ to be the pressure at the base of the layer we have

$$P_a = (P_a)_b \left[\frac{(T_a)_b}{(T_a)_b + L_M(H - H_b)}\right]^{g_r/RL_M} \tag{14}$$

when the temperature gradient, L_M, is not zero. Following the same steps with $L_M = 0$ leads to

$$P_a = (P_a)_b \exp\left[\frac{-g_r (H - H_b)}{R(T_a)_b}\right] \tag{15}$$

Properties which appear in the above equations have been taken from reference 4 and, after converting units, are presented in table 2.

Table 2 - Properties Defining the U.S. Standard Atmosphere, 1962

Altitude, H		Gradient, L	Atmospheric Pressure, P_a	Atmospheric Temperature, T_a
km	feet	°K/foot	in. Hg	°K
0.000			29.92126	288.15
		-1.98120×10^{-3}		
11.000	36,089.24		6.68321	216.65
		0		
20.000	65,616.80		1.61671	216.65
		0.30480×10^{-3}		
32.000	104,986.88		0.25632	228.65
		0.85344×10^{-3}		
47.000	154,199.48		0.032750	270.65
		0		
52.000	170,603.67		0.017423	270.65
		-0.60960×10^{-3}		
61.000	200,131.23		0.0053773	252.65

Pressure, Temperature, and Density Ratios

From the preceding equations, general equations defining pressure, temperature, and density ratios may be found.

From equation (14)

$$\delta = \frac{P_a}{P_{a_{SL}}} = \frac{(P_a)_b}{P_{a_{SL}}}\left[\frac{(T_a)_b}{(T_a)_b + L_M(H - H_b)}\right]^{g_r/RL_M} \tag{16}$$

when $L_M \neq 0$ and, from equation (15)

$$\delta = \frac{P_a}{P_{a_{SL}}} = \frac{(P_a)_b}{P_{a_{SL}}} \exp\left[\frac{-g_r\,(H - H_b)}{R(T_a)_b}\right] \tag{17}$$

when $L_M = 0$.

The general equation for temperature ratio from equation (12) is

$$\theta = \frac{T_a}{T_{a_{SL}}} = \frac{1}{T_{a_{SL}}}\left[(T_a)_b + L_M(H - H_b)\right] \tag{18}$$

From the perfect gas law $\delta_a = \sigma\theta_a$ so that from equations (16) and (18)

$$\sigma = \sigma_b\left[\frac{(T_a)_b}{(T_a)_b + L_M(H - H_b)}\right]^{\frac{g_r}{RL_M} + 1} \tag{19}$$

when $L_M \neq 0$ and, from equations (17) and (18)

$$\sigma = \sigma_b \exp\left[\frac{-g_r (H - H_b)}{R(T_a)_b}\right] \tag{20}$$

when $L_M = 0$

Geometric Altitude

In flight test applications the calculation of geometric (tapeline) altitude is frequently required. Geometric altitudes cannot be computed directly for off-standard conditions; an integration procedure must be resorted to using continuous profiles of pressure and temperature. From $dP_a/P_a = d(\ln P_a)$ equation (3) becomes

$$d(\ln P_a) = -\frac{g_L}{RT_a} dh \tag{21}$$

From the inverse-square law of gravitation (reference equation (19) in the section, Geophysical Properties)

$$g_L = g_{SL} \frac{R_e^2}{(R_e + h)^2} \tag{22}$$

Substituting equation (22) in equation (21) and rearranging

$$dh = -\frac{R}{g_{SL}} T_a \left(\frac{R_e + h}{R_e}\right)^2 d(\ln P_a) \qquad (23)$$

Equation (23) may be written in integral form as

$$\int_{h_{n-1}}^{h_n} dh = -\frac{R}{g_{SL}} \left(\frac{T_{a_n} + T_{a_{n-1}}}{2}\right) \left(\frac{R_e + h_{n-1}}{R_e}\right)^2 \int_{P_{a_{n-1}}}^{P_{a_n}} \frac{dP_a}{P_a} \qquad (24)$$

with the assumptions that the temperature is constant at

$$T_{a_{avg}} = \frac{T_{a_n} + T_{a_{n-1}}}{2}$$

and that

$$\frac{R_e + h}{R_e} = \frac{R_e + h_{n-1}}{R_e}$$

Integrating equation (24)

$$h_n = h_{n-1} + \frac{R}{g_{SL}} \left(\frac{T_{a_n} + T_{a_{n-1}}}{2}\right) \left(\frac{R_e + h_{n-1}}{R_e}\right)^2 \ln \frac{P_{a_{n-1}}}{P_{a_n}} \qquad (25)$$

Geometric altitudes are found by summing increments as indicated by equation (25).

STRUCTURE OF THE ATMOSPHERE

The atmposphere has been broken up into four major regions which are associated with physical characteristics listed in table 3. The names of atmospheric shells and boundaries used in the table have been adopted by the World Meteorological Organization.

Table 3 - Description of Atmospheric Shells

Name	Description
Troposphere	The region nearest the earth's surface having a uniform decrease in temperature with altitude. The troposphere is the domain of weather where turbulence caused by convection occurs. At the tropopause (top of the troposphere) high winds are common and the highest cirrus clouds are found.
Stratosphere	The region above the troposphere having a constant temperature followed by increasing temperatures, reaching a maximum at the stratopause. Maximum of atmospheric ozone is found near the top of this region. Turbulence is infrequent.
Mesosphere	Temperature remains constant with altitude above the stratopause and then decreases. This region is in radiative equilibrium between ultraviolet ozone heating by the upper fringe of ozone region and the infrared ozone and carbon dioxide cooling by radiation to space.
Thermosphere	The region of rising temperature above the major temperature minimum. No upper altitude limit.

COMPARISON OF ATMOSPHERIC MODELS IN RECENT USE

Standard atmospheres which have been used during recent years are:

(1) International Civil Aviation Organization Standard Atmosphere, 1952 adopted by the National Advisory Committee for Aeronautics and published in NACA Report 1235

(2) Air Research and Development Command Model Atmosphere, 1956

(3) U.S. Extension to the ICAO Standard Atmosphere, 1958

(4) ARDC Model Atmosphere, 1959

(5) U.S. Standard Atmosphere, 1962

The International Civil Aviation Organization Standard Atmosphere was adopted by the NACA on November 20, 1952 and is contained in NACA Report 1235, Standard Atmosphere - Tables and Data for Altitudes to 65,800 Feet. The equations of this report were used to extend the tables to 80,000 feet and appear in reference 2. To an altitude of 80,000 feet, the properties such as θ, δ, σ, and a from NACA Report 1235 are identical with those in the ARDC Model Atmosphere, 1956, the U.S. Extension to the ICAO Standard Atmosphere, 1958 and the ARDC Model Atmosphere, 1959.

Some important changes were made in the U.S. Standard Atmosphere, 1962. The principal difference between the U.S.

1962 and previous models is that the altitude at the top of the stratosphere is 65,616.8 geopotential feet in the former and 82,021.0 feet in (2), (3), and (4) from the list above. Above 65,616.8 feet, the U.S. 1962 Atmosphere has a temperature gradient of 0.3048°K/1000 feet as depicted in figure 1.

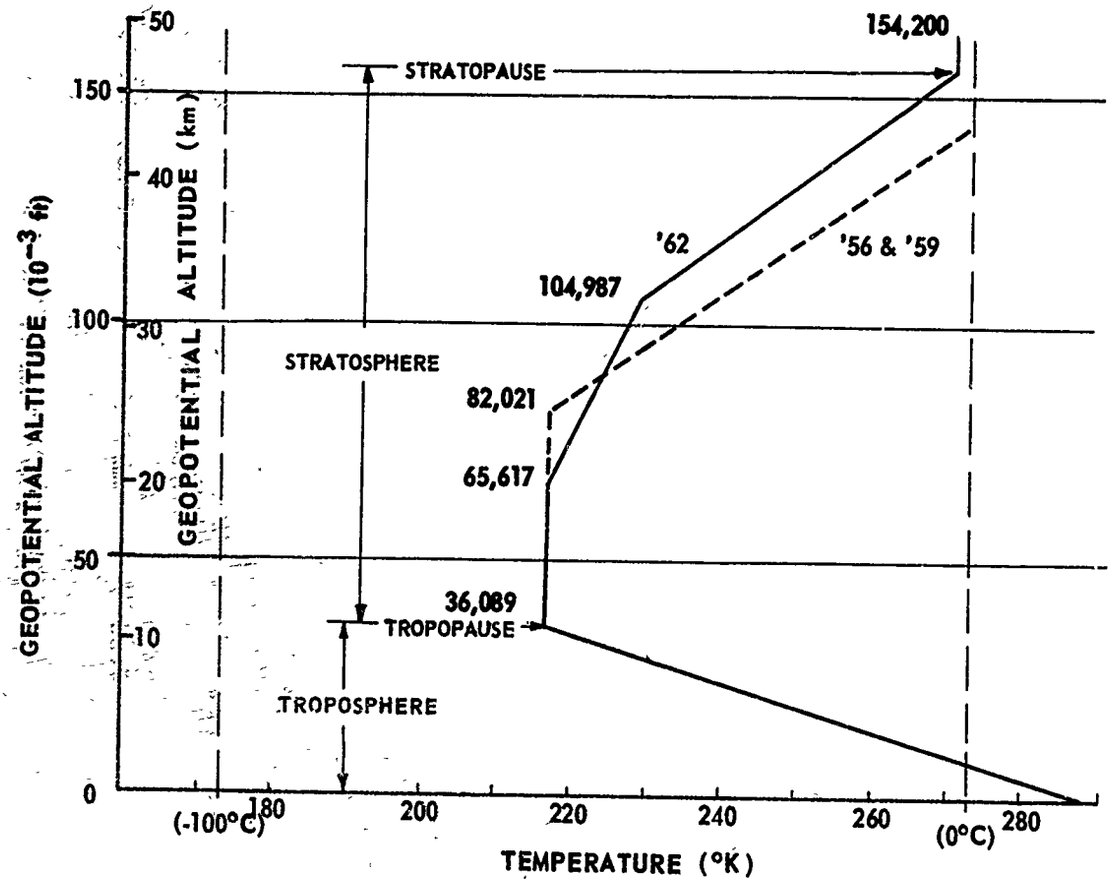

Comparison of Temperature Profiles in Standard Atmospheres

Figure 1

The temperature in the U.S. 1962 atmosphere is 4.4° Kelvin higher at an altitude of 80,000 feet; thus, an airspeed of 700 knots (for example) at this altitude would represent M = 1.208 in the 1962 atmosphere and M =1.220 in the others. The difference in temperature produces differences in tabulated properties at altitudes over 65,000 feet (e.g., θ, δ, etc).

REFERENCES

1. Kolacz, Paul A. Contemplation of the Official Standard Atmosphere, FTC-TIM-68-1003, Air Force Flight Test Center, California, February 1968.
2. Herrington, Russel M, et al. Flight Test Engineering Handbook, AF Technical Report No 6273, Air Force Flight Test Center, California, revised January 1966.
3. King, James J, et al. Aerodynamics Handbook for Performance Flight Testing Vol I, AFFTC-TN-60-28, Air Force Flight Test Center, California, July 1960.
4. Anon, U.S. Standard Atmosphere, 1962, U.S. Government Printing Office, Washington, D.C., December 1962.
5. Anon, Standard Atmosphere - Tables and Data for Altitudes to 65,800 Feet, NACA Report 1235, U.S. Government Printing Office, Washington, D.C., 1955.
6. Minzner, R.A., et al. The ARDC Model Atmosphere, 1959, AFCRC-TR-59-267, Air Force Cambridge Research Center, Bedford, Massachusetts, August 1959.

THIS PAGE LEFT BLANK FOR PRESENTATION PURPOSES

SECTION IV

FLIGHT PARAMETERS FROM SENSED ENVIRONMENT (ON-BOARD STATIC AND TOTAL PRESSURE, AND TOTAL TEMPERATURE)

SUMMARY

The information in this section on airspeeds, temperatures, etc., is similar to that found in other documents (e.g., AF Technical Report 6273, Flight Test Engineering Handbook), but has been included for the sake of completeness and to have a source of basic equations for use in subsequent sections. In addition, an examination has been made of the effects of high speed on the usual assumptions that air obeys the equation of state $P = \rho RT$ and has a constant ratio of specific heats.

TABLE OF CONTENTS

SYMBOLS USED IN THIS SECTION

Symbol	Definition	Units
a	speed of sound	ft/sec
C_L	airplane lift coefficient	dimensionless
g	acceleration due to gravity	ft/sec^2
h	enthalpy	BTU/lb
J	mechanical equivalent of heat	ft-lb/BTU
K	temperature probe recovery factor	dimensionless
M	flight Mach number	dimensionless
ΔM_{pc}	correction to Mach number for position error	dimensionless
n_z	load factor along the z-axis	dimensionless
p_a	ambient pressure	lb/ft^2
p_i	indicated pressure	lb/ft^2
p_s	static pressure	lb/ft^2
p_t	total pressure	lb/ft^2
Δp_p	static pressure source position error	lb/ft^2
q_c	impact pressure	lb/ft^2
R	universal gas constant	$ft^2/sec^2 \cdot K$
S	wing area	ft^2
T_a	ambient temperature	deg K
T_t	total temperature	deg K
V_c	calibrated airspeed	ft/sec
ΔV_c	compressibility correction to calibrated airspeed	ft/sec

Symbol	Definition	Units
V_e	equivalent airspeed	ft/sec
V_t	true airspeed	ft/sec
ΔV_{pc}	correction for airspeed position error	ft/sec
W	airplane gross weight	lb
Z	compressibility factor	dimensionless
α	angle of attack	rad
γ	ratio of specific heats: C_p/C_v	dimensionless
δ_a	ambient pressure ratio	dimensionless
λ	pressure lag constant	sec
μ	absolute viscosity	lb-sec/ft^2
ρ	air density	slugs/ft^3
Subscripts		
ic	indicated corrected for instrument error	
ℓ	corrected for lag	
s	static	
SL	sea level	
t	total	

INTRODUCTION

Pressure altitude, airspeed, Mach number, and free air temperature are basic parameters in the performance of aircraft. Conventional instruments used to measure these quantities are the altimeter, the airspeed indicator, the machmeter, and the free air temperature probe. (Mach numbers deduced from altimeter and airspeed readings are preferred to those from machmeters.) Relationships of the basic parameters to environmental conditions sensed on board an aircraft (static and total pressures, and total temperature) are developed in this section. More comprehensive derivations of equations and descriptions of the construction and calibration of instruments may be found in reference 2. It should be noted that in this reference the usual simplifying assumptions are made (e.g., constant ratio of specific heats). These assumptions lead to errors in calibrated air data when Mach numbers get much above two. Real gas effects as they influence calibrated air data together with equations which may be used at high supersonic and hypersonic speeds are presented in this section.

PRESSURE ALTITUDE

From the general equations relating pressure and altitude (equations (18) and (19) in the section, Atmospheric Environment) we have, after substituting constants appropriate to the U.S. Standard 1962 atmosphere from table 2, for $\delta_a = P_a/P_{a_{SL}}$.

$$\delta_a = (1 - 6.87558 \times 10^{-6} H)^{5.2559} \qquad (1)$$

for $-16{,}404.20 \leq H \leq 36{,}089.24$ geopotential feet

$$\delta_a = 0.223360 \exp[-4.80637 \times 10^{-5}(H - 36089.24)] \qquad (2)$$

for $36{,}089.24 \leq H \leq 65{,}616.80$ geopotential feet

$$\delta_a = 0.0540322[1 + 1.40688 \times 10^{-6}(H - 65.616.80)]^{-34.1634} \qquad (3)$$

for $65{,}616.80 \leq H \leq 104{,}986.88$ geopotential feet

$$\delta_a = 0.00856649[1 + 3.73252 \times 10^{-6}(H - 104{,}986.88)]^{-12.2012} \qquad (4)$$

for $104{,}986.88 \leq H \leq 154{,}199.48$ geopotential feet

Altimeters are built and calibrated according to these relationships (or perhaps to another model atmosphere). Differences in altitude between the various model atmospheres are fairly small (reference 1, pages 13 - 15); however, the standard used for instrument calibration should be known. If laboratory calibrations are made using a model atmosphere other than the one desired, corrections

can be easily made through the general pressure-altitude equations and properties defining the two atmospheres. The static pressure sensed at the static source of the altimeter, P_s, may differ slightly from the atmospheric pressure, P_a, because of pressure lag and position error. These errors are discussed in a later paragraph.

CALIBRATED AIRSPEED

The airspeed indicator senses the difference between two pressures; total pressure, P_t, and static pressure, P_s. The difference in pressure is converted to a speed through Bernoulli's compressible equation for frictionless adiabatic (isentropic) flow in which airspeed is expressed as the difference between total and static pressures. Assuming that $P_s = P_a$, Bernoulli's equation may be expressed as

$$\frac{P_t - P_a}{P_a} = \frac{q_c}{P_a} = \left[1 + \frac{\gamma - 1}{2}\left(\frac{V_t}{a}\right)^2\right]^{\frac{\gamma}{\gamma - 1}} - 1 \qquad (5)$$

for subsonic speeds.

With $\gamma = 1.40$, equation (5) becomes

$$\frac{q_c}{P_a} = \left[1 + 0.2\left(\frac{V_t}{a}\right)^2\right]^{3.5} - 1 \qquad (6)$$

At supersonic speeds a detached shock wave forms in front of the total pressure probe, and equation (5) is no

longer valid. In this case the Rayleigh supersonic pitot formula

$$\frac{q_c}{P_a} = \left[\frac{\gamma+1}{2}\left(\frac{V_t}{a}\right)^2\right]^{\frac{\gamma}{\gamma-1}}\left[\frac{\gamma+1}{1-\gamma+2\gamma\left(\frac{V_t}{a}\right)^2}\right]^{\frac{1}{\gamma-1}} - 1 \qquad (7)$$

relating total pressure behind the shock to the free stream ambient (atmospheric) pressure is used. It should be noted that $q_c = P_t' - P_a$ where the total pressure, P_t', sensed at the pitot head is behind the shock and is not equal to the free stream total pressure, P_t, at supersonic speeds. Substituting 1.40 for γ and simplifying, equation (7) becomes

$$\frac{q_c}{P_a} = \frac{166.921\left(\frac{V_t}{a}\right)^7}{\left[7\left(\frac{V_t}{a}\right)^2 - 1\right]^{2.5}} - 1 \qquad (8)$$

Examination of the above equations shows that true speed, V_t, is dependent on the speed of sound, a, and atmospheric pressure, P_a, in addition to the differential pressure, q_c. Therefore, an airspeed indicator measuring differential pressure can be made to read true airspeed at only one set of atmospheric conditions. Sea level standard has been selected arbitrarily, and the dials of airspeed indicators are scaled so that a given differential pressure will indicate a speed in accordance with equations (6) and (8) in which sea level standard and P_a are inserted. This sea level standard value of V_t is defined as calibrated airspeed, V_c, and is found

from airspeed indicator readings after corrections have been made for instrument and position errors.

Accordingly, equations (6) and (8) may be rewritten as

$$\frac{q_c}{P_{a_{SL}}} = [1 + 0.2(\frac{V_c}{a_{SL}})^2]^{3.5} - 1 \qquad (9)$$

and

$$\frac{q_c}{P_{a_{SL}}} = \frac{166.921(\frac{V_c}{a_{SL}})^7}{[7(\frac{V_c}{a_{SL}})^2 - 1]^{2.5}} - 1 \qquad (10)$$

EQUIVALENT AIRSPEED

The equivalent airspeed, V_e, is the result of correcting the calibrated airspeed for compressibility effects. The airspeed indicator is calibrated to read correctly at standard sea level conditions and thus has a compressibility correction appropriate for these conditions. When an aircraft is operated at altitude, however, the compensation is inadequate and an additional correction must be applied. Hence, V_c and V_e are related by

$$V_c = V_e + \Delta V_c \qquad (11)$$

Equivalent airspeed coupled with standard sea level density produces the same dynamic pressure as the true airspeed (speed relative to the airmass) coupled with the

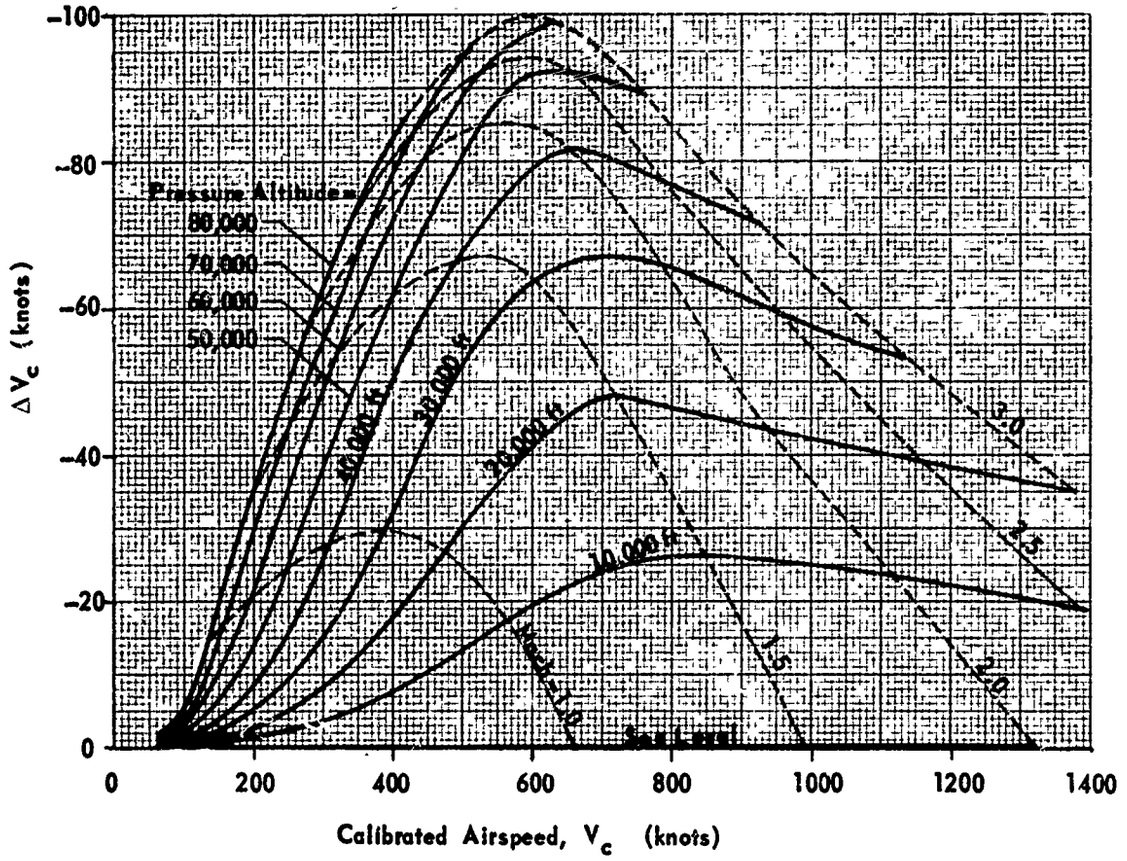

Figure 1 - Compressibility Correction to Calibrated Airspeed

actual air density at flight conditions. Therefore

$$V_t^2 \rho = V_e^2 \rho_{SL} \tag{12}$$

or

$$V_e = V_t \sqrt{\sigma} \tag{13}$$

For subsonic flight, solving equation (5) for V_t^2,

$$V_t^2 = 5a^2[(\frac{q_c}{P_a} + 1)^{2/7} - 1] \tag{14}$$

Combining equations (4) and (5) from the section, Atmospheric Environment, the speed of sound in a perfect gas may be expressed as

$$a = (\frac{\gamma P_a}{\rho})^{1/2} \tag{15}$$

Replacing V_t^2 by V_e^2/σ and $a^2\sigma$ by $\gamma P_a/\rho_{SL}$:

$$V_e = \{\frac{7P_a}{\rho_{SL}}[(\frac{q_c}{P_a} + 1)^{2/7} - 1]\}^{1/2} \tag{16}$$

Solving equation (6) for calibrated airspeed:

$$V_c = \{\frac{7P_{aSL}}{\rho_{SL}}[(\frac{q_c}{P_a} + 1)^{2/7} - 1]\}^{1/2} \tag{17}$$

The difference between equations (16) and (17) is the compressibility correction, ΔV_c, in equation (11). If $P_a = P_{a_{SL}}$ calibrated and equivalent airspeeds are the same and ΔV_c is zero regardless of the magnitude of q_c. Also, ΔV_c can be calculated for any altitude and calibrated airspeed since a value of V_c determines q_c.

MACH NUMBER

Mach number is defined as the ratio of true airspeed to the local speed of sound:

$$M = \frac{V_t}{a} \tag{18}$$

From Bernoulli's equation with isentropic flow of a perfect gas

$$\frac{P_t}{P_a} = (1 + \frac{\gamma - 1}{2} M^2)^{\frac{\gamma}{\gamma - 1}} \tag{19}$$

This equation relates Mach number to free stream total and static pressures and is applicable for supersonic as well as subsonic flight. It should be remembered, however, that P_t' rather than P_t is sensed by a pitot probe in supersonic flight.

Substituting 1.40 for γ, equation (19) becomes

$$\frac{P_t}{P_a} = (1 + 0.2M^2)^{3.5} \tag{20}$$

The machmeter equation for subsonic flight is found by substituting the definition for Mach number in equation (5)

$$\frac{q_c}{P_a} = [1 + \frac{\gamma - 1}{2} M^2]^{\frac{\gamma}{\gamma-1}} - 1 \qquad (21)$$

Solving for M

$$M = [\frac{2}{\gamma - 1}(\frac{q_c}{P_a} + 1)^{\frac{\gamma-1}{\gamma}} - 1]^{1/2} \qquad (22)$$

With $\gamma = 1.40$

$$M = \{5[(\frac{q_c}{P_a} + 1)^{2/7} - 1]\}^{1/2} \qquad (23)$$

For supersonic flight from equation (7)

$$\frac{q_c}{P_a} = (\frac{\gamma + 1}{2} M^2)^{\frac{\gamma}{\gamma-1}} (\frac{\gamma + 1}{1 - \gamma + 2\gamma M^2})^{\frac{1}{\gamma-1}} - 1 \qquad (24)$$

This equation cannot be solved explicitly for Mach number. It can, however, be put in the form

$$M = [\frac{(\frac{q_c}{P_a} + 1)(\gamma + 1) + \gamma - 1}{2\gamma(\frac{\gamma + 1}{2} M^2 \frac{\gamma + 1}{1 - \gamma + 2\gamma M^2})^{\frac{\gamma}{\gamma-1}}}]^{1/2} \qquad (25)$$

which may be solved by iteration.

Substituting 1.40 for γ and rearranging

$$M = [0.7766628(\frac{q_c}{P_a} + 1)(1 - \frac{1}{7M^2})^{5/2}]^{1/2} \quad (26)$$

TOTAL TEMPERATURE

If the air surrounding a temperature probe is brought to a complete stop adiabatically the resulting temperature, T_t, if sensed correctly is

$$T_t = T_a(1 + \frac{\gamma - 1}{2}M^2) \quad (27)$$

For various reasons, such as radiation or heat leakage, most probes do not register the full adiabatic temperature rise. Introducing a probe recovery factor, K, the equation

$$T_t = T_a(1 + K\frac{\gamma - 1}{2}M^2) \quad (28)$$

may be written to account for a lack of complete adiabatic temperature rise. The magnitude of K is between 0.95 and 1.00 for most installations and can often be assumed constant. Variations with altitude and Mach number should be expected, however, particularly at supersonic speeds. Methods for determining K for a given installation are discussed in reference 2.

CALIBRATED AIR DATA AT HIGH SPEEDS

For flight at speeds below Mach 2 it is generally adequate to assume that air behaves as an ideal gas obeying the equation of state $P = \rho RT$ and having a constant ratio

of specific heats taken to be $\gamma = 1.40$. However, at speeds slightly above Mach 2 and for higher Mach numbers this assumption becomes invalid. In general it is necessary to account for real-gas effects where the specific heats are functions of temperature and pressure, and the equation of state must be expanded to include the effects of intermolecular attraction at high densities and dissociation and ionization at high temperatures and low pressures. A general form of the equation of state includes the compressibility factor, Z, as follows

$$P = \rho Z R T \tag{29}$$

Without the assumption of constant specific heats it is impractical to obtain an analytic expression for parameters such as the total temperatures and pressures in front of and behind the shock. A method has been employed to compute these parameters by interpolating air thermodynamic properties from a comprehensive set of tables (reference 3) and computing the total and behind the shock conditions using the conservation equations of mass, momentum, and energy as follows:

$$\rho_2 V_2 = \rho_1 V_1 \tag{30}$$

$$P_2 + \rho_2 V_2^2 = P_1 + \rho_1 V_1^2 \tag{31}$$

$$h_2 + \frac{V_2^2}{2Jg} = h_1 + \frac{V_1^2}{2Jg} = h_t \qquad (32)$$

The free stream temperature, pressure, and density are defined by the ambient conditions at a given altitude, and the ambient enthalpy and entropy can be interpolated from the thermodynamic tables of reference 3. The total enthalpy at each Mach number is given by equation (32), and by definition the total (isentropic) temperature and pressure, T_t and P_t, can be interpolated at this total enthalpy and the ambient entropy.

The static properties behind the shock can be obtained by an iterative solution of equations (29), (30), (31), and (32); and then the entropy behind the shock can be interpolated from the thermodynamic tables. The total temperature and pressure behind the shock, T_t' and P_t' can then be interpolated from the same tables as a function of the total enthalpy and the behind-the-shock entropy.

The values of T_t, P_t, T_t', and P_t' obtained by this method will generally differ from the values given by equations (20), (24) and (27). However, these differences in no way affect the physical operation of the airspeed indicator. Consequently, the definition of differential pressure $q_c = P_t' - P_a$, and the equations for calibrated airspeed, equations (9) and (10) are still applicable. As an

illustration of the real gas effects on the values of T_t and P_t a comparison with the values from the ideal gas equations is presented in figure 2. The real gas temperature ratio diverges from the real gas value immediately above Mach 2. The pressure remains within plus or minus one percent up past Mach 3 but diverges beyond this point. The differences in calibrated airspeed are not as large, being much less than one percent up to Mach 5.

Figure 2 can be used as a tool to decide when the real gas method described here should be used for data reduction. Computer programs have been developed to perform these calculations, and a set of tables of temperature and pressure ratios and calibrated airspeeds has been produced. These are described in reference 4.

ERRORS IN PRESSURE MEASUREMENT

In addition to the usual instrument error, altimeters and airspeed indicators are subject to two additional errors. They are position error and pressure lag error and are discussed in the following paragraphs.

POSITION ERROR

To determine the speed and altitude at which an aircraft is flying, values of dynamic and ambient pressure are required as indicated by the preceding equations.

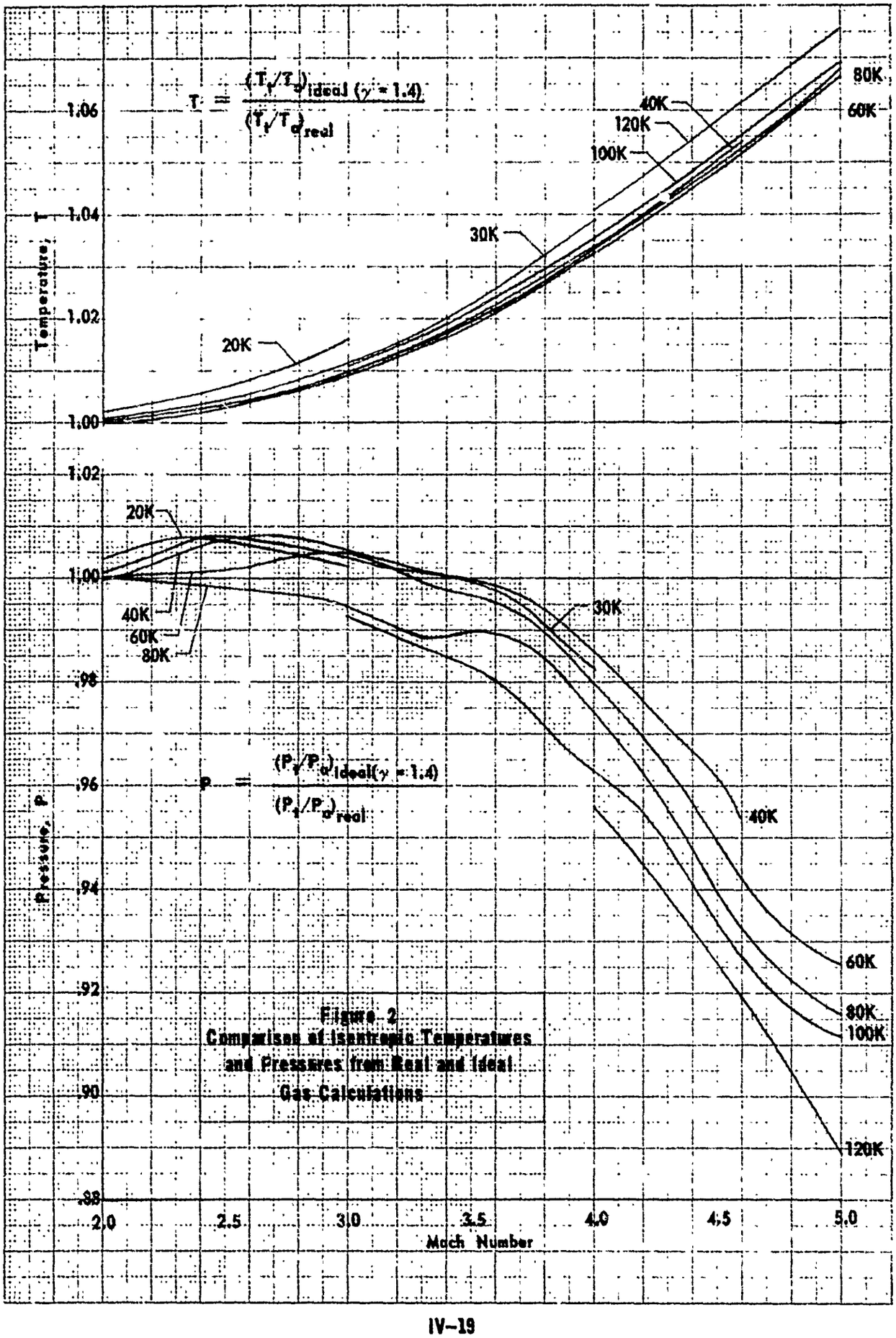

Figure 2
Comparison of Isentropic Temperatures and Pressures from Real and Ideal Gas Calculations

The pressures registered by a pitot-static system will, in general, differ from the desired values. Distortions in flow are caused by the presence of the aircraft and by the system itself; pressure sensors are located in a flow field which is different from the flow field distant from the aircraft. The resulting errors are called position errors.

Total Pressure Error

At subsonic speeds the flow perturbations due to the aircraft static pressure field are very nearly isentropic and hence do not affect the total pressure. Therefore, as long as the total pressure source is not located in a wing wake, in a boundary layer, or in a region of local supersonic flow, the total pressure error due to the position of the total pressure head will usually be negligible.

Nose boom pitot-static systems are installed on supersonic aircraft so that the total pressure pickup will be located ahead of any shock waves formed by the aircraft. The shock wave due to the pickup itself is accounted for by the equation against which airspeed indicators are calibrated (reference equation (10)).

Failure of the total pressure sensor to register the local pressure may result from the shape of the head, inclination of the flow, or burred or misshapen pitot lips. Since pitot-static probes are tested in wind tunnels before intallation to assure good design and commonly used probes produce no significant

errors due to inclination to the relative wind up to approximately 20 degrees, there should be no significant errors in total pressure measurement. In flight test applications it is usually presumed that all of the position error originates in the static pressure source. The possibility of a total pressure error must, however, be considered, and airspeed calibrations should be investigated to find if position errors in total pressure do exist.

Static Pressure Error

The static pressure field surrounding an aircraft in flight is a function of speed and altitude as well as the secondary parameters: angle of attack, Mach number, and Reynolds number. Hence, it is seldom possible to find a location for the static pressure source where the free stream pressure will be sensed under all flight conditions. Therefore, an error in the measurement of the static pressure due to the position of the static pressure source in the aircraft pressure field will generally exist.

At subsonic speeds it is often possible to find some position on the aircraft fuselage where the static pressure error is small under all flight conditions, and flush static ports are usually installed on the fuselages of subsonic aircraft. Nose booms are generally installed on supersonic aircraft to minimize the possibility of total pressure error; static pressure sensed on a boom has the advantage that in

supersonic flight the bow wave formed by the aircraft is downstream of the static pressure ports so that the pressure measured is unaffected by pressure field of the aircraft.

Not considering Reynolds number and assuming that sideslip angles are small, the functional statement

$$\frac{P_s}{P_a} = f(M, \alpha) \tag{33}$$

may be written. Defining the position error, ΔP_p, as

$$\Delta P_p = P_s - P_a \tag{34}$$

equation (33) may be modified to

$$\frac{\Delta P_p}{P_a} = f(M, \alpha) \tag{35}$$

Since q_c/P_a is related to Mach number only, equation (35), in terms of indicated values corrected for instrument error, can be changed to

$$\frac{\Delta P_p}{q_{c_{ic}}} = f(M_{ic}, \alpha_{ic}) \tag{36}$$

or

$$\frac{\Delta P_p}{q_{c_{ic}}} = f(M_{ic}, C_{L_{ic}}) \tag{37}$$

Since M_{ic} is related to $q_{c_{ic}}/P_s$ and a good approximation of lift coefficient is

$$C_{L_{ic}} = \frac{2n_z W}{\delta_{ic} \gamma M_{ic}^2 S P_{a_{SL}}} \tag{38}$$

the position error coefficient may be defined as

$$\frac{\Delta P_p}{q_{c_{ic}}} = f(M_{ic}, \frac{n_z W}{\delta_{ic}}) \tag{39}$$

At low Mach numbers the effects of compressibility on pressure error may be considered negligible and the pressure coefficient assumed to be a function of C_L only.

Since

$$C_L = \frac{n_z W}{\rho_{SL} V_e^2 S/2} \tag{40}$$

and in the low Mach number range $V_c \approx V_e$ it can be assumed that

$$C_{L_{ic}} = \frac{n_z W}{\rho_{SL} V_{ic}^2 S/2} \tag{41}$$

so that

$$\frac{\Delta P_p}{q_{c_{ic}}} = f(\frac{n_z W}{V_{ic}}) \tag{42}$$

For constant $n_z W$

$$\frac{\Delta P_p}{q_{c_{ic}}} = f(V_{ic}) \text{ only} \tag{43}$$

From subsequent derivations of equations (67) and (70) it can be seen that

$$\Delta V_{pc} = f\left(\frac{\Delta P_p}{q_{c_{ic}}}, V_{ic}\right) \tag{44}$$

Since $\Delta P_p/q_{c_{ic}} = f(V_{ic})$ only in the low Mach number range from equation (43)

$$\Delta V_{pc} = f(V_{ic}) \text{ only} \tag{45}$$

for constant $n_z W$ in the absence of Mach number effects.

At higher speeds, when there may be both M_{ic} and $C_{L_{ic}}$ effects, airspeed calibrations may be put in the form $\Delta P_p/q_{c_{ic}}$ or ΔM_{pc} versus M_{ic}. Data from nose booms or wing tip booms will usually form a single line for Mach numbers greater than about 0.6. At lower speeds variation in $n_z W/\delta_{ic}$ may be of consequence especially for large airplanes which have large changes in weight.

For aircraft equipped with nose booms the static pressure error increases very rapidly with Mach number in the vicinity of Mach one. The bow wave passes behind the static ports at

M_{ic} = 1.03 or so, and the pressure error becomes quite small (perhaps zero).

In summary, the form in which data from airspeed calibrations is put depends on the type of airspeed system, speed range, and importance of Mach number and weight effects.

Calculation of Calibrated Airspeed and Calibrated Altitude

The three cases noted below are generally used. Equations for making corrections for position error to both airspeed and altitude are presented for these three cases assuming that no error exists in the total pressure source. With this assumption a common value of ΔP_p is applied to airspeed and to altitude.

Case I:

$$\frac{\Delta P_p}{q_{c_{ic}}} = f(M_{ic}, \frac{n_z W}{\delta_{ic}}) \tag{46}$$

or its alternate

$$\frac{\Delta P_p}{q_{c_{ic}}} = f(M_{ic}, C_{L_{ic}}) \tag{47}$$

$\Delta P_p/q_{c_{ic}}$ is readily found at the test conditions and ΔP_p from

$$\Delta P_p = \frac{\Delta P_p}{q_{c_{ic}}} q_{c_{ic}} \tag{48}$$

where $q_{c_{ic}}$ is computed from the modified form of equation (9).

$$q_{c_{ic}} = P_{a_{SL}}\{[1 + 0.2(\frac{V_{ic}}{a})^2]^{3.5} - 1\} \tag{49}$$

Case II: $\Delta M_{pc} = f(M_{ic})$

By definition

$$\Delta P_p = P_s - P_a \tag{50}$$

which can be written as

$$\frac{\Delta P_p}{P_s} = 1 - \frac{P_a}{P_s} \tag{51}$$

From equation (20) for subsonic flight

$$\frac{\Delta P_p}{P_s} = 1 - \frac{(1 + 0.2M_{ic}^2)^{3.5}}{(1 + 0.2M^2)^{3.5}} \tag{52}$$

Expansion of equation (52) in a Taylor series about M_{ic} through the first two terms produces

$$\frac{\Delta P_p}{P_s} = \frac{1.4M_{ic}\Delta M_{pc}}{1 + 0.2M_{ic}^2} + \frac{0.7(1 - 1.6M_{ic}^2)\Delta M_{pc}^2}{(1 + 0.2M_{ic})^2} \tag{53}$$

From the machmeter equation for supersonic flight

$$\frac{P_t'}{P_s} = \frac{166.921M_{ic}^7}{(7M_{ic}^2 - 1)^{2.5}} \tag{54}$$

and

$$\frac{P_t'}{P_a} = \frac{166.921 M^7}{(7M^2 - 1)^{2.5}} \tag{55}$$

Following the same procedure that was used with the subsonic equations

$$\frac{\Delta P_p}{P_s} = \frac{7(2M_{ic}^2 - 1)\Delta M_{pc}}{M_{ic}(7M_{ic}^2 - 1)} - \frac{7(21M_{ic}^4 - 23.5M_{ic}^2 + 4)\Delta M_{pc}^2}{M_{ic}^2(7M_{ic}^2 - 1)^2} \tag{56}$$

Rewriting equation (6) as

$$\frac{q_{c_{ic}}}{P_s} = (1 + 0.2M_{ic}^2)^{3.5} - 1 \tag{57}$$

and dividing equation (53) by equation (57)

$$\frac{\Delta P_p}{q_{c_{ic}}} = \frac{\dfrac{1.4M_{ic}\Delta M_{pc}}{(1 + 0.2M_{ic}^2)} + \dfrac{0.7(1 - 1.6M_{ic}^2)\Delta M_{pc}^2}{(1 + 0.2M_{ic}^2)^2}}{[(1 + 0.2M_{ic}^2)^{3.5} - 1]} \tag{58}$$

for $M_{ic} \leq 1.0$. The equivalent expression for the supersonic case is obtained by dividing equation (56) by

$$\frac{q_{c_{ic}}}{P_s} = \frac{166.921 M_{ic}^7}{(7M_{ic}^2 - 1)^{2.5}} - 1 \tag{59}$$

which results from equation (8), to give

$$\frac{\Delta P_p}{q_{c_{ic}}} = \frac{\dfrac{7(2M_{ic}^2-1)\Delta M_{pc}}{M_{ic}(7M_{ic}^2-1)} - \dfrac{7(21M_{ic}^4-23.5M_{ic}^2+4)\Delta M_{pc}^2}{M_{ic}^2(7M_{ic}^2-1)^2}}{\left[\dfrac{166.921M_{ic}^7}{(7M_{ic}^2-1)^{2.5}}-1\right]} \tag{60}$$

As for Case I, ΔP_p is determined from

$$\Delta P_p = \frac{\Delta P_p}{q_{c_{ic}}} q_{c_{ic}} \tag{61}$$

requiring equations (59) and (49) for subsonic flight. At supersonic speeds equation (60) and the modified form of equation (10)

$$q_{c_{ic}} = P_{a_{SL}}\left\{\frac{166.921\left(\frac{V_{ic}}{a}\right)^7}{\left[7\left(\frac{V_{ic}}{a}\right)^2-1\right]^{2.5}}-1\right\} \tag{62}$$

are used.

Case III: $\Delta V_{pc} = f(V_{ic})$

From the relationship

$$\Delta P_p = (P_t' - P_a) - (P_t' - P_s) \tag{63}$$

ΔP_p is

$$\Delta P_p = q_c - q_{c_{ic}} = f(V_c) - f(V_{ic}) \tag{64}$$

From equations (9) and (49)

$$\Delta P_p = P_{a_{SL}} \{ [1 + 0.2(\frac{V_c}{a_{SL}})^2]^{3.5} - [1 + 0.2(\frac{V_{ic}}{a_{SL}})^2]^{3.5} \} \tag{65}$$

Expanding equation (65) in a Taylor series through the first two terms and evaluating at $V_c = V_{ic}$

$$\Delta P_p = \frac{1.4 P_{a_{SL}} V_{ic}}{a_{SL}^2} [1 + 0.2(\frac{V_{ic}}{a_{SL}})^2]^{2.5} \Delta V_{pc} + \frac{0.7 P_{a_{SL}}}{a_{SL}^2} [1 + 0.2(\frac{V_{ic}}{a_{SL}})^2]^{1.5} [1 + 1.2(\frac{V_{ic}}{a_{SL}})^2] \Delta V_{pc}^2 \tag{66}$$

or dividing by ΔV_{pc}

$$\frac{\Delta P_p}{\Delta V_{pc}} = \frac{1.4 P_{a_{SL}} V_{ic}}{a_{SL}^2} [1 + 0.2(\frac{V_{ic}}{a_{SL}})^2]^{2.5} + \frac{0.7 P_{a_{SL}}}{a_{SL}^2} [1 + 0.2(\frac{V_{ic}}{a_{SL}})^2]^{1.5} [1 + 1.2(\frac{V_{ic}}{a_{SL}})^2] \Delta V_{pc} \tag{67}$$

Following the same procedure for supersonic flight, from equation (10)

$$\Delta P_p = P_{a_{SL}} \{ \frac{166.921 (\frac{V_c}{a_{SL}})^7}{[7(\frac{V_c}{a_{SL}})^2 - 1]^{2.5}} - \frac{166.921 (\frac{V_{ic}}{a_{SL}})^7}{[7(\frac{V_{ic}}{a_{SL}})^2 - 1]^{2.5}} \} \tag{68}$$

Expanding equation (68) in a Taylor series through the first two terms and evaluating at $V_c = V_{ic}$

$$\Delta P_p = \frac{7 \times 166.921 P_{a_{SL}} \left(\frac{V_{ic}}{a_{SL}}\right)^6}{a_{SL}} \left\{ \frac{2\left(\frac{V_{ic}}{a_{SL}}\right)^2 - 1}{\left[7\left(\frac{V_{ic}}{a_{SL}}\right)^2 - 1\right]^{3.5}} \right\} \Delta V_{pc}$$

$$+ \frac{7 \times 166.921 P_{a_{SL}}}{2} \left(\frac{V_{ic}}{a_{SL}}\right)^5 \frac{\left[14\left(\frac{V_{ic}}{a_{SL}}\right)^4 - 9\left(\frac{V_{ic}}{a_{SL}}\right)^2 + 6\right] \Delta V_{pc}^2}{\left[7\left(\frac{V_{ic}}{a_{SL}}\right)^2 - 1\right]^{4.5}} \quad (69)$$

or dividing by ΔV_{pc}

$$\frac{\Delta P_p}{\Delta V_{pc}} = \frac{1168.45 P_{a_{SL}} \left(\frac{V_{ic}}{a_{SL}}\right)^6}{a_{SL}} \left\{ \frac{2\left(\frac{V_{ic}}{a_{SL}}\right)^2 - 1}{\left[7\left(\frac{V_{ic}}{a_{SL}}\right)^2 - 1\right]^{3.5}} \right\}$$

$$+ \frac{584.224 P_{a_{SL}}}{a_{SL}^2} \left(\frac{V_{ic}}{a_{SL}}\right)^5 \frac{\left[14\left(\frac{V_{ic}}{a_{SL}}\right)^4 - 9\left(\frac{V_{ic}}{a_{SL}}\right)^2 + 6\right] \Delta V_{pc}}{\left[7\left(\frac{V_{ic}}{a_{SL}}\right)^2 - 1\right]^{4.5}} \quad (70)$$

ΔP_p for Case III is found from

$$\Delta P_p = \frac{\Delta P_p}{\Delta V_{pc}} \Delta V_{pc} \quad (71)$$

ΔP_p can be determined as described above for each of the three cases and then used to find both H_c and V_c from H_{ic} and

V_{ic}. To calculate H_c, P_s is first found from the appropriate pressure - altitude relationship (equations (1) through (4)) at H_{ic}. Then ambient pressure is computed from

$$P_a = P_s - \Delta P_p \tag{72}$$

H_c, corresponding to P_a, may then be found through the same pressure - altitude relationships.

V_c may be found in a similar fashion by computing $q_{c_{ic}}$, corresponding to V_{ic}, from equation (49) or equation (62); then impact pressure from

$$q_c = q_{c_{ic}} + \Delta P_p \tag{73}$$

V_c, corresponding to q_c, may be computed from equation (9) or from equation (10) through an iterative method.

PRESSURE LAG ERROR

Pressure gages such as airspeed indicators and altimeters are subject to pressure lag errors when airspeed or altitude are changing. Pressure at the source differs from that registered by a pressure measuring device because of:

(1) pressure drops in tubing resulting from viscous friction between the moving air and the walls of the tubing

(2) inertia of the air in the tubing

(3) pressure drops across orifices and restrictions

(4) acoustic lag, i.e., the time required for a pressure disturbance to travel the length of the tubing, and

(5) instrument damping, inertia, and friction

Since an altimeter is an absolute pressure measuring instrument the effect of lag on indicated altitude readings is fairly obvious. For example, during a climb the indicated altitude tends to be less than the actual altitude; an airspeed indicator, being a differential pressure gage is affected by lags in both total and static pressures so that the error may be either positive or negative.

Since the error in both pressures is in the same direction the net effec on impact pressure and hence calibrated airspeed is compensating. Corrections to altitude are, in general, of more consequence than corrections to airspeed.

From the above list of factors which affect the indicated pressure in an airspeed system it is apparent that a complete mathematical treatment of the response to varying pressure would be prohibitly complex. It has been found, however, that lag can be attributed largely to viscous friction and that the system can be adequately described by the equation

$$\lambda \frac{dP_i}{dt} + P_i = P(t) \qquad (74)$$

where λ is the time by which the indicated pressure lags

behind the source pressure. Use of this equation assumes that

(1) the mass of the air in the system is zero

(2) the rate of change of the applied pressure is nearly constant

(3) laminar flow exists (For this to be true it is necessary that the Reynolds number be less than 2000; in typical airspeed systems a value of 500 is seldom exceeded in flight.)

(4) the pressure lag is small compared with the applied pressure (This is generally the case; however, at very high altitudes this assumption becomes critical.)

(5) the acoustic lag is negligible (This assumption can be easily checked by computing acoustic lag from the length of tubing and the speed of sound in the tubing and comparing it to λ from equation (74)).

(6) the pressure drop across the orifices and restrictions is negligible (This is true only if a minimum of such restrictions exist so that the tubing is nearly a smooth, straight "pipe" of uniform diameter.)

For a constant rate of change of applied pressure, $P(t) = (dP/dt)t$ and equation (74) may be solved as

$$\lambda \frac{dP_i}{dt} + P_i = P \qquad (75)$$

From dimensional analysis it can be shown that, for a particular installation,

$$\lambda \propto \frac{\mu}{P} \tag{76}$$

Hence if the lag constant is obtained at one value of μ/P it may be extrapolated to other values by the expression

$$\frac{\lambda_1}{\lambda_2} = \frac{\mu_1 P_2}{\mu_2 P_1} \tag{77}$$

Usually, experimental data are used to compute a sea level lag constant from which the lag constant at any values of μ and P can be obtained, using the equation

$$\lambda = \lambda_{SL} \frac{\mu}{\mu_{SL}} \frac{P_{SL}}{P} \tag{78}$$

With the lag constants for the static and total pressure systems known, the error in altimeter and airspeed indicator readings due to pressure lag can be calculated for any set of test conditions.

Corrections to Altitude

The lag constant for the static pressure system, λ_s, can be defined from equation (75) as

$$\lambda_s = \frac{P_{s_\ell} - P_s}{dP_{s_\ell}/dt} = \frac{\Delta P_{s_\ell}}{dP_{s_\ell}/dt} \tag{79}$$

With the approximation that $dP_{s_\ell}/dt = dP_s/dt$ equation (79) becomes

$$\lambda_s = \frac{\Delta P_{s_\ell}}{dP_s/dt} \tag{80}$$

From the assumption of hydrostatic equilibrium

$$dP_s = -\rho g dH_{ic} \tag{81}$$

Then from equations (80) and (81) the altimeter lag correction is

$$\Delta H_{ic_\ell} = \lambda_s \frac{dH_{ic}}{dt} \tag{82}$$

Replacing $P_s/P_{a_{SL}}$ with δ_s, equation (78) may be written as

$$\lambda_s = \lambda_{SL} \frac{\mu_{H_{ic}}}{\mu_{SL}} \frac{1}{\delta_s} \tag{83}$$

The altimeter lag correction can be evaluated from the experimentally determined value of λ_{SL}, $\mu_{H_{ic}}/\mu_{SL}$ (a function of temperature from figure 3), δ_s corresponding to H_{ic}, and dH_{ic}/dt the rate of change of observed altitude corrected for instrument error.

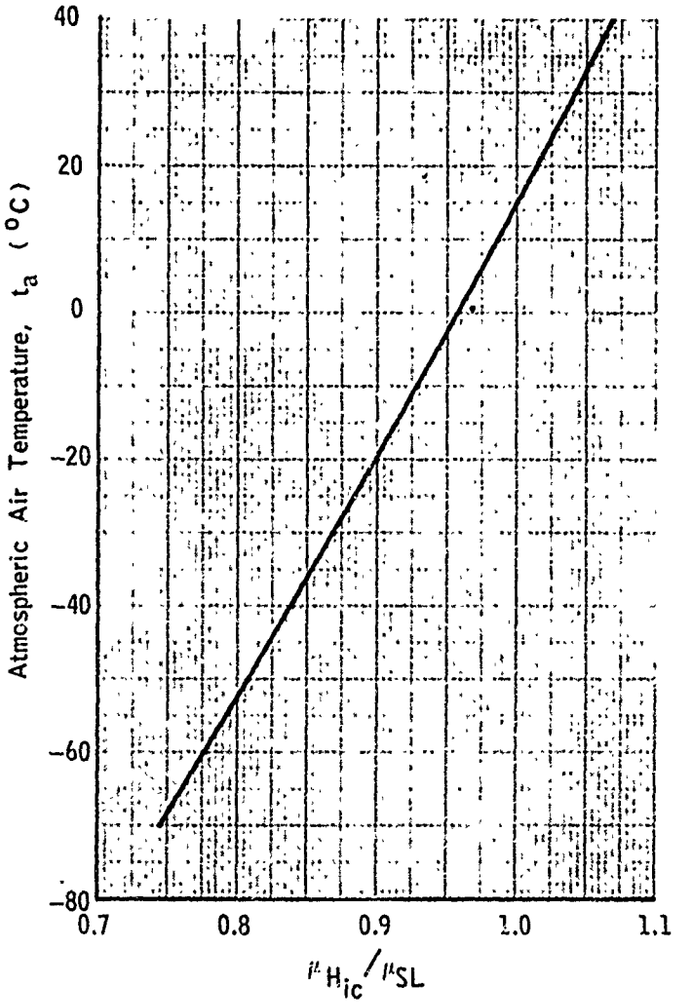

FIGURE 3

The indicated altitude corrected for instrument and lag errors is then

$$H_{ic_\ell} = H_{ic} + \Delta H_{ic_\ell} \qquad (84)$$

Corrections to Airspeed

Lag in both the total and static pressure systems may be accounted for by

$$q_{c_{ic_\ell}} = P_{t_\ell}' - P_{s_\ell} \tag{85}$$

The error in impact pressure due to lag is, by definition

$$\Delta q_{c_{ic_\ell}} = q_{c_{ic_\ell}} - q_{c_{ic}} \tag{86}$$

which may be stated as

$$\Delta q_{c_{ic_\ell}} = (P_{t_\ell}' - P_t') - (P_{s_\ell} - P_s) \tag{87}$$

It follows from equation (75) that

$$\Delta q_{c_{ic_\ell}} = \lambda_t \frac{dP_{t_\ell}'}{dt} - \lambda_s \frac{dP_{s_\ell}}{dt} \tag{88}$$

Differentiating equation (85) with respect to time

$$\frac{dq_{c_{ic_\ell}}}{dt} = \frac{dP_{t_\ell}'}{dt} - \frac{dP_{s_\ell}}{dt} \tag{89}$$

Substituting equation (89) in equation (88)

$$\Delta q_{c_{ic_\ell}} = \lambda_t \frac{dq_{c_{ic_\ell}}}{dt} - (\lambda_s - \lambda_t)\frac{dP_{s_\ell}}{dt} \tag{90}$$

With the approximations

$$\frac{\Delta q_{c_{ic\ell}}}{dt} = \frac{dq_{c_{ic}}}{dt}$$

and

$$\frac{dP_{s_\ell}}{dt} = \frac{dP_s}{dt}$$

equation (90) becomes

$$\Delta q_{c_{ic\ell}} = \lambda_t \frac{dq_{c_{ic}}}{dt} - (\lambda_s - \lambda_t)\frac{dP_s}{dt} \qquad (91)$$

Differentiating equation (81)

$$dP_s = -\rho g\, dH_{ic} \qquad (92)$$

and differentiating the subsonic airspeed equation (equation (49))

$$dq_{c_{ic}} = \frac{1.4 P_{a_{SL}} V_{ic}}{a_{SL}^2}\left[1 + 0.2\left(\frac{V_{ic}}{a_{SL}}\right)^2\right]^{2.5} dV_{ic} \qquad (93)$$

Dividing by dt

$$\frac{dq_{c_{ic}}}{dt} = \frac{1.4 P_{a_{SL}} V_{ic}}{a_{SL}^2}\left[1 + 0.2\left(\frac{V_{ic}}{a_{SL}}\right)^2\right]^{2.5} \frac{dV_{ic}}{dt} \qquad (94)$$

Differentiating equation (88) and substituting together with equations (89) and (90) in equation (87) the airspeed indicator correction expressed as a finite difference is

$$\Delta V_{ic_\ell} = \lambda_t \frac{dV_{ic}}{dt} + \frac{(\lambda_s - \lambda_t)\rho g \frac{dH_{ic}}{dt}}{\frac{1.4 P_{a_{SL}}}{a_{SL}^2} V_{ic}\left[1 + 0.2\left(\frac{V_{ic}}{a_{SL}}\right)^2\right]^{2.5}} \tag{95}$$

for $V_{ic} \leq a_{SL}$

With the supersonic airspeed equation, equation (59)

$$\Delta V_{ic_\ell} = \lambda_t \frac{dV_{ic}}{dt} + \frac{(\lambda_s - \lambda_t)\rho g \frac{dH_{ic}}{dt}}{\frac{3738.11\left(\frac{V_{ic}}{a_{SL}}\right)^6\left[2\left(\frac{V_{ic}}{a_{SL}}\right)^2 - 1\right]}{\left[7\left(\frac{V_{ic}}{a_{SL}}\right)^2 - 1\right]^{3.5}}} . \tag{96}$$

Indicated airspeed corrected for instrument and lag error, V_{ic_ℓ}, may be found from the above equations and

$$V_{ic_\ell} = V_{ic} + \Delta V_{ic_\ell} \tag{97}$$

As in the case of the altimeter, $\lambda_s = \lambda_{SL}(\mu_{H_{ic}}/\mu_{SL})(1/\delta_s)$; similarly

$$\lambda_t = \lambda_{t_{SL}} \frac{\mu_{H_{ic}}}{\mu_{SL}} \frac{P_{a_{SL}}}{P_s + q_{c_{ic}}} \tag{98}$$

REFERENCES

1. Caldwell, Donald M., Jr., Standard Atmospheres for Flight Test, AC-64-5, Flight Research Division Office Memo, Air Force Flight Test Center, California, September 1964.

2. Herrington, Russel M., et. al., Flight Test Engineering Handbook, AF Technical Report No. 6273, Air Force Flight Test Center, California, revised January 1966.

3. Brahinsky, H. S., and Nell, C. A., Tables of Equilibrium Thermodynamic Properties of Air, Volume I. Constant Temperature, Volume II, Constant Pressure, Volume III. Constant Entropy, AEDC-TR-69-89, Volumes I, II, and III, Arnold Engineering Development Center, April 1969.

4. Porter, M. B., Calibrated Air Data at High Speeds, Flight Research Branch Office Memo, Air Force Flight Test Center, California, June 1969.

SECTION V

DETERMINATION OF EXCESS THRUST

SUMMARY

Excess thrust has a number of advantages to recommend it as a basic parameter in defining the performance of an aircraft. For example, corrections in terms of excess thrust, are most easily derived from equations of motion, and procedures common to both climbs and level accelerations may be set up using excess thrust as a basis for arriving at the desired parameters in both cases. Various means of computing excess thrust are available. The advantages and disadvantages of each are discussed, and the equations for computing it are derived in detail.

TABLE OF CONTENTS

LIST OF ILLUSTRATIONS

SYMBOLS USED IN THIS SECTION

Symbol	Definition	Units
a_x, a_y, a_z	components of acceleration	ft per sec^2
A_f	acceleration factor	dimensionless
A_{fE}	acceleration factor associated with energy height	dimensionless
B	roll angle about the airspeed vector	rad
C_{L_α}	$\partial C_L / \partial \alpha$	per rad
D	drag	lb
F_n	net thrust	lb
g_L	local effective acceleration due to gravity	ft per sec^2
g_r	reference acceleration due to gravity	ft per sec^2
g_x, g_y, g_z	components of acceleration of gravity	ft per sec^2
h	tapeline altitude	ft
H_c	pressure altitude	ft
H_E	energy height	ft
$\bar{I}, \bar{j}, \bar{k}$	unit vectors	- - -
i_T	thrust angle of incidence	rad
I_y	moment of inertia about y axis	slug-ft^2
j	$\sqrt{-1}$	dimensionless
J_2, J_3, J_4	coefficients of the zonal harmonics of the earth's gravitational potential	dimensionless
ℓ_v	distance from vane to aircraft cg	ft

L	lift	lb
M	flight Mach number	dimensionless
n_x, n_y, n_z	components of load factor	dimensionless
p	roll rate	rad per sec
p_a	ambient pressure	lb per ft^2
q	pitch rate	rad per sec
$\bar{q}$	dynamic pressure	lb per ft^2
r	local radius of the earth	ft
r	yaw rate	rad per sec
r_o	equatorial radius of the earth	ft
s	Laplace operator	- - -
S_v	characteristic area of vane	ft^2
t	time	sec
V_g	horizontal component of aircraft speed relative to the ground	ft per sec
V_I	inertial speed	ft per sec
V_t	true airspeed	ft per sec
V_w	wind speed	ft per sec
$V_{\omega_\oplus}$	aircraft velocity induced by the earth's rotation	ft per sec
W	airplane gross weight	lb
x, y, z	Cartesian coordinate system (subscripts denote particular axes system)	- - -
α	angle of attack	rad

$\Delta\alpha_{\text{boom bending}}$	change in sensed angle of attack due to boom bending	rad
$\Delta\alpha_q$	change in sensed angle of attack due to pitch rate	rad
$\Delta\alpha_u$	change in sensed angle of attack due to upwash	rad
$\Delta\alpha_\omega$	change in sensed angle of attack due to dynamic lag	rad
γ	flightpath climb angle measured from the geocentric horizontal plane	rad
δ_D	aircraft geodetic latitude	rad
δ_L	aircraft geocentric latitude	rad
ϵ_{ma}	misalinement angle	rad
ζ	damping ratio	dimensionless
$\Delta\lambda_L$	difference between the aircraft longitude and the longitude of the radar coordinate origin	rad
$\mu_\oplus$	product of the universal gravitational constant and the mass of the earth	ft^3 per sec^2
σ	flightpath heading angle measured from true north	rad
σ_g	vehicle ground-track heading angle measured from true north	rad
ϕ	bank angle	rad
ϕ_r	angle between radar X_r-axis and true north	rad
ψ	direction from which the wind blows (from true north)	

ω	frequency	rad per sec
ω_n	undamped natural frequency	rad per sec
ω_w	rotational velocity of wind-axes system	rad per sec
$\omega_\oplus$	angular velocity of the earth	rad per sec

Subscripts

b	body axes
cg	center of gravity
e	geocentric axes
g	local-geocentric axes
ic	indicated corrected for instrument error
m	measured
o	maximum value
r	radar axes
v	vane
w	wind axes

GENERAL DISCUSSION OF THE VARIOUS METHODS

Airplane performance data can be determined by several different methods requiring different instrumentation. These methods, which have received varying degrees of use, are:

a. Airspeed-altitude

b. Accelerometer

c. Position measurement

d. Time history of dynamic pressure

e. Rate of climb indicator connected to total pressure

f. Air temperature thermometer

Methods d, e, and f are described in reference 1 and in Chapter 7 of reference 2 but are excluded from further discussion since they have never received popular acceptance. Of the remaining three, the airspeed-altitude method has been widely used for many years; accelerometers have been used during numerous flight test programs; position measurement (e.g., radar) has been employed in some isolated instances.

The most convenient parameter with which to work in standardizing airplane performance data is excess thrust. Corrections, in terms of excess thrust, are most easily derived from equations of motion. Excess thrust can be related easily to rate of climb, turning performance, and

other performance parameters. Standardization procedures common to both climbs and level accelerations may be set up using test excess thrust as a basis for arriving at the desired standard parameters in both cases. Equations defining test excess thrust are derived in subsequent paragraphs for the three methods, a, b, and c, starting from the same basic equations of motion.

Since the quality of standarized data can be expected to be no better than that of the test data, some observations in regard to the calculation of excess thrust are set down for the three methods. Advantages and disadvantages of each are considered.

AIRSPEED-ALTITUDE METHOD

The bulk of the performance test programs which have been conducted up to the present time have made use of measurements of airspeed, altitude, and time (usually an airspeed indicator, and altimeter, and a clock mounted on a photo-panel) to gather performance data. This method has been in routine use since the early 1950's. Several schemes for processing the data have been tried. The one in most common use in later years for both climbs and accelerations has been to compute total energy as a function of time, then curve fit and differentiate to find rate of change of energy (or excess thrust).

The chief merits of the airspeed-altitude method are (1) the instruments are always available since they are needed on board any test aircraft as a part of its test instrumentation system. Hence "special" instrumentation (viz sensitive accelerometers) or ground based positioning equipment is not needed, and (2) the instruments are very reliable and usually quite consistent in behavior so that relatively little data compared to sensitive accelerometer systems should be lost because of instrument malfunction. Their reliability is also generally superior to that of position measuring equipment since contact with an aircraft is occasionally lost due to excessive range, clouds, etc.

The airspeed-altitude method of calculating excess thrust has been found to be the least accurate of the methods described. (See reference 3, for example). There are several factors which contribute to the inaccuracy of this method, the most important being the errors in determining true airspeed and tapeline rate of climb due to errors in ambient temperature, pressure lag during climbs, readability of instruments, etc. The reason these errors are so important is because excess thrust is computed by differentiating specific energy, E/W (energy height, H_E)

$$\frac{E}{W} = H_E = H + \frac{V_t^2}{2g}$$

and any errors in these parameters are amplified by the differentiation process. Also, the magnitude of the time interval used for curve fitting and differentiating to obtain rates of change of specific energy (and consequently excess thrust) may have a decided bearing on the results. If small intervals are used, spurious variations are introduced into the calculation of excess thrust. On the other hand, when excessively large intervals are used, variations which actually existed are eliminated, or at least reduced in size.

Another disadvantage of the airspeed-altitude method is that corrections for wind gradients are needed which are frequently quite substantial for climbs. In contrast only relatively minor corrections for variations in normal load factor are required to standardize climb performance when using any of the other methods.

As flight speeds and altitudes increase, the accuracy inherent in the airspeed-altitude method becomes worse. Above a Mach number of, say, two, other means of obtaining excess thrust should be used, if possible.

ACCELEROMETER METHOD

Flight tests to evaluate the practicability of measuring longitudinal accelerations by means of a sensitive

accelerometer were conducted in the mid-1950's. (See reference 4.) Sensitive accelerometers were installed in category test aircraft for use as a prime source of performance data starting in the early 1960's. Accuracy of the data recorded during these days was comparable to that acquired with airspeed-altimeter measurements; however, with improvements in accelerometers, installation design, and means of recording, data from accelerometers are at present, decidedly more accurate than that from the airspeed-altitude method.

Two different types of installation have been tried. In the first, a sensitive accelerometer has been mounted on a vane (similar to that used to measure angle of attack) so that the sensitive axis of the accelerometer remains

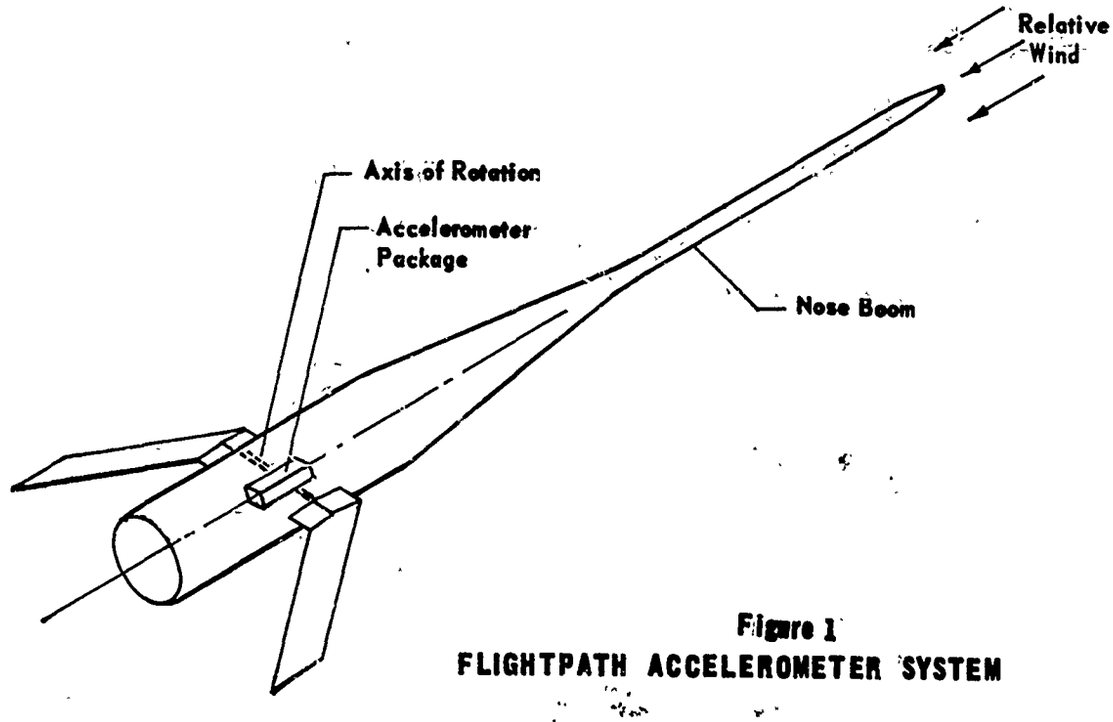

Figure 1
FLIGHTPATH ACCELEROMETER SYSTEM

aligned with the local airflow. Unfortunately, the upwash angle caused by the presence of the pitot head and perhaps the nose of the aircraft is significant, and accurate calibrations must be made in order for the desired component of acceleration along the airplane's velocity vector to be found. Secondary effects which may be of consequence if the pitch angle is changing rapidly are due to pitch rate, pitch accelerations, and dynamic effects causing a lag in the position of the vane. These effects can be expected to be negligible during level accelerations and probably during climbs but may require minor corrections to measured accelerations during roller coaster maneuvers or other tests when pitch rates are high. In the second type of installation, a sensitive accelerometer is hard-mounted at or near the airplane's center of gravity. In this case the location of the sensitive axis of the accelerometer must be very well known. Further, the acceleration must be resolved through the angle of attack and corrections have to be made to it similar to those described for the vane mounted accelerometer.

The most attractive features of the accelerometer method are that load factor, n_x, along the flight path is obtained, after making the corrections and axis transformation described above. The resultant force is the engine

thrust minus the airplane drag (F_{ex}) neither of which are affected greatly by wind gradients. Also, instantaneous values are recorded, and uncertainties incurred by data smoothing and differentiation required by the other methods are avoided.

The reliability of the flightpath accelerometer is better than that of position measuring equipment (radar and Askania camera) since the accelerometer is carried with the aircraft and there is no danger of incomplete flight coverage; however, experience has shown the flightpath accelerometer to be less reliable than the airspeed-altitude instruments.

The most recent accelerometer installations have been a two-axis accelerometer system which measures normal load factor as well as load factor along the flight path. This makes for a considerable improvement in the accuracy of the resultant acceleration along the flight path together with an improved normal load factor for use in the standarization equations.

In addition to one- and two-axis accelerometer systems, three-axis accelerometer data from an inertial navigation system have been used with marked success as a prime source of performance information. Data from a three-axis system

mounted on a stable platform has the considerable advantage that neither upwash angle nor angle of attack need be known if orientation angles to locate the acceleration components are known; they are generally available from on-board computers in aircraft which have inertial navigation systems as standard equipment. Drawbacks to the use of these systems are: additional complexity with attendant maintenance requirements, and need for pre-flight and post-flight checks. Also, operable navigation systems have not been installed, in general, in aircraft used for category performance testing.

POSITION MEASUREMENT METHOD

Radar and Askania camera data have been used to compute performance information in only isolated instances, although both have yielded satisfactory results (reference 3). Since the data from both sources are used in the same way, except for processing of raw data to find position and velocity components, they are discussed together.

The accuracy in both cases depends primarily on the quality of the tracking data, which in turn depends on such factors as number of recording stations, range, elevation angle, etc. As in the airspeed-altitude method, any errors in tracking data are amplified in the differentiation process required to compute excess thrust.

The accuracy inherent in these systems, however, will produce excess thrust of higher quality than will the airspeed-altitude method. A serious disadvantage may be that coverage is not always available, especially for high performance aircraft. Also, data turnaround time may be excessive.

Like the accelerometer method, only slight corrections for wind gradients (for normal load factor) are needed.

Table 1 shows a rating of each method from the standpoint of accuracy, reliability, aircraft equipment required (the least amount being considered best), and data processing effort (least required by engineering personnel considered best).

Table 1 - Comparison of Methods for Calculating Excess Thrust

Rating	Accuracy	Reliability	Aircraft Equipment Required	Data Processing Effort
1	Flight Path Accelerometer	Airspeed-Altitude	Askania	Radar
2	Askania	Flight Path Accelerometer	Radar	Flight Path Accelerometer
3	Radar	Radar	Flight Path Accelerometer	Askania
4	Airspeed-Altitude	Askania	Airspeed-Altitude	Airspeed-Altitude

EQUATIONS OF MOTION

Components of the earth's gravitational attraction taken from the section, Geophysical Properties, are

$$g_{x_g} = -\left(\frac{\mu_\oplus}{r_o^2}\right)\left(\frac{r_o}{r+h}\right)^4\left[3J_2\sin\delta_L - \frac{3}{2}J_3\left(\frac{r_o}{r+h}\right)\left(1-5\sin^2\delta_L\right) - \frac{5}{2}J_4\left(\frac{r_o}{r+h}\right)^2\left(3-7\sin^2\delta_L\right)\sin\delta_L\right]\cos\delta_L \qquad (1)$$

and

$$g_{z_g} = \left(\frac{\mu_\oplus}{r_o^2}\right)\left(\frac{r_o}{r+h}\right)^2\left[1+\frac{3}{2}J_2\left(\frac{r_o}{r+h}\right)\left(1-3\sin^2\delta_L\right) + 2J_3\left(\frac{r_o}{r+h}\right)^3\left(3-5\sin^2\delta_L\right)\sin\delta_L - \frac{5}{8}J_4\left(\frac{r_o}{r+h}\right)^4\left(3-30\sin^2\delta_L+35\sin^4\delta_L\right)\right] \qquad (2)$$

in a north-, geocentrically-directed system. Because of the earth's equatorial bulge, g_{x_g} is always pointed toward the equator (i.e., toward the south in the northern hemisphere and toward the north in the southern hemisphere). g_{y_g} is assumed to be zero and g_{z_g} is directed toward the earth's center. By transforming these components of gravitational attraction through the angles σ, γ, and B, the resultant along the velocity vector is found. The longitudinal equation of motion in the wind-axes system

is, then, for the general case in banked flight

$$F_n \cos(\alpha + i_T) - D - \frac{W}{g_r}\left(g_{Z_g} \sin\gamma - g_{X_g} \cos\gamma \cos\sigma\right) = \frac{W}{g_r} a_{X_W} \tag{3}$$

Similarly, in the lateral direction we have

$$\frac{W}{g_r}\left[g_{X_g}(-\cos B \sin\sigma + \sin B \sin\gamma \cos\sigma)\right] + g_{Z_g} \sin B \cos\gamma = \frac{W}{g_r} a_{Y_W} \tag{4}$$

As pointed out in deriving a_{Y_W} (equation (47)), the lateral acceleration tends to produce a sideslip but that effects on aircraft performance can be safely ignored.

The normal equation of motion in the direction of the lift is

$$L + F_n \sin(\alpha + i_T) - \frac{W}{g_r}\left[g_{X_g}(\sin B \sin\sigma + \cos B \sin\gamma \cos\sigma) + g_{Z_g} \cos B \cos\gamma\right] = \frac{W}{g_r}(-a_{Z_W}) \tag{5}$$

In most flight tests the bank angle is kept small and can be assumed to be zero. For this case the longitudinal and normal equations reduce to

$$F_n \cos(\alpha + i_T) - D - \frac{W}{g_r}\left(g_{Z_g} \sin\gamma - g_{X_g} \cos\gamma \cos\sigma\right) = \frac{W}{g_r} a_{X_W} \tag{6}$$

and

$$L + F_n \sin(\alpha + i_T) - \frac{W}{g_r}(g_{Z_g}\cos\gamma + g_{X_g}\sin\gamma\cos\sigma) \tag{7}$$

It is convenient to combine gravitational attraction and aircraft acceleration by defining load factors along the airspeed vector and along the lift vector. Accelerometers sense these load factors directly. Along the airspeed vector the load factor is

$$n_{X_w} = \frac{1}{g_r}(g_{Z_g}\sin\gamma - g_{X_g}\cos\gamma\cos\sigma + a_{X_w}) \tag{8}$$

In the vertical direction along the lift vector, the load factor is

$$n_{Z_w} = \frac{1}{g_r}(g_{Z_g}\cos\gamma + g_{X_g}\sin\gamma\cos\sigma - a_{Z_w}) \tag{9}$$

Equations (6) and (7) may then be rewritten as

$$F_n\cos(\alpha + i_T) - D = n_{X_w} W \tag{10}$$

and

$$L + F_n\sin(\alpha + i_T) = n_{Z_w} W \tag{11}$$

AIRSPEED-ALTITUDE METHOD

Precise derivations of equations are made which may be used with on-board measurements of airspeed and altitude to give excess thrust. The magnitude of some of the terms is quite small, and considering the inaccuracies in conventional instruments, they may be safely eliminated. If, however, improved instrumentation becomes available, use of the precise equations may be found desirable.

DERIVATION OF GENERAL EQUATIONS

Inertial Velocity in Wind-Axes System

Referring to figure 4 in the section, Coordinate Systems and Transformations, the inertial velocity may be expressed as

$$\bar{V}_I = \bar{V}_t + \bar{V}_{\omega_\oplus} + \bar{V}_w \tag{12}$$

In the wind-axes system the airspeed, $\bar{V}_t$, is $V_t\bar{i}$. Performing transformations, first through the angle σ, then through γ and B, the velocity due to the earth's rotation is

$$[V_{\omega_\oplus}] = [M]\begin{bmatrix} 0 \\ \omega_\oplus(r+h)\cos\delta_L \\ 0 \end{bmatrix} \tag{13}$$

where $$[M] = \begin{bmatrix} 1 & 0 & 0 \\ 0 & \cos B & \sin B \\ 0 & -\sin B & \cos B \end{bmatrix}\begin{bmatrix} \cos\gamma & 0 & -\sin\gamma \\ 0 & 1 & 0 \\ \sin\gamma & 0 & \cos\gamma \end{bmatrix}\begin{bmatrix} \cos\sigma & \sin\sigma & 0 \\ -\sin\sigma & \cos\sigma & 0 \\ 0 & 0 & 1 \end{bmatrix}$$

The product of the matrices composing [M] is shown in equation (15) of the section, Coordinate Systems and Transformations. In expanded form equation (2) becomes

$$\bar{V}_{\omega_\oplus} = \omega_\oplus (r+h)\cos\delta_L [\cos\gamma \sin\sigma\, \bar{i} + (\sin\gamma \sin\sigma \sin B + \cos\sigma \cos B)\bar{j} + (\sin\gamma \sin\sigma \cos B - \cos\sigma \sin B)\bar{k}] \tag{14}$$

The velocity due to local winds as obtained from rawinsonde data is found by making transformation through the angles σ, γ, and B, as above so that

$$[V_w] = [M] \begin{bmatrix} -V_w \cos\psi \\ -V_w \sin\psi \\ 0 \end{bmatrix} \tag{15}$$

Expanding as before

$$\begin{aligned} V_w = {} & [-V_w \cos\psi \cos\gamma \cos\sigma - V_w \sin\psi \cos\gamma \sin\sigma]\bar{i} + [-V_w \cos\psi (\sin\gamma \cos\sigma \sin B - \sin\sigma \cos B) \\ & - V_w \sin\psi (\sin\gamma \sin\sigma \sin B + \cos\sigma \cos B)]\bar{j} + [-V_w \cos\psi (\cos\sigma \sin\gamma \cos B + \sin\sigma \sin B) \\ & - V_w \sin\psi (\sin\gamma \sin\sigma \cos B - \cos\sigma \sin B)]\bar{k} \end{aligned} \tag{16}$$

Equation (16) may be simplified to become

$$\begin{aligned} \bar{V}_w = {} & -V_w \{\cos\gamma \cos(\psi - \sigma)\bar{i} + [\sin\gamma \sin B \cos(\psi - \sigma) + \cos B \sin(\psi - \sigma)]\bar{j} \\ & + [\sin\gamma \cos B \cos(\psi - \sigma) - \sin B \sin(\psi - \sigma)]\bar{k}\} \end{aligned} \tag{17}$$

Adding terms as indicated by equation (12) the inertial velocity in the wind-axes system becomes

$$\begin{aligned}\bar{V}_I = {} & [V_t - V_w\cos\gamma\cos(\psi-\sigma) + \omega_\oplus(r+h)\cos\delta_L\cos\gamma\sin\sigma]\bar{i} + \Big\{-V_w[\sin\gamma\sin B\cos(\psi-\sigma) \\ & + \cos B\sin(\psi-\sigma)] + \omega_\oplus(r+h)\cos\delta_L(\sin\gamma\sin\sigma\sin B + \cos\sigma\cos B)\Big\}\bar{j} \\ & + \Big\{-V_w[\sin\gamma\cos B\cos(\psi-\sigma) - \sin B\sin(\psi-\sigma)] \\ & + \omega_\oplus(r+h)\cos\delta_L(\sin\gamma\sin\sigma\cos B - \cos\sigma\sin B)\end{aligned} \tag{18}$$

where the earth's radius, r, from equation (5) in section Geophysical Properties, is

$$r = 20.925781\times10^6(0.99832172 + .00167616\cos2\delta_L + .00000211\cos4\delta_L) \tag{19}$$

Inertial Accelerations in Wind-Axes System

Since accelerations must be expressed in an inertial system so they can be related to changes in excess thrust, the following equation is used:

$$\bar{a}_{\substack{\text{inertial}\\\text{system}}} = \left.\frac{d\bar{V}_I}{dt}\right|_{\substack{\text{wind-axes}\\\text{system}}} + \bar{\omega}_{\substack{\text{wind-axes}\\\text{system}}} \times \bar{V}_I \tag{20}$$

First, the term $\left.\frac{d\bar{V}_I}{dt}\right|_{\substack{\text{wind-axes}\\\text{syetem}}}$ is evaluated by expressing the velocity in the wind-axes sytem as

$$\bar{V}_I = V_x\bar{i} + V_y\bar{j} + V_z\bar{k} \tag{21}$$

The acceleration becomes

$$\left.\frac{d\bar{V}_I}{dt}\right|_w = \dot{V}_x\bar{i} + \dot{V}_y\bar{j} + \dot{V}_z\bar{k} \tag{22}$$

which may be found by differentiating equation (18):

$$\begin{aligned}\dot{V}_x = {} & \dot{V}_t - \dot{V}_w\cos\gamma\cos(\psi-\sigma) + V_w[\dot{\gamma}\sin\gamma\cos(\psi-\sigma) + (\dot{\psi}-\dot{\sigma})\cos\gamma\sin(\psi-\sigma)] \\ & + \omega_\oplus(r+h)\cos\delta_L\cos\gamma\sin\sigma + \omega_\oplus(r+h)(-\dot{\delta}_L\sin\delta_L\cos\gamma\sin\sigma - \dot{\gamma}\cos\delta_L\sin\gamma\sin\sigma \\ & + \dot{\sigma}\cos\delta_L\cos\gamma\cos\sigma)\end{aligned} \tag{23}$$

$$\begin{aligned}\dot{V}_y = {} & -\dot{V}_w[\sin\gamma\sin B\cos(\psi-\sigma) + \cos B\sin(\psi-\sigma)] - V_w[\dot{\gamma}\cos\gamma\sin B\cos(\psi-\sigma) \\ & + \dot{B}\sin\gamma\cos B\cos(\psi-\sigma) - (\dot{\psi}-\dot{\sigma})\sin\gamma\sin B\sin(\psi-\sigma) - \dot{B}\sin B\sin(\psi-\sigma) \\ & + (\dot{\psi}-\dot{\sigma})\cos B\cos(\psi-\sigma)] + \omega_\oplus(r+h)\cos\delta_L(\sin\gamma\sin\sigma\sin B + \cos\sigma\cos B \\ & - \omega_\oplus(r+h)\dot{\delta}_L\sin\delta_L(\sin\gamma\sin\sigma\sin B + \cos\sigma\cos B) + \omega_\oplus(r+h)\cos\delta_L(\dot{\gamma}\cos\gamma\sin\sigma\sin B \\ & + \dot{\sigma}\sin\gamma\cos\sigma\sin B + \dot{B}\sin\gamma\sin\sigma\cos B - \dot{\sigma}\sin\sigma\cos B - \dot{B}\cos\sigma\sin B)\end{aligned} \tag{24}$$

$$\begin{aligned}\dot{V}_z = {} & -\dot{V}_w[\sin\gamma\cos B\cos(\psi-\sigma) - \sin B\sin(\psi-\sigma)] - V_w[\dot{\gamma}\cos\gamma\cos B\cos(\psi-\sigma) \\ & - \dot{B}\sin\gamma\sin B\cos(\psi-\sigma) - (\dot{\psi}-\dot{\sigma})\sin\gamma\cos B\sin(\psi-\sigma) - \dot{B}\cos B\sin(\psi-\sigma) \\ & - (\dot{\psi}-\dot{\sigma})\sin B\cos(\psi-\sigma)] + \omega_\oplus(r+h)\cos\delta_L(\sin\gamma\sin\sigma\cos B - \cos\sigma\sin B) \\ & - \omega_\oplus(r+h)\dot{\delta}_L\sin\delta_L(\sin\gamma\sin\sigma\cos B - \cos\sigma\sin B) + \omega_\oplus(r+h)\cos\delta_L(\dot{\gamma}\cos\gamma\sin\sigma\cos B \\ & + \dot{\sigma}\sin\gamma\cos\sigma\cos B - \dot{B}\sin\gamma\sin\sigma\sin B + \dot{\sigma}\sin\sigma\sin B - \dot{B}\cos\sigma\cos B)\end{aligned} \tag{25}$$

If no rate of roll exists,* as may be expected during performance flight testing, $\dot{B}$, may be set equal to zero and equations (24) and (25) reduced to the following:

$$\dot{V}_y = -\dot{V}_w[\sin\gamma\sin B\cos(\psi-\sigma) + \cos B\sin(\psi-\sigma)] - V_w[\dot{\gamma}\cos\gamma\sin B\cos(\psi-\sigma) - (\dot{\psi}-\dot{\sigma})\sin\gamma\sin B\sin(\psi-\sigma) + (\dot{\psi}-\dot{\sigma})\cos B\cos(\psi-\sigma)] + \omega_\oplus(r+h)\cos\delta_L(\sin\gamma\sin\sigma\sin B + \cos\sigma\cos B) - \omega_\oplus(r+h)\dot{\delta}_L\sin\delta_L(\sin\gamma\sin\sigma\sin B + \cos\sigma\cos B) + \omega_\oplus(r+h)\cos\delta_L(\dot{\gamma}\cos\gamma\sin\sigma\sin B + \dot{\sigma}\sin\gamma\cos\sigma\sin B - \dot{\sigma}\sin\sigma\cos B) \quad (26)$$

$$\dot{V}_z = -\dot{V}_w[\sin\gamma\cos B\cos(\psi-\sigma) - \sin B\sin(\psi-\sigma)] - V_w[\dot{\gamma}\cos\gamma\cos B\cos(\psi-\sigma) - (\dot{\psi}-\dot{\sigma})\sin\gamma\cos B\sin(\psi-\sigma) - (\dot{\psi}-\dot{\sigma})\sin B\cos(\psi-\sigma)] + \omega_\oplus(r+h)\cos\delta_L(\sin\gamma\sin\sigma\cos B - \cos\sigma\sin B) - \omega_\oplus(r+h)\dot{\delta}_L\sin\delta_L(\sin\gamma\sin\sigma\cos B - \cos\sigma\sin B) + \omega_\oplus(r+h)\cos\delta_L(\dot{\gamma}\cos\gamma\sin\sigma\cos B + \dot{\sigma}\sin\gamma\cos\sigma\cos B + \dot{\sigma}\sin\sigma\sin B) \quad (27)$$

Next, referring back to equation (20), it is necessary to define the rotational velocity of the wind-axes system. This is first determined in the north, east, down system, denoted by the subscript g:

$$\bar{\omega}_w = [(\omega_\oplus + \dot{\lambda})\cos\delta_L - \dot{\gamma}\sin\sigma]\bar{i}_g + (\dot{\gamma}\cos\sigma - \dot{\delta}_L)\bar{j}_g + [\dot{\sigma} - (\omega_\oplus + \dot{\lambda})\sin\delta_L]\bar{k}_g \quad (28)$$

---

*$\dot{B}$ has no influence on a_{x_w}, a_{y_w}, or a_{z_w}. This can be shown by retaining terms which contain $\dot{B}$ in equations (23) and (25) as well as in subsequent equations which define $\bar{\omega}_w$. All terms containing $\dot{B}$ then vanish due to cancellation of terms.

with the rotational velocity due to a rate of roll set equal to zero.

Transforming, as before, to the wind-axes system

$$\begin{bmatrix} \omega_{w_x} \\ \omega_{w_y} \\ \omega_{w_z} \end{bmatrix} = [M] \begin{bmatrix} (\omega_\oplus + \dot{\lambda})\cos\delta_L - \dot{\gamma}\sin\sigma \\ \dot{\gamma}\cos\sigma - \dot{\delta}_L \\ \dot{\sigma} - (\omega_\oplus + \dot{\lambda})\sin\delta_L \end{bmatrix} \tag{29}$$

Performing the matrix multiplication

$$\omega_{w_x} = [(\omega_\oplus + \dot{\lambda})\cos\delta_L - \dot{\gamma}\sin\sigma]\cos\gamma\cos\sigma + [\dot{\gamma}\cos\sigma - \dot{\delta}_L]\cos\gamma\sin\sigma - [\dot{\sigma} - (\omega_\oplus + \dot{\lambda})\sin\delta_L]\sin\gamma \tag{30}$$

$$\omega_{w_y} = [(\omega_\oplus + \dot{\lambda})\cos\delta_L - \dot{\gamma}\sin\sigma](\sin\gamma\cos\sigma\sin B - \sin\sigma\cos B) + (\dot{\gamma}\cos\sigma - \dot{\delta}_L)(\sin\gamma\sin\sigma\sin B + \cos\sigma\cos B) + [\dot{\sigma} - (\omega_\oplus + \dot{\lambda})\sin\delta_L]\cos\gamma\sin B \tag{31}$$

$$\omega_{w_z} = [(\omega_\oplus + \dot{\lambda})\cos\delta_L - \dot{\gamma}\sin\sigma](\cos\sigma\sin\gamma\cos B + \sin\sigma\sin B) + (\dot{\gamma}\cos\sigma - \dot{\delta}_L)(\sin\gamma\sin\sigma\cos B - \cos\sigma\sin B) + [\dot{\sigma} - (\omega_\oplus + \dot{\lambda})\sin\delta_L]\cos\gamma\cos B \tag{32}$$

Simplifying equations (30), (31) and (32) we have

$$\omega_{w_x} = (\omega_\oplus + \dot{\lambda})(\cos\delta_L\cos\gamma\cos\sigma + \sin\delta_L\sin\gamma) - \dot{\delta}_L\cos\gamma\sin\sigma - \dot{\sigma}\sin\gamma \tag{33}$$

$$\omega_{w_y} = (\omega_\oplus + \dot{\lambda})(\cos\delta_L \sin\gamma\cos\sigma \sin B - \cos\delta_L \sin\sigma \cos B - \sin\delta_L \cos\gamma \sin B) + \dot{\gamma}\cos B$$
$$- \dot{\delta}_L(\sin\gamma\sin\sigma \sin B + \cos\sigma \cos B) + \dot{\sigma}\cos\gamma\sin B \qquad (34)$$

$$\omega_{w_z} = (\omega_\oplus + \dot{\lambda})(\cos\delta_L \cos\sigma \sin\gamma\cos B + \cos\delta_L \sin\sigma \sin B - \sin\delta_L \cos\gamma\cos B) - \dot{\gamma}\sin B$$
$$- \dot{\delta}_L(\sin\gamma\sin\sigma \cos B - \cos\sigma \sin B) + \dot{\sigma}\cos\gamma\cos B \qquad (35)$$

Again referring back to equation (20), to evaluate the acceleration due to the rotation of the wind-axes system we have

$$\bar{\omega}_w \times \bar{V}_I = \begin{bmatrix} \bar{i} & \bar{j} & \bar{k} \\ \omega_{w_x} & \omega_{w_y} & \omega_{w_z} \\ V_x & V_y & V_z \end{bmatrix} \qquad (36)$$

Components of acceleration are

$$a_{\omega_x} = \omega_{w_y} V_z - \omega_{w_z} V_y \qquad (37)$$

$$a_{\omega_y} = \omega_{w_z} V_x - \omega_{w_x} V_z \qquad (38)$$

$$a_{\omega_z} = \omega_{w_x} V_y - \omega_{w_y} V_x \qquad (39)$$

Substituting terms from equations (18), (30), (31), and (32) we have

$$a_{\omega_x} = \omega_\oplus(\omega_\oplus + \dot{\lambda})(r + h)(\cos\delta_L \sin\delta_L \cos\gamma\cos\sigma - \cos^2\delta_L \sin\gamma) - V_w(\omega_\oplus + \dot{\lambda})[\cos\gamma \sin(\psi - \sigma)\sin\delta_L$$
$$- \sin\gamma\cos\delta_L \sin\psi] + \dot{\gamma}\omega_\oplus(r + h)\cos\delta_L \sin\gamma\sin\sigma - \dot{\sigma}\omega_\oplus(r + h)\cos\delta_L \cos\gamma\cos\sigma$$
$$- \dot{\gamma} V_w \sin\gamma\cos(\psi - \sigma) + \dot{\delta} V_w \sin\gamma\cos\psi + V_w \dot{\sigma}\cos\gamma \sin(\psi - \sigma) \qquad (40)$$

$$a_{\omega_y} = V_t(\omega_\oplus + \dot{\lambda})(\cos\delta_L \cos\sigma \sin\gamma\cos B + \cos\delta_L \sin\sigma \sin B - \sin\delta_L \cos\gamma\cos B) - V_t\dot{\gamma}\sin B$$
$$- V_t\dot{\delta}_L(\sin\gamma\sin\sigma\cos B - \cos\sigma \sin B) + V_t\dot{\sigma}\cos\gamma\cos B + V_w(\omega_\oplus + \dot{\lambda})[\cos(\psi - \sigma)\sin\delta_L \cos B$$
$$- \cos\gamma\cos\delta_L \sin\psi\sin B - \sin\gamma\sin(\psi - \sigma)\sin\delta_L \sin B] + V_w\dot{\gamma}\cos\gamma\cos(\psi - \sigma)\sin B$$
$$- V_w\dot{\delta}_L\cos\gamma\cos\psi\sin B - V_w\dot{\sigma}[\cos(\psi - \sigma)\cos B - \sin\gamma\sin(\psi - \sigma)\sin B]$$
$$+ \omega_\oplus(\omega_\oplus + \dot{\lambda})(r + h)[-\sin\sigma\cos\delta_L \sin\delta_L \cos B + \cos\gamma\cos^2\delta_L \sin B + \sin\gamma\cos\sigma\cos\delta_L \sin\delta_L \sin B]$$
$$- \dot{\gamma}\omega_\oplus(r + h)\cos\gamma\sin\sigma\cos\delta_L \sin B + \dot{\sigma}\omega_\oplus(r + h)(\sin\sigma\cos\delta_L \cos B - \sin\gamma\cos\sigma\cos\delta_L \sin B) \qquad (41)$$

$$a_{\omega_z} = -V_t[(\omega_\oplus + \dot{\lambda})(\cos\delta_L \sin\gamma\cos\sigma\sin B - \cos\delta_L \sin\sigma\cos B - \sin\delta_L \cos\gamma\sin B) + \dot{\gamma}\cos B$$
$$- \dot{\delta}_L(\sin\gamma\sin\sigma\sin B + \cos\sigma\cos B) + \dot{\sigma}\cos\gamma\sin B] - V_w(\omega_\oplus + \dot{\lambda})[\cos\gamma\sin\psi\cos\delta_L \cos B$$
$$+ \cos(\psi - \sigma)\sin\delta_L \sin B + \sin\gamma\sin(\psi - \sigma)\sin\delta_L \cos B] + \omega_\oplus(\omega_\oplus + \dot{\lambda})(r + h)\cos\delta_L(\cos\gamma\cos\delta_L \cos B$$
$$+ \sin\sigma\sin\delta_L \sin B + \sin\gamma\cos\sigma\sin\delta_L \cos B) - V_w\dot{\delta}_L\cos\gamma\cos\psi\cos B + V_w\dot{\sigma}[\cos(\psi - \sigma)\sin B$$
$$+ \sin\gamma\sin(\psi - \sigma)\cos B] + V_w\dot{\gamma}\cos\gamma\cos(\psi - \sigma)\cos B - \dot{\gamma}\omega_\oplus(r + h)\cos\gamma\sin\sigma\cos\delta_L \cos B$$
$$- \dot{\sigma}\omega_\oplus(r + h)\cos\delta_L(\sin\sigma\sin B + \sin\gamma\cos\sigma\cos B) \qquad (42)$$

To obtain total accelerations in the $\bar{I}$, $\bar{j}$, and $\bar{k}$, directions, as indicated by equation (20), we combine terms as follows:

$$a_{x_w} = \dot{V}_x + a_{\omega_x} \tag{43}$$

$$a_{y_w} = \dot{V}_y + a_{\omega_y} \tag{44}$$

$$a_{z_w} = \dot{V}_z + a_{\omega_z} \tag{45}$$

From equations (23) and (40)

$$\begin{aligned} a_{x_w} = {} & \dot{V}_t - \dot{V}_w \cos\gamma \cos(\psi - \sigma) + V_w \dot{\psi} \cos\gamma \sin(\psi - \sigma) + \omega_\oplus (r + h) \cos\delta_L \cos\gamma \sin\sigma \\ & - \omega_\oplus (r + h) \dot{\delta}_L \sin\delta_L \cos\gamma \sin\sigma + V_w \dot{\delta}_L \sin\gamma \cos\psi - V_w (\omega_\oplus + \dot{\lambda}) [\cos\gamma \sin(\psi - \sigma) \sin\delta_L \\ & - \sin\gamma \cos\delta_L \sin\psi] + \omega_\oplus (\omega_\oplus + \dot{\lambda}) (r + h) (\cos\delta_L \sin\delta_L \cos\gamma \cos\sigma - \cos^2\delta_L \sin\gamma) \end{aligned} \tag{46}$$

Combining equations (24) and (41)

$$\begin{aligned} a_{y_w} = {} & V_t (\omega_\oplus + \dot{\lambda}) (\cos\delta_L \cos\sigma \sin\gamma \sin B + \cos\delta_L \sin\sigma \sin B - \sin\delta_L \cos\gamma \cos B) \cdot\cdot V_t \dot{\gamma} \sin B \\ & - V_t \dot{\delta}_L (\sin\gamma \sin\sigma \cos B - \cos\sigma \sin B) + V_t \dot{\sigma} \cos\gamma \cos B + V_w (\omega_\oplus + \dot{\lambda}) [\cos(\psi - \sigma) \sin\delta_L \cos B \\ & - \cos\gamma \cos\delta_L \sin B \sin\psi - \sin\gamma \sin(\psi - \sigma) \sin\delta_L \sin B] - V_w \dot{\delta}_L \cos\gamma \cos\psi \sin B \\ & - \dot{V}_w [\sin\gamma \sin B \cos(\psi - \sigma) + \cos B \sin(\psi - \sigma)] + V_w \dot{\psi} [\sin\gamma \sin(\psi - \sigma) \sin B \\ & - \cos(\psi - \sigma) \cos B] + [\omega_\oplus (r + h) \cos\delta_L - \omega_\oplus (r + h) \dot{\delta}_L \sin\delta_L] (\sin\gamma \sin\sigma \sin B + \cos\sigma \cos B \\ & + \omega_\oplus (\omega_\oplus + \dot{\lambda}) (r + h) (-\sin\sigma \cos\delta_L \sin\delta_L \cos B + \cos\gamma \cos^2\delta_L \sin B + \sin\gamma \cos\sigma \cos\delta_L \sin\delta_L \sin B) \end{aligned} \tag{47}$$

Equations (25) and (42) yield

$$a_{Z_W} = -V_t\dot{\gamma}\cos B + V_t\dot{\delta}_L(\sin\gamma\sin\sigma\sin B + \cos\sigma\cos B) - V_t\dot{\sigma}\cos\gamma\sin B - V_t(\omega_\oplus + \dot{\lambda})(\sin\gamma\cos\sigma\cos\delta_L\sin B$$
$$- \sin\sigma\cos\delta_L\cos B - \cos\gamma\sin\delta_L\sin B) - \dot{V}_w[\sin\gamma\cos(\psi - \sigma)\cos B - \sin(\psi - \sigma)\sin B]$$
$$+ V_w\dot{\psi}[\sin\gamma\sin(\psi - \sigma)\cos B + \cos(\psi - \sigma)\sin B] - V_w(\omega_\oplus + \dot{\lambda})[\cos\gamma\sin\psi\cos\delta_L\cos B$$
$$+ \cos(\psi - \sigma)\sin\delta_L\sin B + \sin\gamma\sin(\psi - \sigma)\sin\delta_L\cos B] + \omega_\oplus(r + h)\cos\delta_L(\sin\gamma\sin\sigma\cos B$$
$$- \cos\sigma\sin B) - \omega_\oplus(r + h)\dot{\delta}_L\sin\delta_L(\sin\gamma\sin\sigma\cos B - \cos\sigma\sin B) + \omega_\oplus(\omega_\oplus + \dot{\lambda})(r + h)\cos\delta_L \cdot$$
$$\cdot(\cos\gamma\cos\delta_L\cos B + \sin\sigma\sin\delta_L\sin B + \sin\gamma\cos\sigma\sin\delta_L\cos B) - V_w\dot{\delta}_L\cos\gamma\cos\psi\cos B \qquad (48)$$

The lateral acceleration, a_{y_w}, will tend to produce a sideslip, the magnitude of which will depend on the aerodynamic characteristics of the airplane. The resulting increase in drag, even in extreme cases, will be slight, and the effect of a_{y_w} on aircraft performance can be safely ignored.

Equations (46) and (48) may be modified to more easily compute accelerations in the x_w and z_w directions based on on-board measurements of airspeed and altitude. In doing this the parameters $\dot{V}_w$, $\dot{\psi}$, $\dot{\delta}_L$, and $\dot{\lambda}$ will be replaced by more basic quantities.

In the preceding derivations accelerations have been expressed in terms of parameters in a geocentric reference

system. The flightpath climb angle in a geodetic reference system, however, is desired. From equation (9) of the section, Geophysical Properties,

$$\delta_L = \delta_D - 0.19323889 \sin 2\delta_D \qquad (49)$$

with angles expressed in degrees. Equation (49) can then be used to relate the geocentric and geodetic flightpath climb angles by an extension of the relation illustrated in figure 2.

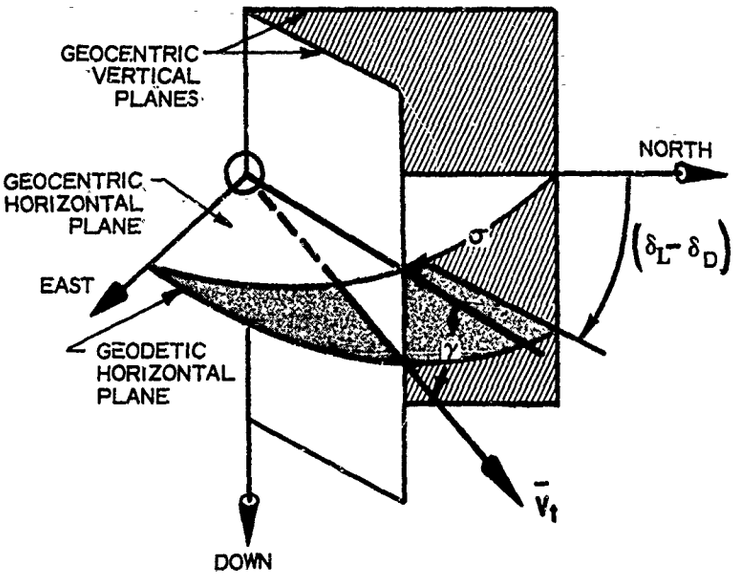

Figure 2 GEOCENTRIC FLIGHTPATH ANGLE FOR GEODETIC HORIZONTAL FLIGHT

$$\gamma = \gamma_D + (\delta_L - \delta_D)\cos\sigma \tag{50}$$

or substituting equation (49)

$$\gamma = \gamma_D - 0.19323889 \sin 2\delta_D \cos\sigma \tag{51}$$

The inverse equation for geodetic climb angle is

$$\gamma_D = \gamma + 0.19323889 \sin 2\delta_D \cos\sigma \tag{52}$$

where the geodetic latitude, δ_D, can be replaced by the geocentric latitude, δ_L, with little loss in accuracy.

From the definitions of geocentric and geodetic climb angles the following equations for rate of climb are

$$\dot{h} = V_t \sin\gamma_D \tag{53}$$

and

$$\dot{h} + \dot{r} = V_t \sin\gamma \tag{54}$$

Next, the ground speed may be expressed as

$$\bar{V}_g = (V_t \cos\gamma \cos\sigma - V_w \cos\psi)\bar{i}_g + (V_t \cos\gamma \sin\sigma - V_w \sin\psi)\bar{j}_g \quad (55)$$

The heading angle of an airplane's ground track, σ_g, is then

$$\sigma_g = \tan^{-1} \frac{V_t \cos\gamma \sin\sigma - V_w \sin\psi}{V_t \cos\gamma \cos\sigma - V_w \cos\psi} \quad (56)$$

which may be used to evaluate the rates of change of latitude and longitude.

$$\dot{\delta}_L = \frac{V_g \cos\sigma_g}{r + h} \quad (57)$$

and

$$\dot{\lambda} = \frac{V_g \sin\sigma_g}{(r + h)\cos\delta_L} \quad (58)$$

In the preceding derivations leading to a_{x_w} and a_{z_w} (equations (46) and (48)) winds have been specified in a

geocentric reference system. As an aid in the following development it will be assumed that the wind can be considered either geocentrically or geodetically horizontal without error. The wind speed and wind direction derivatives may then be expressed through chain differentiation as

$$\dot{V}_w = \frac{dV_w}{dh}\dot{h} = \frac{dV_w}{dh} V_t \sin\gamma_D \tag{59}$$

and

$$\dot{\psi} = \frac{d\psi}{dh}\dot{h} = \frac{d\psi}{dh} V_t \sin\gamma_D \tag{60}$$

The geodetic climb angle can be replaced by a geocentric climb angle in keeping with the assumption noted above.

Introducing these expressions into equations (46) and (48) we obtain directly

$$
\begin{aligned}
a_{x_w} = {} & \dot{V}_t - \frac{dV_w}{dh} V_t \sin\gamma_D \cos\gamma \cos(\psi - \sigma) + V_w \frac{d\psi}{dh} V_t \sin\gamma_D \cos\gamma \sin(\psi - \sigma) \\
& + \omega_\oplus V_t \sin\gamma \cos\gamma \cos\delta_L \sin\sigma - \omega_\oplus (r+h) \frac{V_g \cos\sigma_g}{(r+h)} \sin\delta_L \cos\gamma \sin\sigma \\
& + V_w \frac{V_g \cos\sigma_g}{r+h} \sin\gamma \cos\psi - V_w [\omega_\oplus + \frac{V_g \sin\sigma_g}{(r+h)\cos\delta_L}] \cdot \\
& \cdot [\cos\gamma \sin(\psi - \sigma) \sin\delta_L - \sin\gamma \cos\delta_L \sin\psi] \\
& + \omega_\oplus [\omega_\oplus + \frac{V_g \sin\sigma_g}{(r+h)\cos\delta_L}] (r+h)(\cos\delta_L \sin\delta_L \cos\gamma \cos\sigma \\
& - \cos^2\delta_L \sin\gamma).
\end{aligned} \tag{61}
$$

and

$$
\begin{aligned}
a_{z_w} = {} & - V_t \dot{\gamma} \cos B + V_t \frac{V_g \cos\sigma_g}{r+h} (\sin\gamma \sin\sigma \sin B + \cos\sigma \cos B) \\
& - V_t \dot{\sigma} \cos\gamma \sin B - V_t (\omega_\oplus + \frac{V_g \sin\sigma_g}{(r+h)\cos\delta_L}) (\sin\gamma \cos\sigma \cos\delta_L \sin B \\
& - \sin\sigma \cos\delta_L \cos B - \cos\gamma \sin\delta_L \sin B) \\
& - \frac{dV_w}{dh} V_t \sin\gamma_D [\sin\gamma \cos(\psi - \sigma) \cos B - \sin(\psi - \sigma) \sin B] \\
& + V_w \frac{d\psi}{dh} V_t \sin\gamma_D [\sin\gamma \sin(\psi - \sigma) \cos B + \cos(\psi - \sigma) \sin B] \\
& - V_w [\omega_\oplus + \frac{V_g \sin\sigma_g}{(r+h)\cos\delta_L}] [\cos\gamma \sin\psi \cos\delta_L \cos B - \cos(\psi - \sigma) \sin B \\
& + \sin\gamma \sin(\psi - \sigma) \sin\delta_L \cos B] + \omega_\oplus V_t \sin\gamma \cos\delta_L (\sin\gamma \sin\sigma \cos B \\
& - \cos\sigma \sin B) - \omega_\oplus (r+h) \frac{V_g \sin\sigma_g}{r+h} \sin\delta_L (\sin\gamma \sin\sigma \cos B - \cos\sigma \sin B) \\
& + \omega_\oplus (\omega_\oplus + \frac{V_g \sin\sigma_g}{(r+h)\cos\delta_L}) (r+h) \cos\delta_L (\cos\gamma \cos\delta_L \cos B + \sin\sigma \sin\delta_L \sin B \\
& + \sin\gamma \cos\sigma \sin\delta_L \cos B) - V_w \frac{V_g \cos\sigma_g}{(r+h)}
\end{aligned} \tag{62}
$$

By combining terms, substituting trigonometric identities, and rearranging, equation (50) is reduced to

$$
\begin{aligned}
a_{x_w} = \; & \dot{V}_t - \frac{V_t}{2}\sin 2\gamma\left[\frac{dV_w}{dh}\cos(\psi - \sigma) - V_w\frac{d\psi}{dh}\sin(\psi - \sigma)\right] \\
& + \frac{V_w V_g}{r+h}\left[\sin\gamma\cos(\psi - \sigma_g) - \cos\gamma\tan\delta_L\sin(\psi - \sigma)\sin\sigma_g\right] \\
& - \omega_\oplus(V_g\sin\sigma_g - V_t\cos\gamma\sin\sigma)\sin\gamma\cos\delta_L + \omega_\oplus V_g\sin\delta_L\cos\gamma\sin(\sigma_g - \sigma) \\
& - \omega_\oplus V_w\left[\cos\gamma\sin\delta_L\sin(\psi - \sigma) - \sin\gamma\cos\delta_L\sin\psi\right] \\
& + \omega_\oplus^2(r+h)(\cos\delta_L\sin\delta_L\cos\gamma\cos\sigma - \cos^2\delta_L\sin\gamma) \qquad (63)
\end{aligned}
$$

where γ_D was replaced by γ in the wind gradient terms.

In most cases the bank angle is kept small, and it can be assumed that $\sin\gamma = 0$ and $\cos\gamma = 1$. With this assumption equation (62) can be reduced by combining terms, making substitutions for trigonometric identities, and rearranging to

$$
\begin{aligned}
a_{z_w} = \; & -V_t\dot{\gamma} - V_t\sin^2\gamma\left[\frac{dV_w}{dh}\cos(\psi - \sigma) - V_w\frac{d\psi}{dh}\sin(\psi - \sigma)\right] \\
& + \frac{V_t V_g}{r+h}\cos(\sigma_g - \sigma) - \frac{V_w V_g}{r+h}\cos\gamma\cos(\psi - \sigma_g) \\
& + \sin\gamma\tan\delta_L\sin(\psi - \sigma)\sin\sigma_g\Big] \\
& + \omega_\oplus\cos\delta_L\left[V_t\sin\sigma + (V_t\sin^2\gamma\sin\sigma + V_g\cos\gamma\sin\sigma_g)\right] \\
& - \omega_\oplus V_w\left[\cos\gamma\sin\psi\cos\delta_L + \sin\gamma\sin(\psi - \sigma)\sin\delta_L\right] \\
& + \omega_\oplus V_g\sin\gamma\sin\delta_L\sin(\sigma_g - \sigma) \\
& + \omega_\oplus^2(r+h)(\cos\gamma\cos^2\delta_L + \sin\gamma\cos\delta_L\sin\delta_L\cos\sigma) \qquad (64)
\end{aligned}
$$

where γ_D was again replaced by γ in the wind gradient terms.

The terms containing the products $[\omega_\oplus V_w]$, $[\omega_\oplus (V_g \sin\sigma_g - V_t \cos\gamma \sin\sigma)]$ and $[\omega_\oplus V_g \sin(\sigma_g - \sigma)]$ in equations (20) and (21) can be neglected with little error. If they are dropped the equations reduce to

$$\begin{aligned} a_{x_w} = {} & \dot{V}_t - \frac{V_t}{2} \sin 2\gamma \left[\frac{dV_w}{dh} \cos(\psi - \sigma) - V_w \frac{d\psi}{dh} \sin(\psi - \sigma) \right] \\ & + \frac{V_w V_g}{r + h} \left[\sin\gamma \cos(\psi - \sigma_g) + \cos\gamma \tan\delta_L \sin(\psi - \sigma) \sin\sigma_g \right] \\ & + \omega_\oplus^2 (r + h)(\cos\delta_L \cos\gamma \cos\sigma - \cos^2\delta_L \sin\gamma) \end{aligned} \tag{65}$$

and

$$\begin{aligned} a_{z_w} = {} & - V_t \dot{\gamma} - V_t \sin^2\gamma \left[\frac{dV_w}{dh} \cos(\psi - \sigma) - V_w \frac{d\psi}{dh} \sin(\psi - \sigma) \right] \\ & + \frac{V_t V_g}{r + h} \cos(\sigma_g - \sigma) - \frac{V_w V_g}{r + h} \left[\cos\gamma \cos(\psi - \sigma_g) \right. \\ & \left. + \sin\gamma \tan\delta_L \sin(\psi - \sigma) \sin\sigma_g \right] \\ & + \omega_\oplus \cos\delta_L \left[V_t \sin\sigma + (V_t \sin^2\gamma \sin\sigma + V_g \cos\gamma \sin\sigma_g) \right] \\ & + \omega_\oplus^2 (r + h)(\cos\gamma \cos^2\delta_L + \sin\gamma \cos\delta_L \sin\delta_L \cos\sigma) \end{aligned} \tag{66}$$

ENERGY HEIGHT

In the early days of aviation, a climb amounted chiefly to increasing an airplane's potential energy with changes in kinetic energy being quite small in comparison. As

maximum speeds of airplanes increased, particularly after turbojet engines came into being, it became common practice to account for changes in kinetic energy when computing instantaneous rates of climb and determining "best climb" schedules. The concept of energy height (frequently called specific energy) was introduced by German engineers during World War II and gained world-wide acceptance in dealing with the performance of aircraft powered by turbojet engines.

Energy height is found quite simply by considering the total energy to be the sum of the potential and kinetic energies. That is

$$E = \text{Total energy} = WH_c + \frac{WV_t^2}{2g_r} \tag{67}$$

where total energy is arbitrarily referenced to $H_c = 0$ and $V_t = 0$. H_c is used to compute potential energy, recalling that geopotential altitude is equivalent to the amount of work done in raising a unit mass from mean sea level to a geometric altitude of h. Energy height is, then, the total energy per pound (in the English system) of weight. Thus

$$H_E = H_c + \frac{V_t^2}{2g_r} \tag{68}$$

which is independent of aircraft mass. In its classical form energy height has been defined as $h + V_t^2/2g$; however, when using a model atmosphere in which geopotential rather than geometric altitude is employed, H_c in geopotential feet should be used as a measure of potential energy. Energy height is useful in optimizing climb performance. It is energy height which must be gained mostly rapidly (rather than altitude) to minimize time to climb since potential and kinetic energies are readily interchangeable. Also, energy height has been used (reference the section Standard Climb Schedules) as an independent variable in "optimum" schedules during which altitude is not monotonic increasing. Differentiating equation (68) we have

$$\dot{H}_E = \dot{H}_c + \frac{V_t}{g_r}\dot{V}_t \tag{69}$$

It should be noted that accelerations arising from variations in wind and from the earth's rotation as seen in equation (46), for example, are not accounted for in equation (69).

As in equation (10) of the section Atmospheric Environment

$$g_r\, dH_c = g_L\, dh \tag{70}$$

so that equation (69) may be rewritten as

$$\dot{H}_E = \frac{g_L}{g_r}\dot{h} + \frac{V_t}{g_r}\dot{V}_t \tag{71}$$

LOAD FACTORS

The accelerations from equations (65) and (66) are substituted into equations (8) and (9) to obtain general equations to describe load factors in terms of geocentric parameters. The gravitational and centrifugal relief terms are grouped together:

$$\begin{aligned} n_{x_w} = \frac{1}{g_r}\Big\{ & [g_{z_g} - \omega_\oplus^2 (r+h)\cos^2\delta_L]\sin\gamma \\ & - [g_{x_g} - \omega_\oplus^2 (r+h)\cos\delta_L \sin\delta_L]\cos\gamma\cos\sigma \\ & + \dot{V}_t - \frac{V_t}{2}\sin 2\gamma\left[\frac{dV_w}{dh}\cos(\psi - \sigma) - V_w\frac{d\psi}{dh}\sin(\psi - \sigma)\right] \\ & + \frac{V_w V_g}{r+h}[\sin\gamma\cos(\psi - \sigma_g) + \cos\gamma\tan\delta_L\sin(\psi - \sigma)\sin\sigma_g]\Big\} \end{aligned} \tag{72}$$

and

$$\begin{aligned} n_{z_w} = \frac{1}{g_r}\Big\{ & [g_{z_g} - \omega_\oplus^2 (r+h)\cos^2\delta_L]\cos\gamma \\ & + [g_{x_g} - \omega_\oplus^2 (r+h)\cos\delta_L\sin\delta_L]\sin\gamma\cos\sigma \\ & + V_t\dot{\gamma} + V_t\sin^2\gamma\left[\frac{dV_w}{dh}\cos(\psi - \sigma) - V_w\frac{d\psi}{dh}\sin(\psi - \sigma)\right] \\ & - \frac{V_t V_g}{r+h}\cos(\sigma_g - \sigma) + \frac{V_w V_g}{r+h}[\cos\gamma\cos(\psi - \sigma_g) \\ & + \sin\gamma\tan\delta_L\sin(\psi - \sigma)\sin\sigma_g] - \omega_\oplus\cos\delta_L[V_t\sin\sigma \\ & + (V_t\sin^2\gamma\sin\sigma + V_g\cos\gamma\sin\sigma_g)]\Big\} \end{aligned} \tag{73}$$

where the geocentric components of the acceleration due to gravitational attraction (g_{x_g} and g_{z_g}) are computed from equations (1) and (2).

With zero wind equations (72) and (73) reduce to

$$n_{x_w} = \frac{1}{g_r}\left\{[g_{z_g} - \omega_\oplus^2(r+h)\cos^2\delta_L]\sin\gamma - [g_{x_g} - \omega_\oplus^2(r+h)\cos\delta_L\sin\delta_L]\cos\gamma\cos\sigma + \dot{V}_t\right\} \quad (74)$$

and

$$n_{z_w} = \frac{1}{g_r}\left\{[g_{z_g} - \omega_\oplus^2(r+h)\cos^2\delta_L]\cos\gamma + [g_{x_g} - \omega_\oplus^2(r+h)\cos\delta_L\sin\delta_L]\sin\gamma\cos\sigma + V_t\dot{\gamma} - \frac{V_t^2}{r+h}\cos\gamma - 2\omega_\oplus V_t\cos\delta_L\sin\sigma\right\} \quad (75)$$

Since the local centrifugally relieved acceleration due to gravity is approximately normal to the geoid, equations (72) through (75) can be rewritten including the total resultant gravity vector, g_L:

$$n_{z_w} = \frac{1}{g_r}\left\{g_L\sin\gamma_D + \dot{V}_t - \frac{V_t}{2}\sin 2\gamma\left[\frac{dV_w}{dh}\cos(\psi - \sigma) - V_w\frac{d\psi}{dh}\sin(\psi - \sigma)\right] + \frac{V_w V_g}{r+h}[\sin\gamma\cos(\psi - \sigma_g) + \cos\gamma\tan\delta_L\sin(\psi - \sigma)\sin\sigma_g]\right\} \quad (76)$$

and

$$n_{z_w} = \frac{1}{g_r}\left\{g_L \cos\gamma_D + V_t\dot{\gamma} + V_t\sin^2\gamma\left[\frac{dV_w}{dh}\cos(\psi - \sigma) - V_w\frac{d\psi}{dh}\sin(\psi - \sigma)\right] - \frac{V_t V_g}{r+h}\cos(\sigma_g - \sigma) + \frac{V_w V_g}{r+h}\left[\cos\gamma\cos(\psi - \sigma_g) + \sin\gamma\tan\delta_L\sin(\psi - \sigma)\sin\sigma_g\right] - \omega_\oplus\cos\delta_L\left[V_t\sin\sigma + (V_t\sin^2\gamma\sin\sigma + V_g\cos\gamma\sin\sigma_g)\right]\right\} \quad (77)$$

For zero wind

$$n_{x_w} = \frac{1}{g_r}(g_L\sin\gamma_D + \dot{V}_t) \quad (78)$$

and

$$n_{z_w} = \frac{1}{g_r}\left(g_L\cos\gamma_D + V_t\dot{\gamma} - \frac{V_t^2}{r+h}\cos\gamma - 2\omega_\oplus V_t\cos\delta_L\sin\sigma\right) \quad (79)$$

The load factors of equations (72) through (75) are not exactly equal to those computed with equations (76) through (79) because of the approximations in the derivations including neglect of the differences in the roll and heading angles of an aircraft when referenced to the geocentric instead of the geodetic horizontal plane.

It is frequently convenient to relate the longitudinal load factor, n_{x_w}, to energy height. This may be

done as follows: by rearranging equation (69) and substituting equation (33) we have

$$g_r \frac{\dot{H}_E}{V_t} = g_L \sin\gamma_D + \dot{V}_t \tag{80}$$

Since the right hand side of this equation appears in equations (76) and (78), the left hand side can be introduced into these equations to produce

$$n_{x_w} = \frac{\dot{H}_E}{V_t} + \frac{1}{g_r}\left\{-\frac{V_t}{2}\sin 2\gamma\left[\frac{dV_w}{dh}\cos(\psi - \sigma) - V_w \frac{d\psi}{dh}\sin(\psi - \sigma)\right]\right.$$
$$\left. + \frac{V_w V_g}{r+h}\left[\sin\gamma\cos(\psi - \sigma_g) + \cos\gamma\tan\delta_L \sin(\psi - \sigma)\sin\sigma_g\right]\right\} \tag{81}$$

and for zero wind

$$n_{x_w} = \frac{\dot{H}_E}{V_t} \tag{82}$$

ACCELERATION FACTORS

Equation (71) can be rearranged to produce equations for geometric rate of climb, $\dot{h}$, in terms of either altitude or energy height. Two different acceleration factors result. First, expanding $\dot{V}_t$ by the chain rule, assuming $\dot{h} \neq 0$, equation (71) becomes

$$\dot{H}_E = \frac{g_L}{g_r}\dot{h} + \frac{V_t}{g_r}\frac{dV_t}{dh}\dot{h} \tag{83}$$

Solving for $\dot{h}$

$$\dot{h} = \frac{\dot{H}_E}{\frac{g_L}{g_r}(1 + \frac{V_t}{g_L}\frac{dV_t}{dh})} \tag{84}$$

The denominator is defined as the acceleration factor, A_f, and is used with any of the continuous climbs described in the section, Standard Climb Schedules.

$$A_f = \frac{g_L}{g_r}(1 + \frac{V_t}{g_L}\frac{dV_t}{dh}) \tag{85}$$

With no wind, this provides the following equation for rate of climb using equation (82)

$$\dot{h} = \frac{n_{x_w} V_t}{A_f} \tag{86}$$

The second acceleration factor is useful when climb data are standardized at constant energy height (reference option 4, page 9, Appendix I). Again expanding $\dot{V}_t$ in equation (71) but assuming $\dot{H}_E \neq 0$

$$\dot{H}_E = \frac{g_L}{g_r}\dot{h} + \frac{V_t}{g_r}\frac{dV_t}{dH_E}\dot{H}_E \qquad (87)$$

Solving for $\dot{h}$

$$\dot{h} = \frac{g_r}{g_L}\left(1 - \frac{V_t}{g_r}\frac{dV_t}{dH_E}\right)\dot{H}_E \qquad (88)$$

The acceleration factor is, then

$$A_{fE} = \frac{g_r}{g_L}\left(1 - \frac{V_t}{g_r}\frac{dV_t}{dH_E}\right) \qquad (89)$$

With no wind we have from equation (82)

$$\dot{h} = A_{fE} n_{x_w} V_t \qquad (90)$$

ACCELEROMETER METHODS

In the preceding paragraphs the general equations for computing inertial accelerations and excess thrust of an aircraft were developed for the airspeed-altitude method. Using this method a number of individual terms must be evaluated in order to obtain the total accelerations and resulting forces (e.g., airspeed derivative, rate of climb, wind gradients, Coriolis accelerations, centrifugal relief). Evaluation of some of the terms involves numerical differentiations, and the results are dependent on the numerical data editing and differentiation methods. In addition the basic parameters airspeed and altitude, obtained with conventional instruments, have limited accuracies which are degraded due to complications of position error and pressure lag. Also, it is difficult to evaluate wind gradients precisely because of uncertainties about fluctuations of atmospheric conditions with time of day and with distance from the aircraft flight corridor. The same numerical problems of data editing and differentiation are also encountered when weather balloon position coordinates are successively transformed to wind velocity and gradients.

In light of these uncertainties, methods have been developed to measure an aircraft's accelerations more directly using accelerometers. These methods are not without their own problems, but they do, in general, provide

much superior values of excess thrust. Accelerometers sense the inertial or total accelerations acting on an aircraft and their readings can be converted directly into forces by multiplying by the aircraft weight. Consequently, two of the major problems of the airspeed-altitude method can be eliminated; data editing and differentiation, as well as measurement of atmospheric winds, are not required.

ACCELEROMETER INSTALLATIONS

Sensitive accelerometers have been installed on test aircraft and have produced excess thrust data of significantly better precision than similar data from measurements of airspeed and altitude. (See reference 5, for example.)

Vane Mounted

With an accelerometer mounted on a vane (similar to an angle of attack vane to keep it alined with the local flow), excess thrust could be found immediately, knowing aircraft weight, from

$$F_{ex} = n_{x_w} W \tag{91}$$

The local flow, however, is not coincident with the airplane's velocity vector because of upwash, pitch rate, etc. (Corrections are derived in subsequent paragraphs.) Further, mechanical misalinement of the sensitive axis of the accelerometer relative to the vane may be expected. Hence, the

sensitive axis of the accelerometer is displaced from the local flow at the vane (and, therefore, the longitudinal axis of the vane) by the misalinement angle, ϵ_{ma}. Since accelerations in the wind-axes must be found in order to compute excess thrust, transformations through the angle ϵ_{ma} and other correction angles are required. These transformations are carried out in a later paragraph under Errors in Measured Accelerations.

Fixed cg Mounted

Rather than installing a two-axis accelerometer system on a vane, it may be hard mounted near the aircraft's center of gravity. This has the advantage that errors in measured accelerations caused by changes in attitude are made negligible; however, since these corrections are generally small and can be made easily, the advantage is a slight one. If load factors are measured with accelerometers located near the center of gravity, they must be transformed through any misalinement angle representing the displacement of the sensitive axis of the longitudinal accelerometer from the airplane body axis and through the angle of attack. This permits loads in the direction of and normal to the velocity vector to be found.

The sources of error in the position of a vane to which an accelerometer system is attached also exist in measured angle of attack when sensed by a vane. They appear also

in values obtained from a pressure sensing device with the exception of dynamic response. To avoid degrading the accuracy inherent in the accelerometer system, corrections for the errors described in the following paragraphs should be made and angle of attack should be accurately known (to within, say, 0.1 degrees) when using an accelerometer system mounted near the airplane's center of gravity.

ERRORS IN MEASURED ANGLE OF ATTACK

Angle of attack is generally sensed with a vane mounted on a nose boom well ahead of the aircraft. The accuracy of the sensed value (angular displacement of the relative wind from the airplane body axis) is adequate. Substantial corrections, however, must be applied in order to find true angle of attack. These corrections arise from: bending of the boom, pitching velocity (which adds a component of velocity to the vane not experienced by the airplane's center of gravity), upwash (created by the presence of the boom, nose of the airplane, and its wing), and lag in the vane position caused by rapid motions about the pitch axis.

Angle of attack has been determined less frequently through a differential pressure sensing device attached to the boom to obtain $\Delta P/q_c$, which can be related to indicated angle of attack. Corrections similar to those described

for the angle of attack vane need to be made for this sort of installation with the exception of dynamics response.

Boom Bending

Loads from aerodynamic forces and from inertia cause bending of the boom which results in errors in the measured angle of attack since the position of the vane is referenced to the axis of the boom. Bending from aerodynamic loads is usually negligible although it may be estimated from data contained in reference 6. Adjustments to boom bending for loads due to inertia may be made from a calibration of static deflections of the boom when loaded with weights to represent inertial forces experienced in flight.

Upwash

The largest correction to be made in finding true angle of attack generally stems from upwash. As previously pointed out, upwash is generated by the boom, the nose of the airplane, and the wing. The upwash is most pronounced at high angles of attack and decreases with lift coefficient. At supersonic speeds effects of fuselage and wing disappear, of course. Upwash generated by the boom may be measured in a wind tunnel.

Two-dimensional incompressible flow theory has been used to compute the effects of upwash at low speeds. Figure 3,

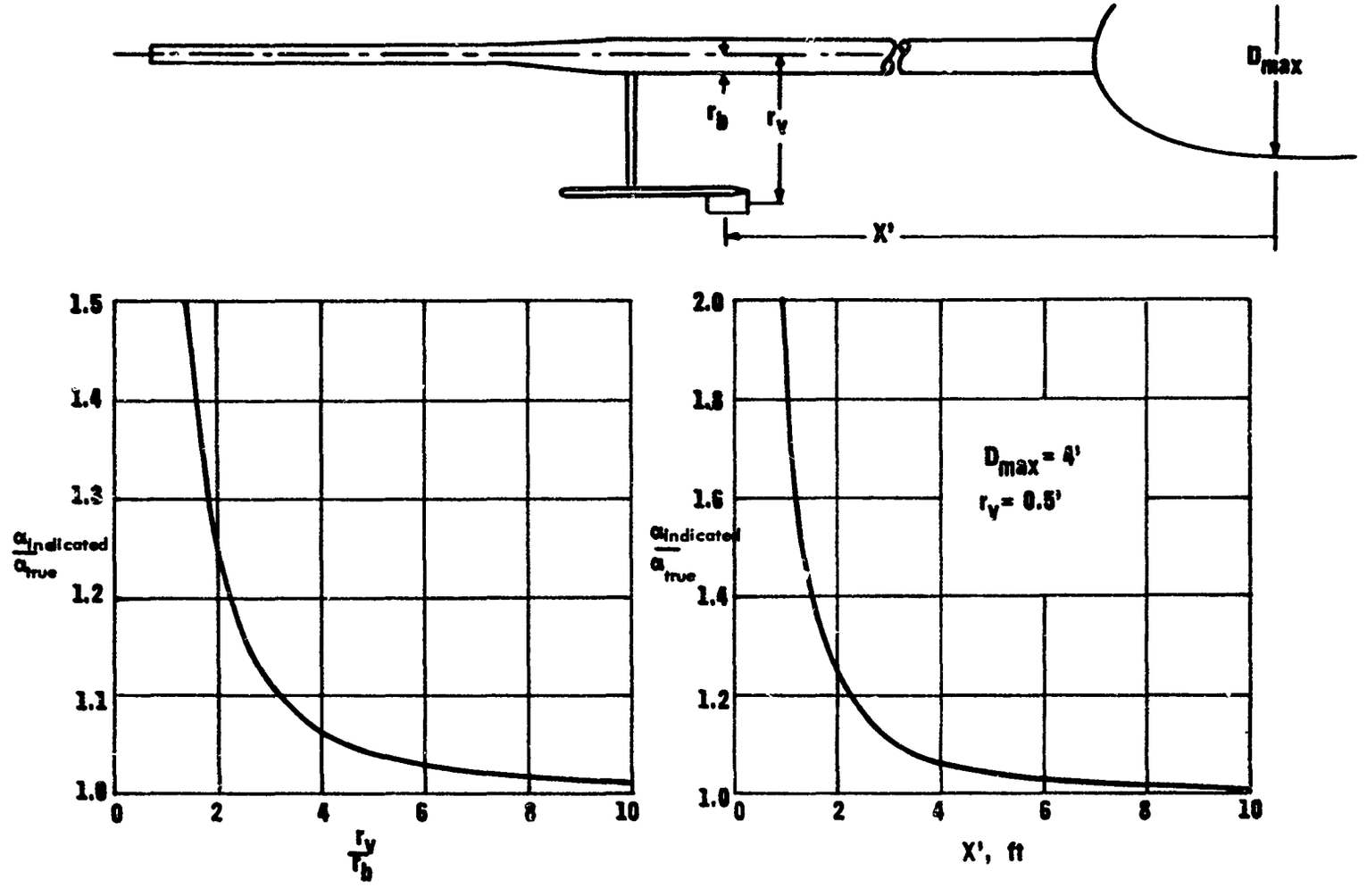

Figure 3 Theoretical Effects on Angle of Attack Measurements of Upwash from the Nose Boom and Fuselage at Low Speeds

taken from reference 7 page 16, shows the results of such computations. Indicated in the figure are variations in angle of attack from the boom itself and from the fuselage, assumed to be a blunt circular cylinder.

In reference 8 equations are presented which may be used to estimate the effects on angle of attack of the fuselage and wing. Effects of the fuselage are found using potential theory, considering the fuselage to be a half rotational body; influence of the wing is computed assuming a bound vortex in the quarter-chord line of the wing section and solving for the induced vertical velocity with a Biot-Savart equation. Estimated upwash angles have been computed using references 7 and 8 and compared to in-flight calibrations obtained with an A-37B (reference 9). Correlation of the estimated angles with those from the calibrations was reasonably good. In flight test applications, however, it is desirable to measure upwash angles from flight data and construct a calibration of upwash angle, $\Delta\alpha_u$, as a function of lift coefficient.

Dynamic Response

An angle of attack vane system* constitutes a torsional spring-mass-damper mechanical system having an undamped natural

*The vane system includes any internal mass balancing, transducer elements, accelerometer package, etc., in addition to the aerodynamic lifting surface.

frequency and damping ratio that describe its dynamic response characteristics. The output of such a system will have errors that are due to signal amplitude and phase-lag characteristics which are functions of the frequency relationship of the exciting signal and the natural frequency of the vane system as well as its damping ratio.

Equations are derived below which may be used to correct for errors in sensed angle of attack. The same equations may also be used to find errors in the position of vane-mounted accelerometers.

Response to Sinusoidal Inputs

An angle of attack vane system is shown schematically in figure 4.

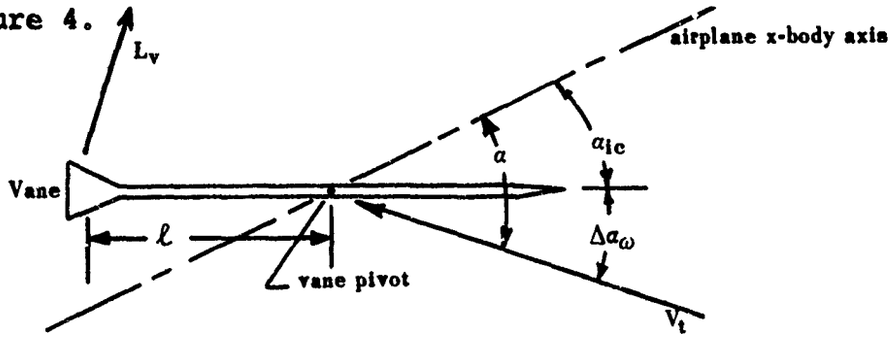

Figure 4 Angle of Attack Vane System

About the vane pivot, taking $\cos \Delta\alpha_\omega = 1$

$$L_v \ell = I_y \ddot{\alpha}_{ic} \tag{92}$$

which may be rewritten as

$$\bar{q} S_v C_{L_\alpha}^{\cdot} \ell \left[(\alpha - \alpha_{ic}) + \frac{\ell}{V_t}(\dot{\alpha} - \dot{\alpha}_{ic})\right] = I_y \ddot{\alpha}_{ic} \tag{93}$$

Rearranging

$$\ddot{\alpha}_{ic} + \frac{\bar{q}S_v \ell^2 C_{L_\alpha}}{I_y V_t}\dot{\alpha}_{ic} + \frac{\bar{q}S_v \ell C_{L_\alpha}}{I_y}\alpha_{ic} = \frac{\bar{q}S_v C_{L_\alpha}}{I_y}\left(\alpha + \frac{\ell}{V_t}\dot{\alpha}\right) \qquad (94)$$

Equation (94) is a second order differential equation describing a system whose dynamic characteristics are given by

$$\omega_n = \left[\frac{\bar{q}S_v \ell C_{L_\alpha}}{I_y}\right]^{1/2} = M\left[\frac{0.7P_a S_v \ell C_{L_\alpha}}{I_y}\right]^{1/2} \qquad (95)$$

$$2\zeta\omega_n = \frac{\bar{q}S_v \ell^2 C_{L_\alpha}}{I_y V} = \frac{0.7P_a M^2 S_v \ell^2 C_{L_\alpha}}{I_y V} \qquad (96)$$

and

$$\zeta = \frac{\ell}{2V_t}\omega_n \qquad (97)$$

It should be noted that the natural frequency and damping of the sytem are not unique properties but are dependent on Mach number and altitude. Thus these properties must be computed for each flight condition at which data are to be collected.

Since the angle of attack vane system is approximately represented by a second-order dynamic system, the first method for correcting angle of attack for dynamic lag

will assume a sinusoidally varying angle of attack. This is a fairly realistic assumption for an aircraft engaged in roller coaster maneuvers. Under these circumstances, then, in Laplace notation considering only the error due to lag

$$\frac{a_{ic}}{a}(s) = \frac{K\omega_n^2}{s^2 + 2\zeta\omega_n s + \omega_n^2} \tag{98}$$

where K is a fixed gain, usually 1.0.
Rearranging this equation and introducing jω for the Laplace operator, s, yields

$$\frac{a_{ic}}{a} = \frac{K e^{-j\tan^{-1}\frac{2\zeta\frac{\omega}{\omega_n}}{[1-(\frac{\omega}{\omega_n})^2]}}}{\left\{[1-(\frac{\omega}{\omega_n})^2]^2 + (2\zeta\frac{\omega}{\omega_n})^2\right\}^{1/2}} \tag{99}$$

This relationship defines the amplitude and phase relationship between the two sinusoidal oscillations in α and α_{ic}. Solving equation (99) for α we have

$$a = a_{ic}\frac{\left\{[1-(\frac{\omega}{\omega_n})^2]^2 + (2\zeta\frac{\omega}{\omega_n})^2\right\}^{1/2}}{K} e^{j\tan^{-1}\frac{2\zeta\frac{\omega}{\omega_n}}{[1-(\frac{\omega}{\omega_n})^2]}} \tag{100}$$

Introducing for α_{ic} the expression

$$a_{ic} = a_{ic_o}\sin\omega t \tag{101}$$

where α_{ic_o} is the maximum amplitude of α_{ic}, it is possible to rearrange the above equations so that a solution is given for $\Delta\alpha_\omega$.

$$\Delta\alpha_\omega = \alpha_{ic_o} r \sin(\omega t + \eta) \tag{102}$$

where

$$r = \left[1 + \frac{\left[1-\left(\frac{\omega}{\omega_n}\right)^2 + \left(2\zeta\frac{\omega}{\omega_n}\right)^2\right]^{1/2}}{K}\left(\frac{\left\{\left[1-\left(\frac{\omega}{\omega_n}\right)^2\right]^2 + \left(2\zeta\frac{\omega}{\omega_n}\right)^2\right\}^{1/2}}{K} - 2\cos\left[\tan^{-1}\frac{2\zeta\frac{\omega}{\omega_n}}{1-\left(\frac{\omega}{\omega_n}\right)^2}\right]\right)\right]^{1/2} \tag{103}$$

and

$$\eta = \tan^{-1}\frac{\frac{2\zeta\frac{\omega}{\omega_n}}{1-\left(\frac{\omega}{\omega_n}\right)^2}}{1 - \frac{1}{\frac{\left\{\left[1-\left(\frac{\omega}{\omega_n}\right)\right]^2 + \left(2\zeta\frac{\omega}{\omega_n}\right)^2\right\}^{1/2}}{K}\cos\left[\tan^{-1}\frac{2\zeta\frac{\omega}{\omega_n}}{1-\left(\frac{\omega}{\omega_n}\right)^2}\right]}} \tag{104}$$

There exists another method for finding $\Delta\alpha_\omega$ for the case where sinusoidal inputs may be assumed and which involves fewer calculations. Given, as before, that the angle of attack vane is a second order system with an undamped natural frequency of oscillation, ω_n, and a damping ratio, ζ, the indicated angle of attack is given by

$$a_{ic}(t) = \frac{K a_0 \sin(\omega t - \phi)}{\left\{[1 - (\frac{\omega}{\omega_n})^2]^2 + (2\zeta\frac{\omega}{\omega_n})^2\right\}^{1/2}} \qquad (105)$$

where K is, as before, a constant gain (usually 1.0) and α_o is the maximum amplitude of α.

Making use of trigonometric identities

$$a_{ic}(t) = \frac{K a_0}{\left\{[1 - (\frac{\omega}{\omega_n})^2]^2 + (2\zeta\frac{\omega}{\omega_n})^2\right\}^{1/2}} (\sin\omega t\cos\phi - \cos\omega t\sin\phi) \qquad (106)$$

where

$$\phi = \tan^{-1}\frac{2\zeta\frac{\omega}{\omega_n}}{1 - (\frac{\omega}{\omega_n})^2} \qquad (107)$$

By rearranging the terms in this equation and making small angle approximations ($\cos\phi = 1$ $\sin\phi = \phi$)

$$\alpha(t) = \frac{\left\{[1-(\frac{\omega}{\omega_n})^2]^2 + (2\zeta\frac{\omega}{\omega_n})^2\right\}^{1/2}}{K} [a_{ic}(t) + a_{ic_0}\phi\cos\omega t] \qquad (108)$$

In the above equation ωt describes the sinusoidally varying α. This is generally not known since α is not

known; however, it can be inferred through knowledge of $\alpha_{ic}(t)$ and a small correction to t. When $\alpha_{ic}(t) = 0$, it can be shown that $\tan \omega t = \phi$, where ωt describes $\alpha(t)$, rather than $\alpha_{ic}(t)$.

Since $t = (1/\omega) \tan^{-1}\phi$ when $\alpha_{ic}(t) = 0$, it can be used to correct the time associated with the observed angle of attack, $\alpha_{ic}(t)$ so that the expression for $\alpha(t)$ becomes

$$\alpha(t_{\alpha_{ic}}) = \frac{\left\{\left[1 + \left(\frac{\omega}{\omega_n}\right)^2\right]^2 + \left(2\zeta\frac{\omega}{\omega_n}\right)^2\right\}^{1/2}}{K} \left\{\alpha_{ic}(t_{\alpha_{ic}}) + \alpha_{ic_o}\phi\cos[\omega(t_{\alpha_{ic}} + \Delta t)]\right\} \tag{109}$$

where

$\alpha_{ic}(t_{\alpha_{ic}})$ = indicated angle of attack at any time, $t_{\alpha_{ic}}$

α_{ic_o} = maximum amplitude of observed angle of attack

$t_{\alpha_{ic}}$ = time from a reference value of the indicated angle of attack

Δt = incremental time correction to $t_{\alpha_{ic}}$ $(1/\omega)\tan^{-1}\phi$

ϕ = phase lag angle between $\alpha(t_{\alpha_{ic}})$ and $\alpha_{ic}(t_{\alpha_{ic}})$

Response to Random Inputs

The previous discussion was concerned with correcting indicated angle of attack when a sinusoidal variation of

the input had been assumed. In the more general case, as in a climb, the angle of attack is changed in a series of quasi-step inputs which are aimed at keeping the aircraft on a desired climb schedule. In correcting the indicated angle of attack in this case, a somewhat more complicated process is used. Since the angle of attack vane system is a second order system, its input-output relationship is given by

$$\frac{\alpha_{ic}}{\alpha}(s) = \frac{K\omega_n^2}{s^2 + 2\zeta\omega s + \omega_n^2} \tag{110}$$

If the operations indicated by the above Laplace-transform expression are performed, the following expression in the time domain results:

$$\alpha(t) = \frac{1}{K\omega_n^2}[\ddot{\alpha}_{ic}(t) + 2\zeta\omega_n\dot{\alpha}_{ic}(t) + \omega_n^2\alpha_{ic}(t)] \tag{111}$$

In general it will be necessary to operate on the indicated angle of attack time history, $\alpha_{ic}(t)$, with a computer program designed to give first and second derivative information about a variable. One such program is called DIRSIT and is described in reference 12. In general, both first and second derivative corrections to indicated angle of attack time histories should be made

since omitting the correction for the second derivative can, in some cases, cause the end result to be as much in error, but in a different sense, as having made no connection at all.

Pitch Rate

The aircraft airspeed vector expressed in the wind-axes is, referring to figure 5

$$\bar{V}_t = V_t \bar{i} \tag{112}$$

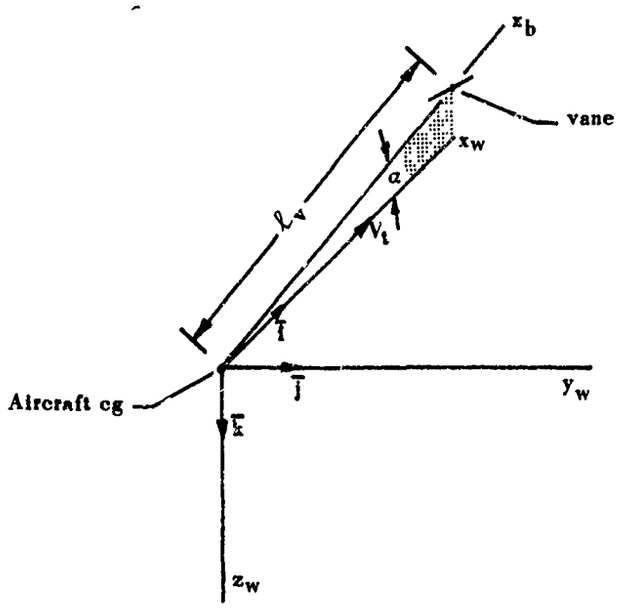

Figure 5 Orientation of Vane

To compute the vane airspeed vector, $\bar{V}_v$, it is assumed that the x_b axis passes through the vane. The following equation may then be written (reference 10, page 440):

$$\bar{V}_v = \bar{V}_t + \bar{\omega}_b \times \bar{\ell}_v \tag{113}$$

When an aircraft is subjected to a pitch rate there will be a difference between the true airspeed of the aircraft's center of gravity and the local airspeed of a vane on a rose boom. Since the vane alines itself with the local flow, the angular alinement error is the angle between the aircraft airspeed and the vane airspeed vectors.

To compute the vane airspeed vector, $\bar{V}_v$, the following equation is used (reference 10, page 440) where the body angular velocity is

$$\bar{\omega}_b = p\bar{i}_b + q\bar{j}_b + r\bar{k}_b \tag{114}$$

Recognizing that

$$\bar{\ell}_v = \ell_v \bar{i}_b \tag{115}$$

we may write

$$\bar{V}_v = \bar{V}_t + \begin{bmatrix} \bar{i}_b & \bar{j}_b & \bar{k}_b \\ p & q & r \\ \ell_v & 0 & 0 \end{bmatrix} \tag{116}$$

Expanding the determinant

$$\bar{V}_v = \bar{V}_t + [\ell_v r\bar{j}_b - \ell_v q\bar{k}_b] \tag{117}$$

To express the velocity in the wind-axes system a transformation is made through α in the negative direction. Making use of the matrix

$$\begin{bmatrix} \cos\alpha & 0 & \sin\alpha \\ 0 & 1 & 0 \\ -\sin\alpha & 0 & \cos\alpha \end{bmatrix}$$

taken from the section, Coordinate Systems and Transformations, the vector in brackets in equation (117) becomes

$$\begin{bmatrix} \cos\alpha & 0 & \sin\alpha \\ 0 & 1 & 0 \\ -\sin\alpha & 0 & \cos\alpha \end{bmatrix} \begin{bmatrix} 0 \\ \ell_v r \\ -\ell_v q \end{bmatrix} = \begin{bmatrix} -\ell_v q\sin\alpha \\ \ell_v r \\ -\ell_v q\cos\alpha \end{bmatrix} \tag{118}$$

In the wind-axes, equation (117) becomes

$$\bar{V}_v = V_t\bar{i} + [-\ell_v q\sin\alpha\bar{i} + \ell_v r\bar{j} - \ell_v q\cos\alpha\bar{k}] \tag{119}$$

Adding components in equation (119)

$$\bar{V}_v = (V_t - \ell_v q \sin\alpha)\bar{i} + \ell_v r\bar{j} - \ell_v q \cos\alpha \bar{k} \qquad (120)$$

Remembering that the unit vector $\bar{k}$ is positive downward and the angle, $\Delta\alpha_q$, is positive upward

$$\tan\Delta\alpha_q = \frac{-(-\ell_v q\cos\alpha)}{V_t - \ell_v q\sin\alpha} \qquad (121)$$

or

$$\Delta\alpha_q = \tan^{-1}\frac{\ell_v q\cos\alpha}{V_t - \ell_v q\sin\alpha} \qquad (122)$$

Since α is not known, an iteration procedure has to be used to compute $\Delta\alpha_q$. In the first iteration the corrections described above are added to the indicated angle of attack so that the angle

$$\alpha_{ic} + \Delta\alpha_u + \Delta\alpha_\omega + \Delta\alpha_{\text{boom bending}}$$

is substituted in place of α in equation (122).

True Angle of Attack

True angle of attack is determined by adding corrections for the errors described above (boom bending, upwash, dynamic

response, and pitch rate). If a pressure sensing device is used, dynamic corrections may be ignored since there are no moving parts. Upwash corrections are generally the largest, particularly at low speeds. Corrections for dynamic response and pitch rate are frequently not required but may be sizable during roller coaster maneuvers, and during climbs, especially for high performance aircraft. If values of pitch rate and pitch acceleration are needed, they are best obtained by direct measurement with on-board instrumentation. In the event that the instrumentation is not available, the required data may be computed using equations derived under the heading, Attitude Rates, in the paragraph, Errors in Measured Accelerations.

ERRORS IN MEASURED ACCELERATIONS

Two types of accelerometer installations have been considered: one in which the accelerometers are attached to a vane located on a nose boom and the other with the accelerometers hard mounted in the aircraft near its center of gravity. In both cases a mechanical misalinement should be considered. For accelerometers on a vane the sensitive axis of the longitudinal accelerometer may not coincide with the axis of the vane. Similarly, for cg mounted accelerometers, the sensitive axis of the accelerometer may not coincide with the airplane's body axis, x_b.

In addition to accounting for mechanical misalinement, axis transformations must be made to find load factors in the wind-axes system. For vane-mounted accelerometers the rotation is made through the net angle which results from combining errors due to boom bending, upwash, dynamic lag, and pitch rate. In the case of fixed cg mounted accelerometers the rotation is made through the angle of attack, but the same errors must be evaluated since they are used to compute angle of attack (excepting dynamic lag when angle of attack is determined from a differential pressure instrument).

With accelerometers on a vane, accelerations are induced at the vane by angular attitude rates and accelerations which are not experienced by the accelerometers when located at the center of gravity. If the accelerometers are on board the aircraft near the center of gravity similar accelerations are generated, but the distance from the center of gravity to the accelerometer should be small enough to make the induced accelerations negligible. However, they should not be eliminated arbitrarily but only after investigation of the particular situation shows these induced accelerations to be trivial.

An additional source of error is incurred with accelerometers on a vane. Dynamic lag resulting from rapid control inputs affects the alinement of the vane (as well as an angle of attack vane) relative to the local flow.

Mechanical Misalinement

It is inevitable that there will be some angular misalinement between the axes of a vane and the sensitive axes of accelerometers (both normal and longitudinal) attached to the vane. Considering the construction of the accelerometer system, it is generally secured as a two-accelerometer package with their orthogonality well enough controlled so there is little error. Also, since acceleration in the y-direction is not measured, misalinement from rotation about the z-axis is not taken into account. The principal source of misalinement is, then, an angular rotation of the accelerometer case about the vane axis as illustrated in figure 6.

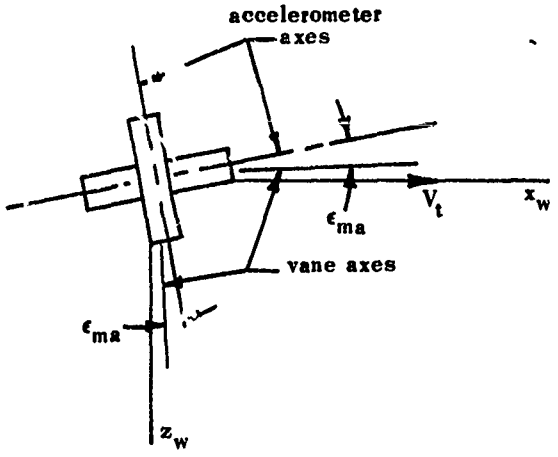

Figure 6 Vane Misalinement Angle

Components of acceleration along and normal to the vane are found by transforming through the angle ϵ_{ma} to obtain

$$n_{x_v} = n_{x_m} \cos \epsilon_{ma} - n_{z_m} \sin \epsilon_{ma} \quad (123)$$

and

$$n_{z_v} = n_{z_m} \cos \epsilon_{ma} + n_{x_m} \sin \epsilon_{ma} \quad (124)$$

where the subscript m refers to measured values. In order to retain the accuracy inherent in sensitive accelerometers, it is necessary to know the magnitude of ϵ_{ma} quite well. To illustrate, suppose the $n_{x_m} = 0g$, $n_{z_m} = 1g$, and $\epsilon_{ma} = 1$ degree. n_{x_v}, arising from the component of n_{z_m} is 0.01745g. Since this is several times the accuracy which may be achieved in the measured quantities, the misalinement angle should be known to within about 0.1 degrees.

Use of a sensitive accelerometer to measure normal load factor is desirable in computing n_{x_v}, (and hence n_{x_w}) particularly for climbs or other maneuvers during which there are significant changes in normal load factor.

A similar misalinement angle should be expected when the accelerometer system is mounted near the center of gravity of the airplane. In this case the misalinement angle is the angular displacement of the sensitive axis of the longitudinal accelerometer from the airplane's body axis, x_b. An axis transformation similar to that indicated

by equations (123) and (124) is made to obtain load factors in the body axes.

$$n_{x_b} = n_{x_m}\cos\epsilon_{ma} - n_{z_m}\sin\epsilon_{ma} \tag{125}$$

and

$$n_{z_b} = n_{z_m}\cos\epsilon_{ma} + n_{x_m}\sin\epsilon_{ma} \tag{126}$$

Observed Load Factors in the Wind-Axes System

It is necessary to make axes transformations through the angle between the sensitive axes of the accelerometers and the wind axes for both types of accelerometer systems considered. This might be done by making the transformation through a single angle in both cases. The resultant load factors have been found, however, by first transforming through the misalinement, ϵ_{ma}, as indicated in equations (123) through (126). In the case of vane-mounted accelerometers, then, an additional transformation through the angle

$$\Delta\alpha_{net} = \Delta\alpha_{\text{boom bending}} + \Delta\alpha_u + \Delta\alpha_\omega + \Delta\alpha_q \tag{127}$$

is required, and observed load factors in wind axes become

$$n_{x_{w'}} = n_{x_v}\cos\Delta\alpha_{net} - n_{z_v}\sin\Delta\alpha_{net} \tag{128}$$

and

$$n_{z_{w'}} = n_{z_v}\cos\Delta\alpha_{net} + n_{x_v}\sin\Delta\alpha_{net} \tag{129}$$

The load factors in equations (128) and (129) are in the wind-axes system but have not been corrected for induced accelerations derived in the following paragraph.

For accelerometer systems hard mounted near the cg, the desired load factors may be found immediately by making a transformation through the angle of attack, which is computed from

$$\alpha = \alpha_{ic} + \Delta\alpha_{\text{boom bending}} + \Delta\alpha_{u} + \Delta\alpha_{\omega} \tag{130}$$

We have, then

$$n_{x_w} = n_{x_b}\cos\alpha - n_{z_b}\sin\alpha \tag{131}$$

and

$$n_{z_w} = n_{x_b}\sin\alpha + n_{z_b}\cos\alpha \tag{132}$$

Accelerations Induced from Attitude Rates

The acceleration at the vane referenced to that at the cg is, from reference 10, page 443

$$\bar{a}_v = \bar{a}_{cg} + \left[\frac{d^2\bar{\ell}_v}{dt^2}\right]_b + \left[\frac{d\bar{\omega}_b}{dt}\right]_b \times \bar{\ell}_v + 2\bar{\omega}_b \times \left[\frac{d\bar{\ell}_v}{dt}\right]_b + \bar{\omega}_b \times (\bar{\omega}_b \times \bar{\ell}_v) \tag{133}$$

where the body-axes system is moving and the terms in the brackets represent derivatives within the moving system.

Since the axis of the vane is assumed to lie on the x_b axis, the first and second derivatives of $\bar{\ell}_v$ are zero.

$$\left[\frac{d\,\bar{\ell}_v}{dt}\right]_b = \left[\frac{d^2\bar{\ell}_v}{dt^2}\right]_b = 0 \tag{134}$$

Evaluating the remaining terms

$$\left[\frac{d\bar{\omega}_b}{dt}\right]_b = \dot{p}\bar{i}_b + \dot{q}\bar{j}_b + \dot{r}\bar{k}_b \tag{135}$$

$$\left[\frac{d\bar{\omega}_b}{dt}\right]_b \times \bar{\ell}_v = \begin{bmatrix} \bar{i}_b & \bar{j}_b & \bar{k}_b \\ \dot{p} & \dot{q} & \dot{r} \\ \ell_v & 0 & 0 \end{bmatrix} = (0)\bar{i}_b + (\ell_v\dot{r})\bar{j}_b - (\ell_v\dot{q})\bar{k}_b \tag{136}$$

and $$\bar{\omega}_b \times (\bar{\omega}_b \times \bar{\ell}_v) = \begin{bmatrix} \bar{i}_b & \bar{j}_b & \bar{k}_b \\ \dot{p} & \dot{q} & \dot{r} \\ 0 & \ell_v r & -\ell_v q \end{bmatrix}$$

$$= -\ell_v(q^2 + r^2)\bar{i}_b + \ell_v qp\bar{j}_b + \ell_v pr\bar{k}_b \tag{137}$$

Substituting equations (135) and (137) in equation (133)

$$\bar{a}_v = \ddot{\bar{a}}_{cg} + \ell_v[-(q^2+r^2)\bar{i}_b + (pq+\dot{r})\bar{j}_b + (pr-\dot{q})\bar{k}_b] \tag{138}$$

Transforming the components to the wind-axes system, as in equation (118)

$$\begin{bmatrix} \cos\alpha & 0 & \sin\alpha \\ 0 & 1 & 0 \\ -\sin\alpha & 0 & \cos\alpha \end{bmatrix} \begin{bmatrix} -\ell_v(q^2 + r^2) \\ \ell_v(qp + \dot{r}) \\ \ell_v(pr - \dot{q}) \end{bmatrix}$$

$$= \begin{bmatrix} \ell_v[-(q^2+r^2)\cos\alpha + (pr-\dot{q})\sin\alpha] \\ \ell_v(qp + \dot{r}) \\ \ell_v[(q^2+r^2)\sin\alpha + (pr-\dot{q})\cos\alpha] \end{bmatrix} \qquad (139)$$

The final equation for acceleration in the wind-axes is

$$\bar{a}_v = \bar{a}_{cg} + \ell_v\{[-(q^2+r^2)\cos\alpha + (pr-\dot{q})\sin\alpha]\bar{i} + (qp+\dot{r})\bar{j} + [(q^2+r^2)\sin\alpha + (pr-\dot{q})\cos\alpha]\bar{k}\} \qquad (140)$$

The induced acceleration is made up of the terms in equation (114) representing the difference between the acceleration at the vane and that at the center of gravity, $(\bar{a}_v - \bar{a}_{cg})$.

Corrected Load Factors in the Wind-Axes System

When induced accelerations as defined in equation (140) become large enough to have significant effects on load factors, it becomes necessary to calculate load factors at the cg in terms of the load factors measured by the accelerometers located on a vane.

The correction to load factor is

$$\frac{1}{g_r}(\bar{a}_{cg} - \bar{a}_v) \qquad (141)$$

so that, from equations (128), (129) and (140) the load factors along and normal to the airplane's velocity vector are

$$n_{x_w} = n_{x_v}\cos\Delta\alpha_{net} - n_{z_v}\sin\Delta\alpha_{net} + \frac{\ell_v}{g_r}[(q^2+r^2)\cos\alpha - (pr-\dot{q})\sin\alpha] \quad (142)$$

and

$$n_{z_w} = n_{z_v}\cos\Delta\alpha_{net} + n_{x_v}\sin\Delta\alpha_{net} + \frac{\ell_v}{g_r}[(q^2+r^2)\sin\alpha + (pr-\dot{q})\cos\alpha] \quad (143)$$

Since these corrections are not usually needed for accelerometers located near the cg, load factors for this sort of installation may be found from equations (131) and (132).

If the corrections to load factors described above (and to angle of attack for pitch rate) are made, the best way to obtain the attitude rates and attitude accelerations is to measure them directly with rate gyros and angular accelerometers. Any other method involves differentiation which will magnify any errors arising from inadequate instrumentation, calibration, data reduction technique, etc. Despite these limitations, corrections can be made by use of equations presented in the following paragraph although it is iterated that the results can be expected to be inferior to direct measurements.

Computed Attitude Rates

To develop body rate equations we begin with the angular velocity of the wind-axes (reference 11, page 22) including only the changes in heading and climb angle, and adding roll rate $\dot{B}\bar{i}$,

$$\bar{\omega}_v = (\dot{B} - \dot{\sigma}\sin\gamma)\bar{i} + (\dot{\gamma}\cos B + \dot{\sigma}\cos\gamma\sin B)\bar{j}$$

$$+ (-\dot{\gamma}\sin B + \dot{\sigma}\cos\gamma\cos B)\bar{k} \qquad (144)$$

Next we add the rate of change of the angle of attack to obtain the angular velocity of the body axes

$$\bar{\omega}_b = (\dot{B} - \dot{\sigma}\sin\gamma)\bar{i} + (\dot{\alpha} + \dot{\gamma}\cos B + \dot{\sigma}\cos\gamma\sin B)\bar{j}$$

$$+ (-\dot{\gamma}\sin B + \dot{\sigma}\cos\gamma\cos B)\bar{k} \qquad (145)$$

Finally, to obtain the body roll, pitch, and yaw rates we transform the components of equation (145) to the body-axes system. The transform matrix is, from the section, Coordinate Systems and Transformations, the inverse of that in equation (139).

$$[\omega_b] = \begin{bmatrix} \cos\alpha & 0 & -\sin\alpha \\ 0 & 1 & 0 \\ \sin\alpha & 0 & \cos\alpha \end{bmatrix} \begin{bmatrix} \dot{B} - \dot{\sigma}\sin\gamma \\ \dot{\alpha} + \dot{\gamma}\cos B + \dot{\sigma}\cos\gamma\sin B \\ -\dot{\gamma}\sin B + \dot{\sigma}\cos\gamma\cos B \end{bmatrix}$$

$$= \begin{bmatrix} (\dot{B} - \dot{\sigma}\sin\gamma)\cos\alpha - (-\dot{\gamma}\sin B + \dot{\sigma}\cos\gamma\cos B)\sin\alpha \\ \dot{\alpha} + \dot{\gamma}\cos B + \dot{\sigma}\cos\gamma\sin B \\ (\dot{B} - \dot{\sigma}\sin\gamma)\sin\alpha + (-\dot{\gamma}\sin B + \dot{\sigma}\cos\gamma\cos B)\cos\alpha \end{bmatrix} \qquad (146)$$

Equating the vector components of equations (114) and (146)

$$p = (\dot{B} - \dot{\sigma}\sin\gamma)\cos\alpha - (-\dot{\gamma}\sin E \cdot \dot{\sigma}\cos\gamma\cos B)\sin\alpha \tag{147}$$

$$q = \dot{\alpha} + \dot{\gamma}\cos B + \dot{\sigma}\cos\gamma\sin B \tag{148}$$

$$r = (\dot{B} - \dot{\sigma}\sin\gamma)\sin\alpha + (-\dot{\gamma}\sin B + \dot{\sigma}\cos\gamma\cos B)\cos\alpha \tag{149}$$

The parameters in these equations can all be computed from airspeed, altitude, and angle of attack except for B, $\dot{B}$, and $\dot{\sigma}$. To evaluate these unknowns $\dot{B}$ is assumed to be zero; then the other two parameters can be obtained by reference to the equations of motion along the wind y- and z-axes. The accelerations along these axes are, neglecting smaller order terms, from equations (47) and (48)

$$a_{y_w} = V_t(\dot{\sigma}\cos\gamma\cos B - \dot{\gamma}\sin B) \tag{150}$$

and

$$a_{z_w} = -V_t(\dot{\gamma}\cos B + \dot{\sigma}\cos\gamma\sin B) \tag{151}$$

The components of the local gravity can be obtained by transforming the component

$$\bar{g}_L = g_L\bar{k}_g \tag{152}$$

in the local geocentric-axes system into the wind-axes system. Applying the transformation matrix from the section, Coordinate Systems and Transformations, results in

$$\bar{g}_L = g_L(-\sin\gamma\bar{i} + \cos\gamma\sin B\bar{j} + \cos\gamma\cos B\bar{k}) \tag{153}$$

Recalling that the normal load factor is positive upwards opposite to the positive z-axis, the total load factor at the cg is

$$\bar{n}_{cg} = n_x\bar{i} + n_y\bar{j} - n_z\bar{k} \tag{154}$$

The vector equation for load factor in terms of aircraft acceleration is

$$n_{cg} = \frac{1}{g_r}(\bar{a}_{cg} - \bar{g}_L) \tag{155}$$

Substituting the components from equations (150), (151), (153) and (154) in equation (155) and picking out the y and z components

$$n_{y_w} = \frac{1}{g_r}[V_t(\dot{\alpha}\cos\gamma\cos B - \dot{\gamma}\sin B) - g_L\cos\gamma\sin B] \tag{156}$$

and

$$n_{z_w} = \frac{1}{g_r}[V_t(\dot{\gamma}\cos B + \dot{\alpha}\cos\gamma\sin B) + g_L\cos\gamma\cos B] \tag{157}$$

With the assumption of zero sideslip the side load factor must be zero. Therefore, from equation (156)

$$V_t(\dot{\sigma}\cos\gamma\cos B - \dot{\gamma}\sin B) = g_L\cos\gamma\sin B \tag{158}$$

Equation (158) can be solved for tan B to give

$$\tan B = \frac{V_t\dot{\sigma}\cos\gamma}{g_L\cos\gamma + V_t\dot{\gamma}} \tag{159}$$

Rearranging equation (157)

$$g_r n_{z_w} - g_L\cos\gamma\cos B + V_t\dot{\sigma}\cos B = (V_t\dot{\sigma}\cos\gamma)\sin B \tag{160}$$

Solving equation (159) for $(V_t\dot{\sigma}\cos\gamma)$, substituting into equation (160), and multiplying by cos B

$$g_r n_{z_w}\cos B - (g_L\cos\gamma + V_t\dot{\gamma})\cos^2 B = (g_L\cos\gamma + V_t\dot{\gamma})\sin^2 B \tag{161}$$

Since $\cos^2 B + \sin^2 B = 1$, equation (161) reduces to

$$\cos B = \frac{g_L\cos\gamma + V_t\dot{\gamma}}{g_r n_{z_w}} \tag{162}$$

Multiplying cosB of equation (162) times tanB of equation (159) the following results

$$\sin B = \frac{V_t\cos\gamma}{g_r n_{z_w}}\dot{\sigma}$$

or solving for $\dot{\sigma}$

$$\dot{\sigma} = \frac{g_r n_{z_w}}{V_t \cos\gamma} \sin B \tag{163}$$

From trigonometry

$$\sin B = (1 - \cos^2 B)^{1/2} \tag{164}$$

so that *

$$\sin B = \left[1 - \left(\frac{g_L \cos\gamma + V_t \dot{\gamma}}{g_r n_{z_w}}\right)^2\right]^{1/2} \tag{165}$$

Substituting into equation (163) and rearranging

$$\dot{\sigma} = \frac{\left[(g_r n_{z_w})^2 - (g_L \cos\gamma + V_t \dot{\gamma})^2\right]^{1/2}}{V_t \cos\gamma} \tag{166}$$

Equations (162) and (166) provide the required values of B and $\dot{\sigma}$ to substitute into the attitude rate equations, ((147) through (149)'. The pitch angular acceleration, $\dot{q}$, required in equations (142) and (143) can be obtained from time differentiation of q in equation (148). These

* sin B and $\dot{\sigma}$ become negative when

$$1 - \left(\frac{g_L \cos\gamma + V_t \dot{\gamma}}{g_r n_{z_w}}\right)^2 < 0.$$

equations include the true normal load factor, which can be approximated satisfactorily by the measured value.

INERTIAL NAVIGATION SYSTEMS

An inertial navigation system from which are obtained the output from a three-axis accelerometer system and sufficient orientation angles to find components in the wind-axis system has a very important advantage over the accelerometer installations previously described. That is, the need for making corrections for boom bending, upwash, dynamic lag, pitch rate or for induced accelerations in values sensed by accelerometers mounted on a vane are eliminated. Since the inherent accuracy of the orientation angles defining the position of the three-axis accelerometer system is superior to conventional angle of attack measurements and the uncertainties associated with above corrections are eliminated, computed load factors in the wind-axes from an inertial navigation system can be expected to be significantly more accurate than those from the accelerometer systems previously described.

Comparative disadvantages of an inertial navigation system may be: increased preflight checkout time, poorer reliability with increased maintenance, and higher cost (presuming that the test aircraft has not been equipped with an operable system).

Because of the variety in design of inertial navigation systems, the orientation of the accelerometers depends on the specific system being used. Hence, the axes transformations to obtain load factors in wind-axes are not presented.

RADAR METHOD

Equations are presented which may be used with data from radar (or position data from some other source such as Askania cameras) to compute load factors and hence excess thrust.

Figure 7 shows the radar system located with respect to the geocentric coordinate system in terms of the geocentric latitude, δ_L, the height above the reference ellipsoid, and the angular deviation of the x_r axis from true north.

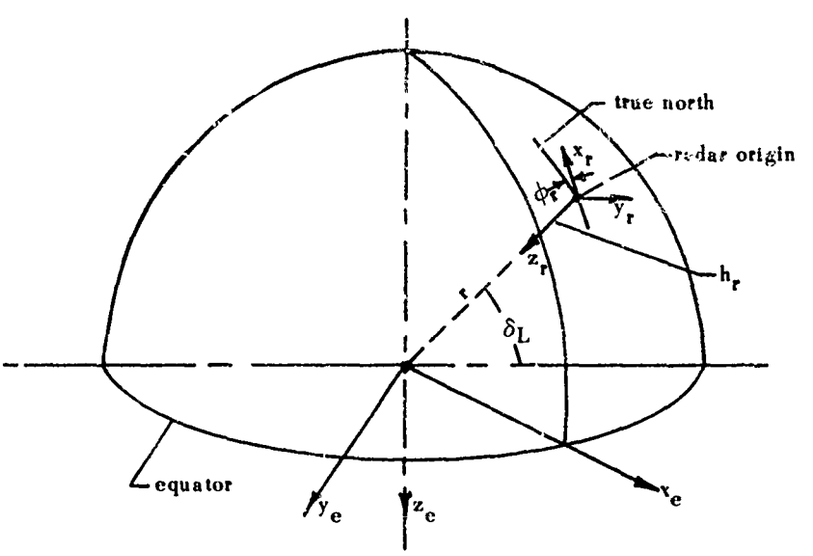

Figure 7 Radar System

The origin of the radar system in geocentric coordinates is given by

$$x_e' = (r + h_r)\cos\delta_L \tag{167}$$

$$y_e' = 0 \tag{168}$$

and

$$z_e' = -(r + h_r)\sin\delta_L \tag{169}$$

r, repeating equation (5) from the section Geophysical Properties, is

$$r = r_0(.99832172 + .0016761\cos 2\delta_L + .0000021\cos 4\delta_L) \tag{170}$$

As may be seen by figure 7, rotations of $(\phi_r+180°)$ and δ_L are necessary to aline the radar system with the geocentric system. These rotations result in a rotation matrix given by

$$[M(\phi_r + \pi, \delta_L)] = \begin{bmatrix} -\sin\delta_L\cos\phi_r & \sin\delta_L\sin\phi_r & -\cos\delta_L \\ -\sin\phi_r & -\cos\phi_r & 0 \\ -\cos\delta_L\cos\phi_r & \cos\delta_L\sin\phi_r & \sin\delta_L \end{bmatrix} \tag{171}$$

The position of an aircraft in geocentric coordinates is obtained by addition of the rotated radar coordinates to the components of the radar origin in geocentric coordinates:

$$\begin{bmatrix} x_{e_m} \\ y_{e_m} \\ z_{e_m} \end{bmatrix} = [M(\phi_r + \pi, \delta_L)] \begin{bmatrix} x_r \\ y_r \\ z_r \end{bmatrix} + \begin{bmatrix} x_e' \\ y_e' \\ z_e' \end{bmatrix} \tag{172}$$

Since x_e', y_e', z_e', and $[M(\phi_r+\pi,\delta_L)]$ are constants, the transformations of aircraft velocities and accelerations are given by

$$\begin{bmatrix} \dot{x}_{e_m} \\ \dot{y}_{e_m} \\ \dot{z}_{e_m} \end{bmatrix} = [M(\phi_r + \pi, \delta_L)] \begin{bmatrix} \dot{x}_r \\ \dot{y}_r \\ \dot{z}_r \end{bmatrix} \tag{173}$$

The components of velocity and acceleration are determined from a smoothing and differentiating process of the position data.

Since the x_r, y_r, z_r system is attached to the earth and rotates with it at an angular rate of $\omega_\oplus$, accelerations

due to $\omega_\oplus$ are generated. In order to find inertial accelerations which may be related to forces acting on the aircraft and to load factors, equations (174) through (176) are used:

$$\ddot{x}_e = \ddot{x}_{e_m} - x_{e_m}\omega_\oplus^2 + 2\dot{y}_{e_m}\omega_\oplus \tag{174}$$

$$\ddot{y}_e = \ddot{y}_{e_m} - y_{e_m}\omega_\oplus^2 - 2\dot{x}_{e_m}\omega_\oplus \tag{175}$$

and

$$\ddot{z}_e = \ddot{z}_{e_m} \tag{176}$$

Next, the above accelerations are transformed to local geocentric axes. This is accomplished by use of the matrix found in the section, Coordinate Systems and Transformations, and results in

$$\begin{bmatrix} \ddot{x}_g \\ \ddot{y}_g \\ \ddot{z}_g \end{bmatrix} = \begin{bmatrix} -\cos\Delta\lambda_L\sin\delta_L & -\sin\Delta\lambda_L\sin\delta_L & -\cos\delta_L \\ \sin\Delta\lambda_L & -\cos\Delta\lambda_L & 0 \\ -\cos\Delta\lambda_L\cos\delta_L & -\sin\Delta\lambda_L\cos\delta_L & \sin\delta_L \end{bmatrix} \begin{bmatrix} \ddot{x}_e \\ \ddot{y}_e \\ \ddot{z}_e \end{bmatrix} \tag{177}$$

$\Delta\lambda_L$ is the difference between the aircraft longitude and the longitude of the radar coordinate origin as shown in figure 3 of that section.

Gravitational attractions as computed from equation (15) of the same section may be readily added to the accelerations from equation (177) and load factors computed:

$$n_{x_g} = \frac{1}{g_r}(\ddot{x}_g - g_{x_g}) \tag{178}$$

$$n_{y_g} = \frac{1}{g_r}\ddot{y}_g \tag{179}$$

and

$$n_{z_g} = -\frac{1}{g_r}(\ddot{z}_g - g_{z_g}) \tag{180}$$

Transformation into wind axes but at zero bank angle is accomplished by means of the matrix $[M(\sigma,\gamma)]$ expressed in equation (14) of the section, Coordinate Systems and Transformations:

$$\begin{bmatrix} n_{x_{w'}} \\ n_{y_{w'}} \\ n_{z_{w'}} \end{bmatrix} = [M(\sigma,\gamma)] \begin{bmatrix} n_{x_g} \\ n_{y_g} \\ n_{z_g} \end{bmatrix} \tag{181}$$

The angles σ and γ when computed from radar data for use in equation (181) require a knowledge of wind speed

and direction as a function of time. Velocities in local geocentric axes are found through the same rotation matrix that was used with accelerations in equation (177):

$$\begin{bmatrix} \dot{x}_{g_m} \\ \dot{y}_{g_m} \\ \dot{z}_{g_m} \end{bmatrix} = \begin{bmatrix} -\cos\Delta\lambda_L \sin\delta_L & -\sin\Delta\lambda_L \sin\delta_L & -\cos\delta_L \\ \sin\Delta\lambda_L & -\cos\Delta\lambda_L & 0 \\ -\cos\Delta\lambda_L \cos\delta_L & -\sin\Delta\lambda_L \cos\delta_L & \sin\delta_L \end{bmatrix} \begin{bmatrix} \dot{x}_{e_m} \\ \dot{y}_{e_m} \\ \dot{z}_{e_m} \end{bmatrix} \quad (182)$$

Velocities in the wind axes become

$$\dot{x}_w = \dot{x}_{g_m} + V_w \cos\psi \quad (183)$$

$$\dot{y}_w = \dot{y}_{g_m} + V_w \cos\psi \quad (184)$$

and

$$\dot{z}_w = \dot{z}_{g_m} \quad (185)$$

with the assumption that winds are in the local geocentric system.

Aircraft velocity with respect to the airmass is

$$V_t = (\dot{x}_w^2 + \dot{y}_w^2 + \dot{z}_w^2)^{1/2} \quad (186)$$

The two angles, γ, and σ, for use in equation (181) become

$$\gamma = \sin^{-1} \frac{-\dot{z}_w}{V_t} \qquad (187)$$

and

$$\sigma = \tan^{-1} \frac{\dot{y}_w}{\dot{x}_w} \qquad (188)$$

Bank angle may be defined as

$$B = \tan^{-1} \frac{n_{y_{w'}}}{n_{z_{w'}}} \qquad (189)$$

A rotation may then be made through B to obtain load factors in banked flight. Performing the transformation the load factors become, with the aid of equation (189)

$$n_{x_w} = n_{x_{w'}} \qquad (190)$$

$$n_{y_w} = 0 \qquad (191)$$

and

$$n_{z_w} = (n_{y_{w'}}^2 + n_{z_{w'}}^2)^{1/2} \qquad (192)$$

REFERENCES

1. Lush, Kenneth J. Optimum Climb Theory and Techniques of Determining Climb Schedules from Flight Test, AFFTC-TN-56-13, Air Force Flight Test Center, California, February 1956.

2. AGARD Flight Test Manual, Vol I, Pergamon Press, 1962.

3. Walker, Richard C. A Comparison of Several Techniques for Determining Aircraft Test Day Climb Performance, AC-65-7, Flight Research Division Office Memo, Air Force Flight Test Center, California, June 1965.

4. Mahoney, John J. and Bennett, Donald A. A Comparative Evaluation of Three Techniques for Measurement of Level Flight Accelerations, AFFTC TN 54-2, Air Force Flight Test Center, California, 1954.

5. Allen, Willie L. and Weight, Robert H. The Use of Flightpath Accelerometers in Performance Flight Testing, Proceedings of the 13th Annual AF Science and Engineering Symposium, September 1966.

6. Allen, H. Julian, and Perkins, Edward W. A Study of Effects of Viscosity on Flow Over Slender Inclined Bodies of Revolution, NACA Report 1048, Ames Aeronautical Laboratory, California, 1951.

7. Beeler, D. E., et al. Flight Techniques for Determining Airplane Drag at High Mach Numbers, NACA TN3821, NACA High Speed Flight Station, Edwards, California, 1956.

8. Strömungsmebgeräte für den Flugversuch (Flow Measuring Apparatus for Flight Test), Technical Brochure of Donier GmbH, Friedrichshafen, Federal Republic of Germany.

9. Berven, Lester H. Use of Flightpath Accelerometers in Performance Flight Testing: Test Techniques, Data Analysis Methods and Typical Results, AFFTC TIM 69-1001, Air Force Flight Test Center, California, July 1969.

10. Etkin, Bernard. Dynamics of Flight, New York: John Wiley and Sons, Inc. 1959.

11. Dunlap, Everett W. and Porter, Milton B. Accelerations on Aircraft Induced by the Earth's Rotation, FTC-TR-66-38, Air Force Flight Test Center, California, February 1967.

12. Schramm, Roland C. and Scott, Maceo T. Derivative Information Recovery By a Selective Integration Technique (DIRSIT), Technical Memorandum 1040, The Army Missile Test and Evaluation Directorate, White Sands Missile Range, New Mexico, November 1962.

SECTION VI

STANDARD CLIMB SCHEDULES

SUMMARY

Various standard climb schedules are considered (e.g., a segment at constant calibrated airspeed followed by one at constant Mach number). Equations are given to compute the break altitude or juncture of these segments. Climb speed derivatives from which acceleration factors may be computed are derived for each schedule.

TABLE OF CONTENTS

SYMBOLS USED IN THIS SECTION

Symbol	Definition	Units
a	speed of sound	knots or ft/sec
A_f	acceleration factor	dimensionless
A_{fE}	acceleration factor associated with energy height	dimensionless
g_r	reference acceleration due to gravity	ft/sec^2
g_L	local effective acceleration due to gravity	ft/sec^2
H_c	pressure altitude	ft
H_E	energy height	ft
M	flight Mach number	dimensionless
P_a	ambient pressure	in. Hg
q_c	impact pressure	in. Hg
V_c	calibrated airspeed	knots
V_e	equivalent airspeed	knots
V_t	true airspeed	knots
δ_a	ambient pressure ratio	dimensionless
θ_a	ambient temperature ratio	dimensionless
σ	air density ratio	dimensionless

INTRODUCTION

It is desirable to present aircraft performance during a continuous climb for an arbitrary (standard) climb schedule; generally the one which the pilot was attempting to follow. Since climb schedules cannot be followed precisely, large deviations in rates of change of potential and kinetic energies occur, although the sum of the two can usually be expected to change quite uniformly. In order to find rates of climb along an arbitrary climb schedule, acceleration factors together with climb potential (rate of climb for zero acceleration along the flight path) are used as described in the section, Standardization of Performance Parameters. The information required to define standard schedules and to compute acceleration factors is presented in the following paragraphs.

STANDARD CLIMB SCHEDULES

DESCRIPTION OF STANDARD SCHEDULES

In standardizing aircraft performance during continuous climbs, it is desirable to make corrections to an arbitrary (standard) climb schedule; generally the one which the pilot was attempting to follow. Since climb schedules cannot be followed precisely and climb potential may vary rapidly with speed, large corrections may result. The largest corrections should be expected when climbing at a high subsonic speed (typical of best climb speed for high performance aircraft) where drag increases very rapidly when Mach numbers exceed those for best climb.

Four standard climb schedules are considered. These are:

(1) Initial segment at constant V_c with the remainder at constant M

(2) True speed specified as a function of altitude - for any arbitrary schedule with altitude montonic increasing (test and standard altitudes taken to be equal)

(3) Initial segment at constant V_e with the remainder at constant M

(4) True speed specified as a function of altitude - for any arbitrary schedule with altitude permitted to decrease but with H_E monotonic increasing (test and standard energy heights taken to be equal)

Constant Mach number, constant V_c, and constant V_e climbs are not listed since they can be considered as special cases of (1) or (3). Equations pertaining to the standardization of climb performance along each of the above schedules are derived in the following paragraphs.

BREAK ALTITUDE

For schedules (1) or (3) it is convenient, when using a digital computer, to load in desired standard values of speed and Mach number and have the intersection of the two segments of the schedule (break altitude) computed.

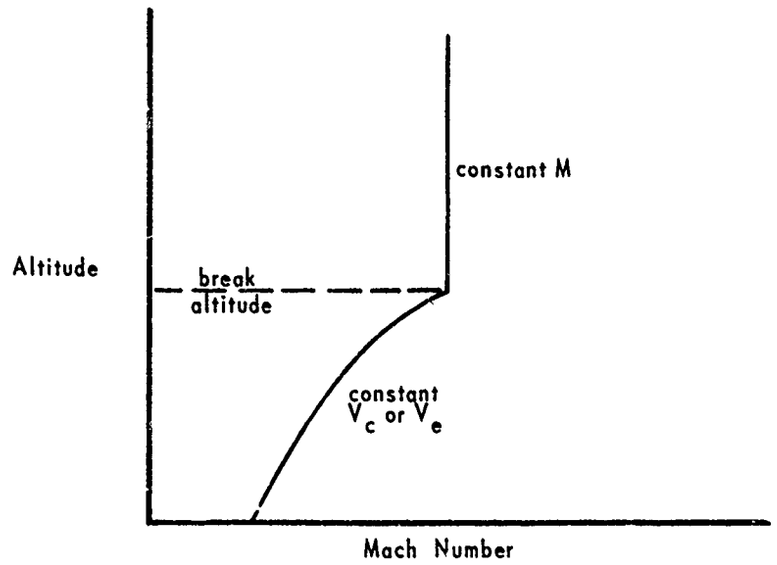

Figure 1 Break Altitude

To do this, combinations of V_c less than or more than a_{SL} and subsonic and supersonic Mach numbers must be considered. (Reference figure 2.) If $V_c > a_{SL}$ then, of course, $M > 1.0$ so that the combination $V_c > a_{SL}$ and $M < 1.0$ cannot exist. Break altitudes for the three remaining combinations of V_c and M are derived as follows:

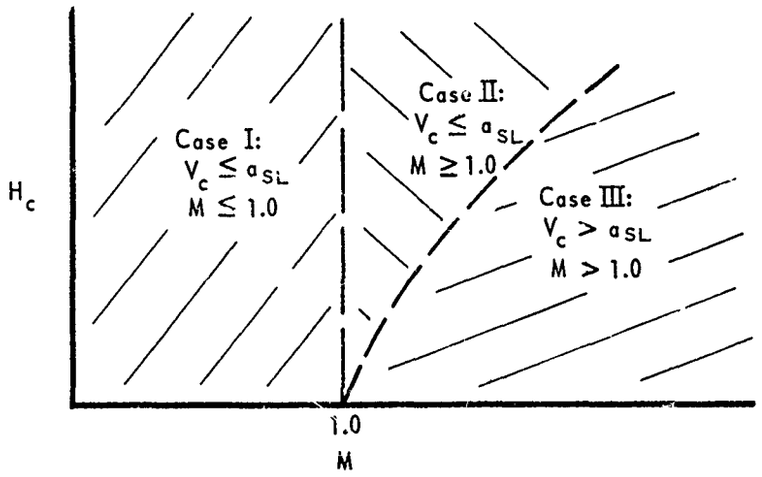

Figure 2 Combinations of V_c and M

CASL I ($V_c \leq a_{SL}$, $M \leq 1.0$)

Substituting $\gamma = 1.40$ in equation (21) of the section, Flight Parameters from Sensed Environment.

$$\frac{q_c}{P_a} = \left[1 + 0.2M^2\right]^{3.5} - 1 \qquad (1)$$

To find the common value of q_c/P_a and hence the break altitude

the above equation is equated to the corresponding relation containing calibrated airspeed

$$\frac{q_c}{P_a} = \frac{1}{\delta_a}\left\{\left[1 + 0.2\left(\frac{V_c}{a_{SL}}\right)^2\right]^{3.5} - 1\right\} \qquad (2)$$

which follows from equation (9) of the section, Flight Parameters from Sensed Environment.

$$\frac{1}{\delta_a}\left\{\left[1 + 0.2\left(\frac{V_c}{a_{SL}}\right)^2\right]^{3.5} - 1\right\} = (1 + 0.2M^2)^{3.5} - 1 \qquad (3)$$

From which

$$\delta_a = \frac{\left[1 + 0.2\left(\frac{V_c}{a_{SL}}\right)^2\right]^{3.5} - 1}{(1 + 0.2M^2)^{3.5} - 1} \qquad (4)$$

δ_a can then be easily converted into altitude. For example, from equation (14) in the section, Atmospheric Environment, for the troposphere in the U.S. 1962 atmosphere

$$H_c = \frac{1 - \delta_a^{1/5.2559}}{6.87558 \times 10^{-6}} \qquad (5)$$

CASE II ($V_c \leq a_{SL}$, $M > 1.0$)

Following the same procedure, from equations (2) and (8) from the section, Flight Parameters from Sensed Environment.

$$\delta_a = \frac{\left[1 + 0.2\left(\frac{V_c}{a_{SL}}\right)^2\right]^{3.5} - 1}{\frac{166.921\,M^7}{(7M^2 - 1)^{2.5}} - 1} \tag{6}$$

CASE III ($V_c > a_{SL}$, $M > 1.0$)

As before, from equations (8) and (10) of the same section

$$\delta_a = \frac{\frac{166.921\left(\frac{V_c}{a_{SL}}\right)^7}{\left[7\left(\frac{V_c}{a_{SL}}\right)^2 - 1\right]^{2.5}} - 1}{\frac{166.921\,M^7}{(7M^2 - 1)^{2.5}} - 1} \tag{7}$$

The break altitude for a constant V_e - constant M schedule can be found more readily. Equation (13), also from the same section, may be restated as

$$V_e = aM\sqrt{\sigma} \tag{8}$$

The velocity of sound in a perfect gas is proportional to the square root of the temperature so that

$$\frac{a}{a_{SL}} = \sqrt{\theta_a} \tag{9}$$

From the perfect gas law $\delta_a = \sigma\theta_a$. Substituting this relationship and equation (9) in equation (8)

$$V_e = a_{SL} M \sqrt{\delta_a} \tag{10}$$

Solving for δ_a

$$\delta_a = \left(\frac{V_e}{a_{SL} M}\right)^2 \tag{11}$$

The break altitude may then be computed, as for the constant V_c - constant M schedule, from equation (5) or other appropriate δ_a - H relation for a given atmospheric layer. Equation (11) is valid for all values of M and V_e.

AIRSPEED-MACH NUMBER RELATIONSHIPS

The airspeed - Mach number relationships which are needed for climbs are presented below. For example, when using schedule (1), Mach numbers at the test altitudes along the constant V_c portion of the climb are desired; conversely, when a constant Mach number is specified the corresponding calibrated airspeeds are desired.

The equations that were used to determine break altitudes for the same combinations of V_c and M are used to calculate both V_c and M.

CALIBRATED AIRSPEED AND MACH NUMBER ($V_c \leq a_{SL}$, $M \leq 1.0$)

V_c is, solving equation (3)

$$V_c = a_{SL}\sqrt{5}\left(\left\{\delta_a\left[(1+0.2M^2)^{3.5}-1\right]+1\right\}^{2/7}-1\right)^{1/2} \qquad (12)$$

and M is

$$M = \sqrt{5}\left(\left\{\frac{\left[1+0.2\left(\frac{V_c}{a_{SL}}\right)^2\right]^{3.5}-1}{\delta_a}+1\right\}^{2/7}-1\right)^{1/2} \qquad (13)$$

CALIBRATED AIRSPEED AND MACH NUMBER ($V_c \leq a_{SL}$, $M > 1.0$)

Solving equation (6) V_c is

$$V_c = a_{SL}\sqrt{5}\left(\left\{\delta_a\left[\frac{166.921M^7}{(7M^2-1)^{2.5}}-1\right]+1\right\}^{2/7}-1\right)^{1/2} \qquad (14)$$

and M is

$$M = \left[\frac{1}{166.921}\left(\frac{1}{\delta_a}\left\{\left[1+0.2\left(\frac{V_c}{a_{SL}}\right)^2\right]^{3.5}-1\right\}+1\right)(7M^2-1)^{5/2}\right]^{1/7} \qquad (15)$$

In this case an iterative solution for M must be made since equation (7) cannot be solved explicitly.

CALIBRATED AIRSPEED AND MACH NUMBER ($V_c > a_{SL}$, $M > 1.0$)

Solving equation (7) for V_c

$$V_c = a_{SL}\left(\frac{1}{166.921}\left\{\delta_a\left[\frac{166.921\,M^7}{(7M^2-1)^{2.5}}+1\right]+1\right\}\left[7\left(\frac{V_c}{a_{SL}}\right)^2-1\right]^{2.5}\right)^{1/7} \quad (16)$$

In this case also, V_c must be found through an iterative procedure. M from equation (7) is

$$M = \left[\frac{1}{166.921}\left(\frac{1}{\delta_a}\left\{\frac{166.921\left(\frac{V_c}{a_{SL}}\right)^7}{\left[7\left(\frac{V_c}{a_{SL}}\right)^2-1\right]^{2.5}}-1\right\}+1\right)(7M^2-1)^{5/2}\right]^{1/7} \quad (17)$$

Here again an iterative procedure is needed to find it.

V_c may be found for the remaining schedules by first converting V_e or V_t to M and then using equation (12), (14), or (16) as appropriate.

CLIMB SPEED DERIVATIVE, dV_t/dH_c

The acceleration factors discussed in the section, Standardization of Performance Parameters, and defined by the equations

$$A_f = \frac{g_L}{g_r}\left(1+\frac{V_t}{g_r}\frac{dV_t}{dH_c}\right) \quad (18a)$$

and

$$A_{fE} = \frac{g_r}{g_L}\left(1-\frac{V_t}{g_r}\frac{dV_t}{dH_E}\right) \quad (18b)$$

are of importance in establishing climb performance. With them, rate of climb along the standard climb schedule may be found from standardized excess thrust. Values of dV_t/dH_c for the

various combinations of V_c and M are derived in the following paragraphs for a constant V_c.

CLIMB SPEED DERIVATIVE, dV_t/dH_c, ($V_c \leq a_{SL}$, $M \leq 1.0$)

From differentiation of the relation $V_t = aM$

$$\frac{dV_t}{dH_c} = M\frac{da}{dH_c} + a\frac{dM}{dH_c} \tag{19}$$

Since V_c/a_{SL} is constant with respect to the differentiation indicated, the term

$$\left[1 + 0.2\left(\frac{V_c}{a_{SL}}\right)^2\right]^{3.5} - 1$$

in equation (13) may be replaced K_1 to give

$$M = \sqrt{5}\left[\left(\frac{K_1}{\delta_a} + 1\right)^{2/7} - 1\right]^{1/2} \tag{20}$$

Differentiation with respect to H_c produces

$$\frac{dM}{dH_c} = -\frac{5K_1\frac{d\delta_a}{dH_c}}{7\delta_a{}^2M\left(\frac{K_1}{\delta_a} + 1\right)^{5/7}} \tag{21}$$

Equation (21) might be used, substituting it in equation (19); a more simple form may be derived, however. From the definition of K_1

$$\left(\frac{M^2}{5} + 1\right)^{3.5} = \frac{K_1}{\delta_a} + 1 \tag{22}$$

Substituting in equation (21)

$$\frac{dM}{dH_c} = -\frac{5\left[(1 + 0.2M^2)^{3.5} - 1\right]\frac{d\delta_a}{dH_c}}{7\delta_a M(1 + 0.2M^2)^{2.5}} \tag{23}$$

But

$$\frac{1}{\delta_a}\frac{d\delta_a}{dH_c} = \frac{d(\ln \delta_a)}{dH_c}$$

so that substitution in equation (19) produces

$$\frac{dV_t}{dH_c} = M\frac{da}{dH_c} - \frac{5a\left[(1 + 0.2M^2)^{3.5} - 1\right]}{7M(1 + 0.2M^2)^{2.5}}\frac{d(\ln \delta_a)}{dH_c} \tag{24}$$

The derivatives da/dH_c and $d(\ell n\ \delta_a)/dH_c$ are presented in subsequent paragraphs.

CLIMB SPEED DERIVATIVE, dV_t/dH_c, ($V_c \leq a_{SL}$, $M > 1.0$)

Equation (15) may be rewritten as

$$166.921M^7 = \left(\frac{K_1}{\delta_a} + 1\right)(7M^2 - 1)^{2.5} \tag{25}$$

Differentiating and collecting terms

$$\frac{dM}{dH_c}\left[7 \times 166.921M^6 - 35M\left(\frac{K_1}{\delta_a} + 1\right)(7M^2 - 1)^{1.5}\right] = -\frac{K_1}{\delta_a}(7M^2 - 1)^{2.5}\frac{d(\ln \delta_a)}{dH_c} \tag{26}$$

Substituting for K_1 from equation (25) and rearranging

$$\frac{dM}{dH_c} = -\frac{\left[166.921M^7 - (7M^2 - 1)^{2.5}\right](7M^2 - 1)\frac{d(\ln \delta_a)}{dH_c}}{1168.45M^6(2M^2 - 1)} \tag{27}$$

Substituting, as before, in equation (19)

$$\frac{dV_t}{dH_c} = M\frac{da}{dH_c} - \frac{a\left[166.921M^7 - (7M^2 - 1)^{2.5}\right](7M^2 - 1)}{1168.45M^6(2M^2 - 1)}\frac{d(\ln \delta_a)}{dH_c} \tag{28}$$

CLIMB SPEED DERIVATIVE, dV_t/dH_c, ($V_c > a_{SL}$, $M > 1.0$)

Rewriting equation (17)

$$166.921M^7 = \left(\frac{1}{\delta_a}\left\{\frac{166.921(\frac{V_c}{a_{SL}})^7}{[7(\frac{V_c}{a_{SL}})^2 - 1]^{2.5}} - 1\right\} + 1\right)(7M^2 - 1)^{2.5} \tag{29}$$

or

$$166.921M^7 = (\frac{K_2}{\delta_a} + 1)(7M^2 - 1)^{2.5} \tag{30}$$

where

$$K_2 = \frac{166.921(\frac{V_c}{a_{SL}})^7}{[7(\frac{V_c}{a_{SL}})^2 - 1]} - 1 \tag{31}$$

Since the form of equation (30) is the same as that of equation (25) the same final equation for dV_t/dH_c will also apply

in this case. Repeating equation (28)

$$\frac{dV_t}{dH_c} = M\frac{da}{dH_c} - \frac{a[166.921M^7 - (7M^2-1)^{2.5}](7M^2-1)}{1168.45M^6(2M^2-1)}\frac{d(\ln\delta_a)}{dH_c} \qquad (32)$$

CLIMB SPEED DERIVATIVE, dV_t/dH_c, (V_c not constant)

Values of dV_t/dH_c during a climb at constant V_e (as during schedule (3)) may be found from differentiation of $V_t = V_e/\sqrt{\sigma}$ to obtain

$$\frac{dV_t}{dH_c} = -\frac{V_e}{2\sigma^{3/2}}\frac{d\sigma}{dH_c} \qquad (33)$$

For the cases where V_t is specified as a function of H_c (schedules (2) and (4)) dV_t/dH_c or dV_t/dH_E must be found by numerical differentiation since they cannot be calculated by analytic means.

When Mach number is maintained constant equation (19) reduces to

$$\frac{dV_t}{dH_c} = M\frac{da}{dH_c} \qquad (34)$$

and values of da/dH_c, as for constant V_c climbs, are found from the following equations.

SPEED OF SOUND DERIVATIVE, da/dH_c

The following equations are given as an aid in computing dV_t/dH_c and are to be used in equations (24), (28), and (32). Differentiating equation (4) from the section Atmospheric Environment, with respect to H_c

$$\frac{da}{dH_c} = \frac{1}{2}\left(\frac{\gamma R}{T_a}\right)^{1/2} \frac{dT_a}{dH_c} \tag{35}$$

Substituting equation (12) from the section Atmospheric Environment, with H replaced by H_c and L_M for dT_a/dH_c

$$\frac{da}{dH_c} = \frac{L_M}{2}\left[\frac{\gamma R}{(T_a)_b + L_M(H_c - H_b)}\right]^{1/2} \tag{36}$$

Substituting constants appropriate to the U.S. 1962 atmosphere

$$\frac{da}{dH_c} = -\frac{0.0651520}{(288.15 - 0.0019812 H_c)^{1/2}} \tag{37}$$

in units of feet/sec/foot for $-16{,}404.20 \leq H_c \leq 36{,}089.24$ feet

$$\frac{da}{dH_c} = 0 \tag{38}$$

for $36{,}089.24 \leq H_c \leq 65{,}616.80$ feet

$$\frac{da}{dH_c} = \frac{0.0100234}{[216.65 + 0.0003048(H_c - H_b)]^{1/2}} \qquad (39)$$

for $65,616.80 \leq H_c \leq 104,986.88$ feet and

$$\frac{da}{dH_c} = \frac{0.0280641}{[228.65 + 0.0008534(H_c - H_b)]^{1/2}} \qquad (40)$$

for $104,986.88 \leq H_c \leq 154,199.48$ feet

PRESSURE RATIO DERIVATIVE, $d(\ln \delta_a)/dH_c$

The following equations are given as an aid in computing dV_t/dH_c and are to be used in equations (24), (28), and (32).

Equation (16) from the section, Atmospheric Environment, may be rewritten as

$$\delta_a = \frac{(P_a)_b}{P_{a_{SL}}}\left[1 + \frac{L_M}{(T_a)_b}(H_c - H_b)\right]^{-g_{SL}/RL_M} \qquad (41)$$

or taking the logarithm

$$\ln \delta_a = -\frac{g_{SL}}{RL_M} \ln \frac{(P_a)_b}{P_{a_{SL}}}\left[1 + \frac{L_M}{(T_a)_b}(H_c - H_b)\right] \qquad (42)$$

Differentiating with respect to H_c

$$\frac{d(\ln \delta_a)}{dH_c} = -\frac{g_{SL}}{R(T_a)_b} \frac{1}{\left[1 + \frac{L_M}{(T_a)_b}(H_c - H_b)\right]} \tag{43}$$

when $L_M \neq 0$.

Taking logs of equation (17) from the section, Atmospheric Environment

$$\ln \delta_a = \ln \frac{(P_a)_b}{P_{a_{SL}}} - \frac{g_{SL}(H_c - H_b)}{R(T_a)_b} \tag{44}$$

Differentiating with respect to H_c

$$\frac{d(\ln \delta_a)}{dH_c} = -\frac{g_{SL}}{R(T_a)_b} \tag{45}$$

when $L_M = 0$.

Substituting constants appropriate to the U.S. 1962 atmosphere

$$\frac{d(\ln \delta_a)}{dH_c} = -0.361374 \times 10^{-4} \left[\frac{1}{1 - 6.875586 \times 10^{-6} H_c}\right] \tag{46}$$

in units of $feet^{-1}$ for $-16,404.20 \leq H_c \leq 36,089.24$ feet

$$\frac{d(\ln \delta_a)}{dH_c} = -0.480637 \times 10^{-4} \tag{47}$$

for $36,089.24 \leq H_c \leq 65,616.80$ feet

$$\frac{d(\ln \delta_a)}{dH_c} = -0.480637 \times 10^{-4}\left[\frac{1}{1 + 1.40688 \times 10^{-6}(H_c - 65{,}616.80)}\right] \quad (48)$$

for $65{,}616.80 \leq H_c \leq 104{,}986.88$ feet and

$$\frac{d(\ln \delta_a)}{dH_c} = -0.455412 \times 10^{-4}\left[\frac{1}{1 + 3.73252 \times 10^{-6}(H_c - 104{,}986.88)}\right] \quad (49)$$

for $104{,}986.88 \leq H_c \leq 154{,}199.48$ feet

DENSITY RATIO DERIVATIVE, $d\sigma/dH_c$

The following equations are listed to provide assistance in computing dV_t/dH_c when V_e is constant, as in equation 33. After differentiating equations (19) and (20) from the section, Atmospheric Environment, we have, after substitution of appropriate constants from the 1962 atmosphere

$$\frac{d\sigma}{dH_c} = -2.92618 \times 10^{-5}(1 - 6.87558 \times 10^{-6} H_c)^{3.2559} \quad (50)$$

in units of feet^{-1} for $-16{,}404.20 \leq H_c \leq 36{,}089.24$ feet

$$\frac{d\sigma}{dH_c} = -1.42785 \times 10^{-5}\exp[-4.80637 \times 10^{-5}(H_c - 36089.24)] \quad (51)$$

for $36{,}089.24 \leq H_c \leq 65{,}616.80$ feet

$$\frac{d\sigma}{dH_c} = -3.55517 \times 10^{-6}[1 + 1.40688 \times 10^{-6}(H_c - 65616.8)]^{-36.1634} \quad (52)$$

for $65,616.8 \leq H_c \leq 104,986.88$ feet and

$$\frac{d\sigma}{dH_c} = -5.31944 \times 10^{-7}[1 + 3.73252 \times 10^{-6}(H_c - 104986.88)]^{-14.2012} \quad (53)$$

for $104986.88 \leq H_c \leq 154,199.48$ feet.

SECTION VII

STANDARDIZATION OF EXCESS THRUST

SUMMARY

Standard excess thrust is found by extrapolating to a set of standard conditions using a Taylor series expansion. From a functional statement defining excess thrust and the equations of motion, partial derivatives of excess thrust with respect to each of the independent variables have been found. The terms are collected into an equation which may be used for both climbs and level accelerations. This has been done for first order terms, which, it is expected, will generally be sufficient; second order terms have been derived so that they may be included if their magnitude warrants it. The standardization equation cannot be solved directly, and an iteration procedure is needed. A description of it is included.

TABLE OF CONTENTS

SYMBOLS USED IN THIS SECTION

Symbol	Definition	Units
C_D	airplane total drag coefficient	dimensionless
C_L	airplane lift coefficient	dimensionless
cg	center of gravity	pct MAC
F_e	engine ram drag	lb
F_{ex}	excess thrust	lb
F_g	gross thrust	lb
F_n	net thrust	lb
g	acceleration due to gravity	ft/sec^2
g_r	reference acceleration due to gravity	ft/sec^2
h	tapeline altitude	ft
H_c	pressure altitude	ft
i_F	thrust angle of incidence	rad
M	flight Mach Number	dimensionless
n_{z_w}	load factor along negative wind z-axis	dimensionless
P_a	ambient pressure	in. Hg
q	dynamic pressure	lb/ft^2
r	local radius of the earth	ft
S	wing area	ft^2
t	time	sec
T_a	ambient temperature	deg K
V_t	true airspeed	knots
W	airplane gross weight	lb

α	angle of attack	rad
γ	flightpath climb angle measured from the geocentric horizontal plane	rad
γ_D	flightpath climb angle measured from the geodetic horizontal plane	rad
δ_L	aircraft geocentric latitude	rad
σ	flightpath heading angle	rad
$\omega_\oplus$	angular velocity of the earth	rad/sec

Subscripts

s	standard day conditions	--
t	test day conditions	--
$(\dot{})$	dot denotes first derivative of a quantity with respect to time	--

INTRODUCTION

The test excess thrust, computed by one of the methods outlined in the section, Determination of Excess Thrust, is extrapolated to a set of standard conditions. In the following analysis, excess thrust is taken to be sensitive to the following parameters: (1) temperature, (2) weight, (3) Mach number, (4) pressure or altitude, (5) normal load factor, (6) power setting, and (7) center of gravity. Of these variables the first five obviously have a bearing on thrust and/or drag and hence on excess thrust. Adjustments to excess thrust for changes in power setting would not be made in most cases but might be desirable for a variety of reasons; for example, a correction may be needed to account for a power lever which has been improperly rigged. Inlet total pressure ratio was not included as an independent variable since it was considered to be a function solely of Mach number, which has been treated as an independent variable. This assumption can, in general, be made quite satisfactorily. As speed is increased and a Mach number of perhaps three is reached, total pressure ratio may become a function of other variables as well as Mach number. In this event, appropriate functional statements, depending on the particular installation, need to be written and corrections to excess thrust made for variations in total pressure ratio.

Standardization of excess thrust is accomplished by first expanding excess thrust in a Taylor series about the test day

point through the first order terms. Then the development of expressions for the partial derivatives of excess thrust with respect to each of the variable test conditions is presented. Next, the equation for the standard excess thrust in terms of flight test data is developed. Finally, a more precise equation for standard excess thrust is derived by following the above steps but carrying the Taylor series expansion through the second order terms.

TAYLOR SERIES EXPANSION OF EXCESS THRUST-FIRST ORDER TERMS

The two equations of motion resulting from force balances along and normal to the airplane's velocity vector are basic to derivatives in the following paragraphs. Excess thrust, from the longitudinal equation of motion is*

$$F_{ex} = F_n \cos(\alpha + i_F) - qSC_D \qquad (1)$$

and the equation of motion normal to the flightpath is

$$qSC_L = n_z W - F_g \sin(\alpha + i_F) \qquad (2)$$

Equation (1) is examined to determine a functional relationship for excess thrust. It is well known that net thrust depends on ambient temperature, Mach number, and pressure (altitude). Power setting, π, is also included so that changes in

*The excess thrust is, properly, $F_g\cos(\alpha+i_F)-F_e-qSC_D$. This is quite a satisfactory approximation, however, and simplifies the following derivations.

power lever angle or other measure of power setting can be made. Hence, $F_n = f(T_a, M, P_a, \pi)$. Both C_L and C_D may be expressed as functions of α, M, and cg ($C_L=f(\alpha, M, cg)$ and $C_D=f(\alpha, M, cg)$) with the center of gravity included to account for changes in trim drag. It is more convenient, however, to express drag coefficient as $C_D=f(C_L, M, cg)$. From these relationships

together with $q=0.7P_aM^2$ and $C_L = \frac{n_z W - F_g \sin(\alpha + i_F)}{qS}$ from equation (2), excess thrust may be completely defined by the functional statement

$$F_{ex} = f(T_a, W, M, P_a, n_z, \pi, cg) \qquad (3)$$

A Taylor series expansion of the excess thrust about the test day point results in the expression for standard excess thrust:

$$\begin{aligned} F_{ex_s} = F_{ext} &+ \frac{\partial F_{ext}}{\partial T_a}(T_{as} - T_{at}) + \frac{\partial F_{ext}}{\partial W}(W_s - W_t) \\ &+ \frac{\partial F_{ext}}{\partial M}(M_s - M_t) + \frac{\partial F_{ext}}{\partial P_a}(P_{as} - P_{at}) \\ &+ \frac{\partial F_{ex}}{\partial n_z}(n_{z_s} - n_{z_t}) + \frac{\partial F_{ex}}{\partial \pi}(\pi_s - \pi_t) \\ &+ \frac{\partial F_{ex}}{\partial cg}(cg_s - cg_t) + \text{higher order terms} \end{aligned} \qquad (4)$$

Magnitudes of the higher order terms are less than those of the first order terms but will, at some test conditions, be significant. The partial derivatives in equation (4) are

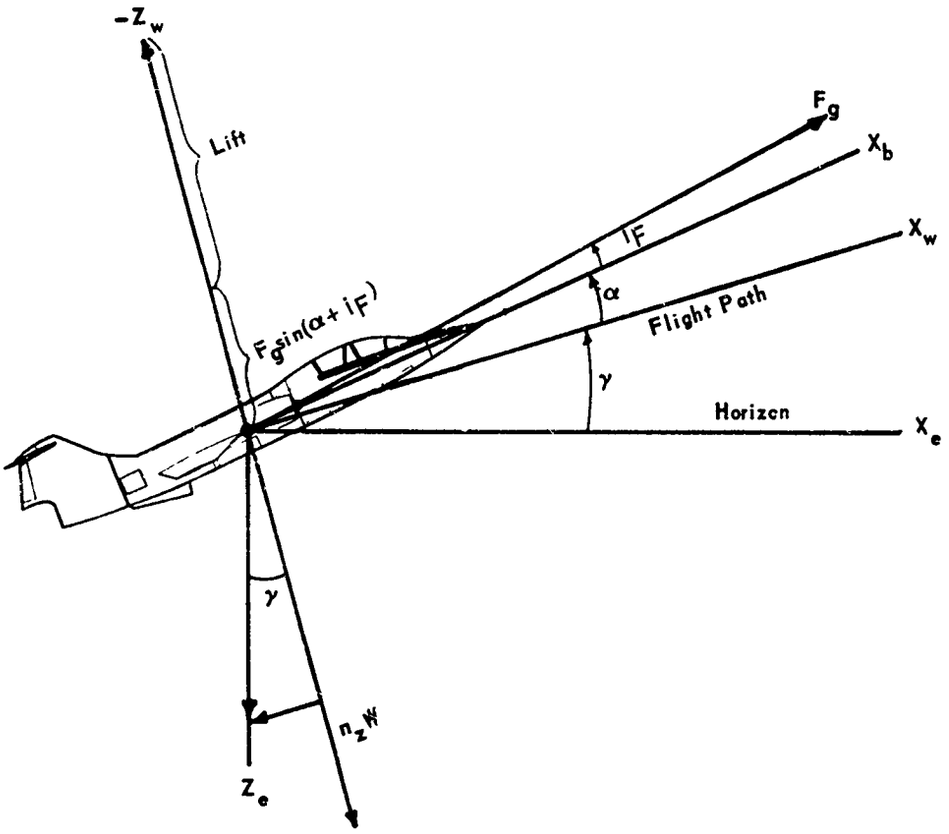

Figure 1 Forces Normal to the Flight Path

evaluated first, and then attention is given to the second order terms.

VARIATION OF EXCESS THRUST WITH TEST CONDITIONS

The partial derivatives in equation (4) are found by differentiating equation (1) with respect to each of the independent variables. It is important to note that, in each case, the normal equation of motion (equation (2)) provides a constraint on the equation for excess thrust. The angle of attack must vary in such a manner that both equations are satisfied simultaneously.

Temperature

To determine how excess thrust varies with temperature, the relationship $q=0.7P_aM^2$ is used and the partial derivative of equation (1) taken with respect to temperature:

$$\frac{\partial F_{ex}}{\partial T_a} = \cos(\alpha + i_F)\frac{\partial F_n}{\partial T_a} - F_n\sin(\alpha + i_F)\frac{\partial \alpha}{\partial T_a} - 0.7P_aM^2S\frac{\partial C_D}{\partial T} \qquad (5)$$

The reason thrust varies with ambient temperature is well known; however, the dependence of angle of attack and drag coefficient on temperature requires an explanation.

Figure 1 shows a component of thrust in the direction of the lift vector. If the thrust is varied, then the angle of attack must vary to adjust the lift to the new condition. The changes in angle of attack and lift cause a change in the induced drag similar to that caused by a weight change.

Chain rule differentiation of $\alpha = f(C_L, M, cg)$ with M and cg held constant produces

$$\frac{\partial \alpha}{\partial T_a} = \frac{\partial \alpha}{\partial C_L}\frac{\partial C_L}{\partial T_a} \tag{6}$$

and similarly

$$\frac{\partial C_D}{\partial T_a} = \frac{\partial C_D}{\partial C_L}\frac{\partial C_L}{\partial T_a} \tag{7}$$

Equation

$$\frac{\partial F_{ex}}{\partial T_a} = \cos(\alpha + i_F)\frac{\partial F_n}{\partial T_a} - \left[F_n \sin(\alpha + i_F)\frac{\partial \alpha}{\partial C_L} + qS\frac{\partial C_D}{\partial C_L}\right]\frac{\partial C_L}{\partial T_a} \tag{8}$$

The partial of the lift coefficient with respect to temperature is found by differentiating the equation of motion normal to the flight path:

$$qS\frac{\partial C_L}{\partial T_a} = -\sin(\alpha + i_F)\frac{\partial F_n}{\partial T_a} - F_n \cos(\alpha + i_F)\frac{\partial \alpha}{\partial T_a} \tag{9}$$

Again using the transformation expressed by equation (6):

$$\frac{\partial C_L}{\partial T_a} = -\frac{\sin(\alpha + i_F)\frac{\partial F_n}{\partial T_a}}{qS + F_n \cos(\alpha + i_F)\frac{\partial \alpha}{\partial C_L}} \tag{10}$$

The equation for the variation of excess thrust with temperature is found by substituting equation (10) in equation (8).

$$\frac{\partial F_{ex}}{\partial T_a} = \cos(\alpha + i_F)\frac{\partial F_n}{\partial T_a} + \sin(\alpha + i_F)\frac{\partial F_g}{\partial T_a}\,\frac{F_n \sin(\alpha + i_F) + qS\dfrac{\partial C_D}{\partial \alpha}}{F_g \cos(\alpha + i_F) + qS\dfrac{\partial C_L}{\partial \alpha}} \qquad (11)$$

Weight

The partial derivative of excess thrust with respect to weight using equation (1) as the expression for excess thrust is

$$\frac{\partial F_{ex}}{\partial W} = -F_n \sin(\alpha + i_F)\frac{\partial \alpha}{\partial W} - qS\frac{\partial C_D}{\partial W} \qquad (12)$$

Again transforming variables through chain rule differentiation with M and $c\sigma$ constant:

$$\frac{\partial \alpha}{\partial W} = \frac{\partial \alpha}{\partial C_L}\frac{\partial C_L}{\partial W} \qquad (13)$$

and

$$\frac{\partial C_D}{\partial W} = \frac{\partial C_D}{\partial C_L}\frac{\partial C_L}{\partial W} \qquad (14)$$

Substituting these transformations into equation (12) and rearranging:

$$\frac{\partial F_{ex}}{\partial W} = -\left[\frac{F_n}{\dfrac{\partial C_L}{\partial \alpha}}\sin(\alpha + i_F) + qS\frac{\partial C_D}{\partial C_L}\right]\frac{\partial C_L}{\partial W} \qquad (15)$$

The partial of the lift coefficient with respect to weight is found by differentiating equation (2).

$$qS\frac{\partial C_L}{\partial W} = n_z - F_g \cos(\alpha + i_F)\frac{\partial \alpha}{\partial W} \qquad (16)$$

Substituting equation (13) in equation (16) we have

$$\frac{\partial C_L}{\partial W} = \frac{n_z}{\frac{F_g}{\frac{\partial C_L}{\partial \alpha}}\cos(\alpha + i_F) + qS} \tag{17}$$

The general expression for the variation of excess thrust with weight from equations (17) and (15) is

$$\frac{\partial F_{ex}}{\partial W} = + - \left[\frac{F_n \sin(\alpha + i_F) + qS\frac{\partial C_D}{\partial \alpha}}{F_g \cos(\alpha + i_F) + qS\frac{\partial C_L}{\partial \alpha}}\right] n_z \tag{18}$$

Mach Number

Inserting the relationship $q=0.7P_aM^2$ in equation (1) and differentiating, we have

$$\frac{\partial F_{ex}}{\partial M} = \frac{\partial F_n}{\partial M}\cos(\alpha + i_F) - F_n \sin(\alpha + i_F)\frac{\partial \alpha}{\partial M} - \frac{2qSC_D}{M} - qS\frac{\partial C_D}{\partial M} \tag{19}$$

Holding cg constant, C_D is a function of M and α, but α is dependent on M so that

$$C_D = f\left[M, \alpha(M)\right] \tag{20}$$

Differentiation of equation (20) with respect to M yields

$$\frac{\partial C_D}{\partial M} = \frac{\partial C_D}{\partial M}\bigg|_\alpha \frac{\partial M}{\partial M} + \frac{\partial C_D}{\partial \alpha}\bigg|_M \frac{\partial \alpha}{\partial M}$$

which reduces to

$$\frac{\partial C_D}{\partial M} = \frac{\partial C_D}{\partial M}\bigg|_\alpha + \frac{\partial C_D}{\partial \alpha}\bigg|_M \frac{\partial \alpha}{\partial M} \tag{21}$$

Differentiating equation (2)

$$\frac{2C_L qS}{M} + qS\frac{\partial C_L}{\partial M} = -\left[\frac{\partial F_g}{\partial M}\sin(\alpha + i_F) + F_g\cos(\alpha + i_F)\frac{\partial \alpha}{\partial M}\right] \qquad (22)$$

Equations similar to (20) and (21) may be written with C_L in place of C_D. Substituting in equation (22)

$$\frac{2C_L qS}{M} + qS\left(\frac{\partial C_L}{\partial M}\bigg|_\alpha + \frac{\partial C_L}{\partial \alpha}\bigg|_M \frac{\partial \alpha}{\partial M}\right) = -\left[\frac{\partial F_g}{\partial M}\sin(\alpha + i_F) + F_g\cos(\alpha + i_F)\frac{\partial \alpha}{\partial M}\right] \qquad (23)$$

Solving for $\frac{\partial \alpha}{\partial M}$

$$\frac{\partial \alpha}{\partial M} = -\left[\frac{\frac{2C_L qS}{M} + qS\frac{\partial C_L}{\partial M}\Big|_\alpha + \frac{\partial F_g}{\partial M}\sin(\alpha + i_F)}{F_g\cos(\alpha + i_F) + qS\frac{\partial C_L}{\partial \alpha}\Big|_M}\right] \qquad (24)$$

Substitution of equation (21) in equation (19) yields

$$\frac{\partial F_{ex}}{\partial M} = \frac{\partial F_n}{\partial M}\cos(\alpha + i_F) - \frac{2C_D qS}{M} - qS\frac{\partial C_D}{\partial M}\Big|_\alpha - \left[F_n\sin(\alpha + i_F) + \frac{\partial C_D}{\partial \alpha}\Big|_M qS\right]\frac{\partial \alpha}{\partial M} \qquad (25)$$

Finally, after substitution of equation (24) in equation (25)

$$\frac{\partial F_{ex}}{\partial M} = \frac{\partial F_n}{\partial M}\cos(\alpha + i_F) - \frac{2C_D qS}{M} - qS\frac{\partial C_D}{\partial M}\Big|_\alpha + \left[F_n\sin(\alpha + i_F) + \frac{\partial C_D}{\partial \alpha}\Big|_M qS\right]\left[\frac{\frac{2C_L qS}{M} + qS\frac{\partial C_L}{\partial M}\Big|_\alpha + \frac{\partial F_g}{\partial M}\sin(\alpha + i_F)}{F_g\cos(\alpha + i_F) + qS\frac{\partial C_L}{\partial \alpha}\Big|_M}\right] \qquad (26)$$

Pressure

Taking the derivative of equation (1) with respect to pressure

$$\frac{\partial F_{ex}}{\partial P_a} = \cos(\alpha + i_F)\frac{\partial F_n}{\partial P_a} - F_n \sin(\alpha + i_F)\frac{\partial \alpha}{\partial P_a} - \frac{qSC_D}{P_a} - qS\frac{\partial C_D}{\partial P_a} \quad (27)$$

Substituting the transformation of variables produced by the same method as previously used

$$\frac{\partial \alpha}{\partial P_a} = \frac{\partial \alpha}{\partial C_L}\frac{\partial C_L}{\partial P_a} \quad (28)$$

and

$$\frac{\partial C_D}{\partial P_a} = \frac{\partial C_D}{\partial C_L}\frac{\partial C_L}{\partial P_a} \quad (29)$$

results in

$$\frac{\partial F_{ex}}{\partial P_a} = \cos(\alpha + i_F)\frac{\partial F_n}{\partial P_a} - \frac{qSC_D}{P_a} - \left[F_n \sin(\alpha + i_F)\frac{\partial \alpha}{\partial C_L} + qS\frac{\partial C_D}{\partial C_L}\right]\frac{\partial C_L}{\partial P_a} \quad (30)$$

The partial derivative of lift coefficient with respect to pressure is evaluated from the equation of motion normal to the flightpath. Differentiating equation (2)

$$qS\frac{\partial C_L}{\partial P_a} + \frac{qSC_L}{P_a} = -\frac{\partial F_g}{\partial P_a}\sin(\alpha + i_F) - F_g \cos(\alpha + i_F)\frac{\partial \alpha}{\partial P_a} \quad (31)$$

Using the transformation

$$\frac{\partial \alpha}{\partial P_a} = \frac{\partial \alpha}{\partial C_L}\frac{\partial C_L}{\partial P_a} \tag{32}$$

equation (31) becomes, after rearranging

$$\frac{\partial C_L}{\partial P_a} = -\frac{\frac{\partial F_g}{\partial P_a}\sin(\alpha + i_F) + \frac{qSC_L}{P_a}}{F_g \cos(\alpha + i_F)\frac{\partial \alpha}{\partial C_L} + qS} \tag{33}$$

Substituting equation (33) in equation (30) we have the general expression for the change in thrust with pressure.

$$\frac{\partial F_{ex}}{\partial P_a} = \cos(\alpha + i_F)\frac{\partial F_n}{\partial P_a} - \frac{qSC_D}{P_a} - \left[\frac{F_n \sin(\alpha + i_F) + qS\frac{\partial C_D}{\partial \alpha}}{F_g \cos(\alpha + i_F) + qS\frac{\partial C_L}{\partial \alpha}}\right]\left[\frac{\partial F_g}{\partial P_a}\sin(\alpha + i_F) + \frac{qSC_L}{P_a}\right] \tag{34}$$

It may be more convenient to make the transformation

$$\frac{\partial F_n}{\partial P_a} = \frac{\partial F_n}{\partial H_c}\frac{\partial H_c}{\partial P_a} \tag{35}$$

and substitute in equation (34) with $\frac{\partial H_c}{\partial P_a}$ being evaluated from the appropriate altitude - pressure relationships. For example, differentiating

$$P_a = P_{a_{SL}}(1 - 6.87558 \times 10^{-6} H_c)^{5.25591} \tag{36}$$

taken from the U.S. Standard Atmosphere, 1962, for altitudes below the tropopause

$$\frac{\partial H_c}{\partial P_a} = \frac{13.0763}{(1 - 6.87558 \times 10^{-6} H_c)^{4.25591}} \tag{37}$$

in the units of feet/lb per square foot.

Load Factor, n_z

Differentiating equation (1) with respect to normal load factor yields

$$\frac{\partial F_{ex}}{\partial n_z} = -F_n \sin(\alpha + i_F) \frac{\partial \alpha}{\partial n_z} - qS \frac{\partial C_D}{\partial n_z} \tag{38}$$

Proceeding as before

$$\frac{\partial \alpha}{\partial n_z} = \frac{\partial \alpha}{\partial C_L} \frac{\partial C_L}{\partial n_z} \tag{39}$$

and

$$\frac{\partial C_D}{\partial n_z} = \frac{\partial C_D}{\partial C_L} \frac{\partial C_L}{\partial n_z} \tag{40}$$

equation (38) becomes

$$\frac{\partial F_{ex}}{\partial n_z} = -F_n \sin(\alpha + i_F) \frac{\partial \alpha}{\partial C_L} \frac{\partial C_L}{\partial n_z} - qS \frac{\partial C_D}{\partial C_L} \frac{\partial C_L}{\partial n_z} \tag{41}$$

The term $\frac{\partial C_L}{\partial n_z}$ is evaluated by taking the partial derivative of

equation (2)

$$qS\frac{\partial C_L}{\partial n_z} = W - F_g \cos(\alpha + i_F)\frac{\partial \alpha}{\partial n_z} \tag{42}$$

From which

$$\frac{\partial C_L}{\partial n_z} = \frac{W}{F_g \frac{\partial \alpha}{\partial C_L}\cos(\alpha + i_F) + qS} \tag{43}$$

Substituting equation (43) in equation (41)

$$\frac{\partial F_{ex}}{\partial n_z} = -\left[\frac{F_n \sin(\alpha + i_F) + qS\frac{\partial C_D}{\partial \alpha}}{F_g \cos(\alpha + i_F) + qS\frac{\partial C_L}{\partial \alpha}}\right] W \tag{44}$$

Power Setting

The expression for the partial of excess thrust with respect to power setting is developed by taking the partial of equation (1) with respect to π,

$$\frac{\partial F_{ex}}{\partial \pi} = \cos(\alpha + i_F)\frac{\partial F_n}{\partial \pi} - F_n \sin(\alpha + i_F)\frac{\partial \alpha}{\partial \pi} - qS\frac{\partial C_D}{\partial \pi} \tag{45}$$

Expressions for the following change of variables may be written following the methods used in the preceding derivations:

$$\frac{\partial \alpha}{\partial \pi} = \frac{\partial \alpha}{\partial C_L}\frac{\partial C_L}{\partial \pi} \tag{46}$$

and

$$\frac{\partial C_D}{\partial \pi} = \frac{\partial C_D}{\partial C_L}\frac{\partial C_L}{\partial \pi} \tag{47}$$

equation (45) becomes

$$\frac{\partial F_{ex}}{\partial \pi} = \cos(\alpha + i_F)\frac{\partial F_n}{\partial \pi} - \left[F_n \sin(\alpha + i_F)\frac{\partial \alpha}{\partial C_L} + qS\frac{\partial C_D}{\partial C_L}\right]\frac{\partial C_L}{\partial \pi} \tag{48}$$

The variation of lift coefficient with power setting is determined by taking the partial derivative of equation (2) with respect to power setting.

$$qS\frac{\partial C_L}{\partial \pi} = -\frac{\partial F_g}{\partial \pi}\sin(\alpha + i_F) - F_g \cos(\alpha + i_F)\frac{\partial \alpha}{\partial \pi} \tag{49}$$

Substituting equation (46) and rearranging

$$\frac{\partial C_L}{\partial \pi} = -\frac{\frac{\partial F_g}{\partial \pi}\sin(\alpha + i_F)}{F_g \frac{\partial \alpha}{\partial C_L}\cos(\alpha + i_F) + qS} \tag{50}$$

The variation of excess thrust with power setting becomes, after substitution of equation (50) in equation (48)

$$\frac{\partial F_{ex}}{\partial \pi} = \cos(\alpha + i_F)\frac{\partial F_n}{\partial \pi} + \frac{F_n \sin(\alpha + i_F) + qS\frac{\partial C_D}{\partial \alpha}}{F_g \cos(\alpha + i_F) + qS\frac{\partial C_L}{\partial \alpha}}\frac{\partial F_g}{\partial \pi}\sin(\alpha + i_F) \tag{51}$$

Trim Drag

Differentiating equation (1) with respect to cg yields

$$\frac{\partial F_{ex}}{\partial cg} = -F_n \sin(\alpha + i_F)\frac{\partial \alpha}{\partial cg} - qS\frac{\partial C_D}{\partial cg} \tag{52}$$

As previously stated $C_D = f(\alpha, M, cg)$. Since trim drag corrections are made at constant Mach number the functional relationship

$$C_D = f\left[cg, \alpha(cg)\right] \tag{53}$$

may be set down. The partial derivative of C_D with respect to cg then becomes

$$\frac{\partial C_D}{\partial cg} = \frac{\partial C_D}{\partial cg}\bigg|_\alpha + \frac{\partial C_D}{\partial \alpha}\bigg|_{cg}\frac{\partial \alpha}{\partial cg} \tag{54}$$

Substituting in equation (52)

$$\frac{\partial F_{ex}}{\partial cg} = -F_n \sin(\alpha + i_F)\frac{\partial \alpha}{\partial cg} - qS\left(\frac{\partial C_D}{\partial cg}\bigg|_\alpha + \frac{\partial C_D}{\partial \alpha}\bigg|_{cg}\frac{\partial \alpha}{\partial cg}\right) \tag{55}$$

From differentiation of equation (2)

$$qS\left(\frac{\partial C_L}{\partial cg}\bigg|_\alpha + \frac{\partial C_L}{\partial \alpha}\bigg|_{cg}\frac{\partial \alpha}{\partial cg}\right) = -F_g \cos(\alpha + i_F)\frac{\partial \alpha}{\partial cg} \tag{56}$$

Solving for $\frac{\partial \alpha}{\partial cg}$

$$\frac{\partial \alpha}{\partial cg} = -\frac{qS\frac{\partial C_L}{\partial cg}\Big|_\alpha}{F_g\cos(\alpha + i_F) + qS\frac{\partial C_L}{\partial \alpha}\Big|_{cg}} \tag{57}$$

Substituting equation (57) in equation (55)

$$\frac{\partial F_{ex}}{\partial cg} = \frac{F_n\sin(\alpha + i_F) + qS\frac{\partial C_D}{\partial \alpha}\Big|_{cg}}{F_g\cos(\alpha + i_F) + qS\frac{\partial C_L}{\partial \alpha}} qS\frac{\partial C_L}{\partial cg}\Big|_\alpha - qS\frac{\partial C_D}{\partial cg}\Big|_\alpha \tag{58}$$

STANDARDIZED EXCESS THRUST

An examination of the preceding derivations shows that the term

$$\frac{F_n\sin(\alpha + i_F) + qS\frac{\partial C_D}{\partial \alpha}\Big|_{M,cg}}{F_g\cos(\alpha + i_F) + qS\frac{\partial C_L}{\partial \alpha}\Big|_{M,cg}}$$

occurs in each of the equations for the partial derivatives. Setting this term equal to A and summing up the corrections as indicated by equation (2) we have

$$\begin{aligned} F_{ex_s} = {} & F_{ex_t} + \left[\cos(\alpha + i_F)\frac{\partial F_n}{\partial T_a} + A\sin(\alpha + i_F)\frac{\partial F_g}{\partial T_a}\right](T_{a_s} - T_{a_t}) \\ & - An_z(W_s - W_t) + \left\{\frac{\partial F_n}{\partial M}\cos(\alpha + i_F) - \frac{2C_D qS}{M} - qS\frac{\partial C_D}{\partial M}\Big|_\alpha\right. \\ & \left. + A\left[\frac{2C_L qS}{M} + qS\frac{\partial C_L}{\partial M}\Big|_\alpha + \frac{\partial F_g}{\partial M}\sin(\alpha + i_F)\right]\right\}(M_s - M_t) \\ & + \left\{\cos(\alpha + i_F)\frac{\partial F_n}{\partial H_c}\frac{\partial H_c}{\partial P_a} - \frac{qSC_D}{P_a} + A\left[\frac{\partial F_g}{\partial H_c}\frac{\partial H_c}{\partial P_a}\sin(\alpha + i_F)\right.\right. \\ & \left.\left. + \frac{qSC_L}{P_a}\right]\right\}(P_{a_s} - P_{a_t}) + \left[\cos(\alpha + i_F)\frac{\partial F_n}{\partial \pi} + A\frac{\partial F_g}{\partial \pi}\sin(\alpha + i_F)\right](\pi_s - \pi_t) \\ & - AW_t(n_{z_s} - n_{z_t}) + \left[Aqs\frac{\partial C_L}{\partial cg}\Big|_\alpha - qS\frac{\partial C_D}{\partial cg}\Big|_\alpha\right](cg_s - cg_t) \end{aligned} \tag{59}$$

Equation (59) can be simplified by considering the total change in net thrust caused by changes in temperature, Mach number, and pressure. The total change in net thrust is

$$F_{n_s} - F_{n_t} = F_n\big|_{T_{a_s}, M_s, P_{a_s}} - F_n\big|_{T_{a_t}, M_t, P_{a_t}} \tag{60}$$

or

$$F_{n_s} - F_{n_t} = \frac{\partial F_n}{\partial T_a}(T_{a_s} - T_{a_t}) + \frac{\partial F_n}{\partial M}(M_s - M_t) + \frac{\partial F_n}{\partial P_a}(P_{a_s} - P_{a_t}) \tag{61}$$

The change in net thrust may be determined from the engine manufacturer's specifications, from computer programs constructed by the engine manufacturer, or from flight test data.

Substitution of equation (61) in equation (59) results in

$$\begin{aligned} F_{ex_s} = {} & F_{ex_t} + \cos(\alpha + i_F)(F_{n_s} - F_{n_t}) + A\sin(\alpha + i_F)(F_{g_s} - F_{g_t}) \\ & - A n_z (W_s - W_t) + \left[-\frac{2 C_D q S}{M} + A\frac{2 C_L q S}{M} + qS\left(A\frac{\partial C_L}{\partial M}\Big|_\alpha \right.\right. \\ & \left.\left. - \frac{\partial C_D}{\partial M}\Big|_\alpha \right)\right](M_s - M_t) + \left(-\frac{qSC_D}{P_a} + A\frac{qSC_L}{P_a}\right)(P_{a_s} - P_{a_t}) \\ & - AW(n_{z_s} - n_{z_t}) + \left[AqS\frac{\partial C_L}{\partial cg}\Big|_\alpha - qS\frac{\partial C_D}{\partial cg}\Big|_\alpha\right](cg_s - cg_t) \end{aligned} \tag{62}$$

TAYLOR SERILS EXPANSION OF EXCESS THRUST-SLCOND ORDLR TERMS

Restating equation (4) but carrying the expansion through the second order terms, we have, omitting power setting

$$
\begin{aligned}
F_{ex_s} = F_{ex_t} &+ \frac{\partial F_{ex}}{\partial T_a}(T_{a_s} - T_{a_t}) + \frac{\partial F_{ex}}{\partial W}(W_s - W_t) + \frac{\partial F_{ex}}{\partial M}(M_s - M_t) \\
&+ \frac{\partial F_{ex}}{\partial P_a}(P_{a_s} - P_{a_t}) + \frac{\partial F_{ex}}{\partial n_z}(n_{z_s} - n_{z_t}) + \frac{\partial F_{ex}}{\partial cg}(cg_s - cg_t) \\
&+ \frac{1}{2}\left[\frac{\partial^2 F_{ex}}{\partial T_a^2}(T_{a_s} - T_{a_t})^2 + 2\frac{\partial^2 F_{ex}}{\partial T_a \partial W}(T_{a_s} - T_{a_t})(W_s - W_t)\right. \\
&+ 2\frac{\partial^2 F_{ex}}{\partial T_a \partial M}(T_{a_s} - T_{a_t})(M_s - M_t) + 2\frac{\partial^2 F_{ex}}{\partial T_a \partial P_a}(T_{a_s} - T_{a_t})(P_{a_s} - P_{a_t}) \\
&+ 2\frac{\partial^2 F_{ex}}{\partial T_a \partial n_z}(T_{a_s} - T_{a_t})(n_{z_s} - n_{z_t}) + 2\frac{\partial^2 F_{ex}}{\partial T_a \partial cg}(T_{a_s} - T_{a_t})(cg_s - cg_t) \\
&+ \frac{\partial^2 F_{ex}}{\partial W^2}(W_s - W_t)^2 + 2\frac{\partial^2 F_{ex}}{\partial W \partial M}(W_s - W_t)(M_s - M_t) \\
&+ 2\frac{\partial^2 F_{ex}}{\partial W \partial P_a}(W_s - W_t)(P_{a_s} - P_{a_t}) + 2\frac{\partial^2 F_{ex}}{\partial W \partial n_z}(W_s - W_t)(n_{z_s} - n_{z_t}) \\
&+ 2\frac{\partial^2 F_{ex}}{\partial W \partial cg}(W_s - W_t)(cg_s - cg_t) + \frac{\partial^2 F_{ex}}{\partial M^2}(M_s - M_t)^2 \\
&+ 2\frac{\partial^2 F_{ex}}{\partial M \partial P_a}(M_s - M_t)(P_{a_s} - P_{a_t}) + 2\frac{\partial^2 F_{ex}}{\partial M \partial n_z}(M_s - M_t)(n_{z_s} - n_{z_t}) \\
&+ 2\frac{\partial^2 F_{ex}}{\partial M \partial cg}(M_s - M_t)(cg_s - cg_t) + \frac{\partial^2 F_{ex}}{\partial P_a^2}(P_{a_s} - P_{a_t})^2 \\
&+ 2\frac{\partial^2 F_{ex}}{\partial P_a \partial n_z}(P_{a_s} - P_{a_t})(n_{z_s} - n_{z_t}) + 2\frac{\partial^2 F_{ex}}{\partial P_a \partial cg}(P_{a_s} - P_{a_t})(cg_s - cg_t) \\
&+ \frac{\partial^2 F_{ex}}{\partial n_z^2}(n_{z_s} - n_{z_t})^2 + 2\frac{\partial^2 F_{ex}}{\partial n_z \partial cg}(n_{z_s} - n_{z_t})(cg_s - cg_t) \\
&+ \left.\frac{\partial^2 F_{ex}}{\partial cg^2}(cg_s - cg_t)^2\right] \qquad (63)
\end{aligned}
$$

Before evaluating the partial derivatives, it should be noted that the total change in net thrust, as identified in

equations (60) and (61) for first order terms, should also include the following terms

$$\frac{\partial^2 F_n}{\partial T_a^2}(T_{a_s} - T_{a_t})^2,\ \frac{\partial^2 F_n}{\partial M^2}(M_s - M_t)^2,\ \frac{\partial^2 F_n}{\partial P_a^2}(P_{a_s} - P_{a_t})^2,\ \frac{\partial^2 F_n}{\partial T_a \partial M}(T_{a_s} - T_{a_t})(M_s - M_t),$$

$$\frac{\partial^2 F_n}{\partial T_a \partial P_a}(T_{a_s} - T_{a_t})(P_{a_s} - P_{a_t}),\ \text{and}\ \frac{\partial^2 F_n}{\partial M \partial P_a}(M_s - M_t)(P_{a_s} - P_{a_t})$$

Evaluation of the partial derivatives using equations (1) and (2) would become quite involved. Since the magnitudes of the second order terms are less than those of the first order terms, the equations of motion can be reduced to

$$F_{ex} = F_n - qSC_D \tag{64}$$

and

$$qSC_L = n_z W \tag{65}$$

and the partial derivatives found much more easily and with little loss in accuracy. With these simplifications the second partial derivatives are (derivations have not been included) as listed below.

$$\frac{\partial^2 F_{ex}}{\partial T_a^2} = \frac{\partial^2 F_n}{\partial T_a^2}$$

$$\frac{\partial^2 F_{ex}}{\partial T_a \partial W} = 0$$

$$\frac{\partial^2 F_{ex}}{\partial T_a \partial M} = \frac{\partial^2 F_n}{\partial T_a \partial M}$$

$$\frac{\partial^2 F_{ex}}{\partial T_a \partial P_a} = \frac{\partial^2 F_n}{\partial T_a \partial P_a}$$

$$\frac{\partial^2 F_{ex}}{\partial T_a \partial n_z} = 0$$

$$\frac{\partial^2 F_{ex}}{\partial T_a \partial cg} = 0$$

$$\frac{\partial^2 F_{ex}}{\partial W^2} = -\frac{\partial^2 C_D}{\partial C_L^2} \frac{n_z^2}{qS}$$

$$\frac{\partial^2 F_{ex}}{\partial W \partial M} = -n_z \left[\frac{\partial^2 C_D}{\partial C_L^2} \left(-\frac{2 C_L}{M} \right) + \frac{\partial \left(\frac{\partial C_D}{\partial C_L} \right)}{\partial M} \bigg|_{C_L} \right]$$

$$\frac{\partial^2 F_{ex}}{\partial W \partial P_a} = \frac{n_z C_L}{P_a} \frac{\partial^2 C_D}{\partial C_L^2}$$

$$\frac{\partial^2 F_{ex}}{\partial W \partial n_z} = -\left(C_L \frac{\partial^2 C_D}{\partial C_L^2} + \frac{\partial C_D}{\partial C_L} \right)$$

$$\frac{\partial^2 F_{ex}}{\partial W \partial cg} = -n_z \left[\frac{\partial \left(\frac{\partial C_D}{\partial C_L} \right)}{\partial cg} \bigg|_{C_L} \right]$$

$$\frac{\partial^2 F_{ex}}{\partial M^2} = \frac{\partial F_n}{\partial M^2} - qS\left[\frac{4}{M}\frac{\partial C_D}{\partial M}\bigg|_{C_L} - \frac{2C_L}{M^2}\frac{\partial C_D}{\partial C_L}\bigg|_M + \frac{\partial^2 C_D}{\partial M^2}\bigg|_{C_L} + \frac{\partial\left(\frac{\partial C_D}{\partial C_L}\right)\Big|_M}{\partial M}\left(-\frac{2C_L}{M}\right) + \frac{2C_D}{M^2}\right]$$

$$\frac{\partial^2 F_{ex}}{\partial M\,\partial P_a} = \frac{\partial^2 F_n}{\partial M\,\partial P_a} - \frac{qS}{P_a}\left[\frac{\partial C_D}{\partial M}\bigg|_{C_L} + \frac{\partial^2 C_D}{\partial C_L^2}\left(\frac{2C_L^2}{M}\right)\right]$$

$$+ .7MS\left[-2C_D + 2\frac{\partial C_D}{\partial C_L}C_L + M\frac{\partial\left(\frac{\partial C_D}{\partial C_L}\right)\Big|}{\partial M}\bigg|_{C_L}C_L\right]$$

NOTE: This correction can be ignored for climbs and level accelerations where either ΔM or $\Delta P_a = 0$. It will take on some value when both M and P_a are corrected as during an 'optimum climb."

$$\frac{\partial^2 F_{ex}}{\partial M\,\partial n_z} = -W\left[\frac{\partial\left(\frac{\partial C_D}{\partial C_L}\right)\Big|}{\partial M}\bigg|_{C_L} - \frac{2C_L}{M}\frac{\partial^2 C_D}{\partial C_L^2}\right]$$

$$\frac{\partial^2 F_{ex}}{\partial M\,\partial cg} = -qS\left[\frac{2}{M}\frac{\partial C_D}{\partial cg}\bigg|_{C_L} + \frac{\partial\left(\frac{\partial C_D}{\partial cg}\right)\Big|}{\partial M}\bigg|_{C_L}\right]$$

$$\frac{\partial^2 F_{ex}}{\partial P_a^2} = \frac{\partial^2 F_n}{\partial P_a^2} + \frac{qSC_L^2}{P_a^2}\frac{\partial^2 C_D}{\partial C_L^2}$$

$$\frac{\partial^2 F_{ex}}{\partial P_a\,\partial n_z} = \frac{C_L W}{P_a}\frac{\partial^2 C_D}{\partial C_L^2}$$

$$\frac{\partial^2 F_{ex}}{\partial P_a \partial cg} = -qS\left[\frac{1}{P_a}\frac{\partial C_D}{\partial cg}\bigg|_{C_L} + \frac{C_L}{P_a}\frac{\partial\left(\frac{\partial C_D}{\partial cg}\right)\Big|_{C_L}}{\partial C_L}\right]$$

$$\frac{\partial^2 F_{ex}}{\partial n_z^2} = -\frac{W^2}{qS}\frac{\partial^2 C_D}{\partial C_L^2}$$

$$\frac{\partial^2 F_{ex}}{\partial n_z \partial cg} = -W\frac{\partial\left(\frac{\partial C_D}{\partial C_L}\right)}{\partial cg}\bigg|_{C_L}$$

$$\frac{\partial^2 F_{ex}}{\partial cg^2} = -qS\frac{\partial^2 C_D}{\partial cg^2}\bigg|_{C_L}$$

Standard excess thrust may be computed by substituting the partial derivatives listed above in equation (63) to find the second order terms. It should be remembered that the total change in net thrust is

$$\begin{aligned} F_{n_s} - F_{n_t} = {} & \frac{\partial F_n}{\partial T_a}(T_{a_s} - T_{a_t}) + \frac{\partial F_n}{\partial M}(M_s - M_t) + \frac{\partial F_n}{\partial P_a}(P_{a_s} - P_{a_t}) \\ & + \frac{1}{2}\frac{\partial^2 F_n}{\partial T_a^2}(T_{a_s} - T_{a_t})^2 + \frac{1}{2}\frac{\partial^2 F_n}{\partial M^2}(M_s - M_t)^2 \\ & + \frac{1}{2}\frac{\partial^2 F_n}{\partial P_a^2}(P_{a_s} - P_{a_t})^2 + \frac{\partial^2 F_n}{\partial T_a \partial M}(T_{a_s} - T_{a_t})(M_s - M_t) \\ & + \frac{\partial^2 F_n}{\partial T_a \partial P_a}(T_{a_s} - T_{a_t})(P_{a_s} - P_{a_t}) + \frac{\partial^2 F_n}{\partial M \partial P_a}(M_s - M_t)(P_{a_s} - P_{a_t}) \end{aligned} \tag{66}$$

Hence only the remaining second order terms in equation (63) need be added to equation (62) to find standard excess thrust for an expansion through the second order terms.

The magnitudes of the second order terms can be expected to be less than those of the first order terms, but they will be of consequence in some instances. It is suggested that for installations having an accuracy of 0.01g or less in n_x consideration be given to including second order terms in the standardization equation. They can be safely ignored when using the airspeed-altitude method since errors introduced by this method are larger than the magnitude of the second order terms.

ITERATION PROCEDURES

Equation (62) cannot be solved directly since (during climbs) standard normal load factor depends on γ_s, $\dot{\gamma}_s$, and standard weight, which must be determined from the fuel consumed. The fuel consumed, in turn, depends on the normal load factor. Procedures are simplified for level accelerations since $\dot{\gamma}_s=0$. Further, trim drag corrections are related to center of gravity position which may be a function of weight, as when automatic fuel sequencing is used. Hence, iteration procedures are required to find standard values of normal load factor, weight, and perhaps center of gravity position. It should be noted that several test points at least must be operated on at one time in order that numerical differentiation to obtain $\dot{\gamma}$ and consequently n_z may be carried out.

For purposes of illustration, the basic steps in the iteration procedure for standardization of a continuous climb are laid out in the following chart.

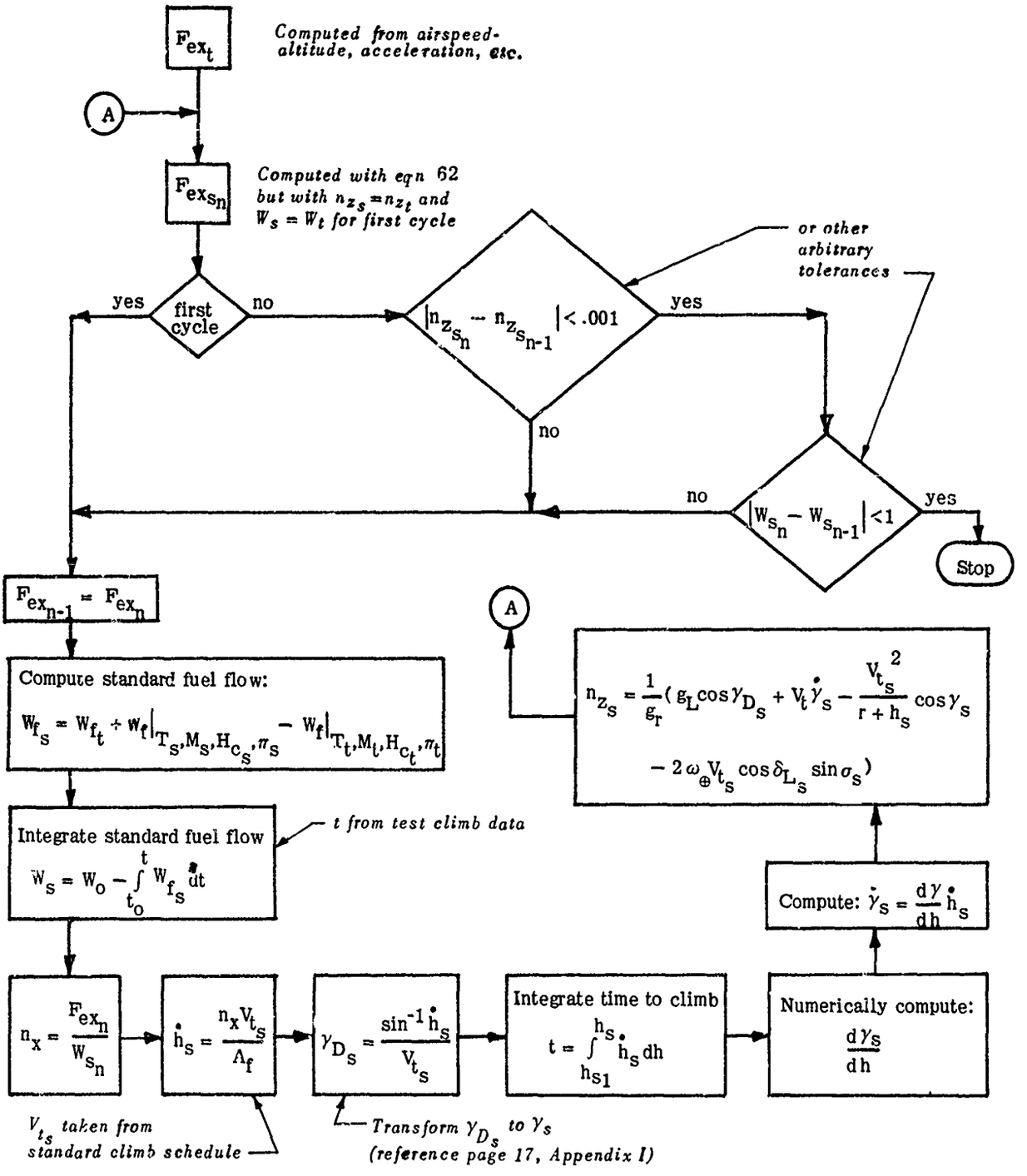
F_{ex_t}
Computed from airspeed-altitude, acceleration, etc.
A
$F_{ex_{s_n}}$
Computed with eqn 62 but with $n_{z_s} = n_{z_t}$ and $W_s = W_t$ for first cycle
first cycle
yes
no
$|n_{z_{s_n}} - n_{z_{s_{n-1}}}| < .001$
yes
or other arbitrary tolerances
no
$|W_{s_n} - W_{s_{n-1}}| < 1$
no
yes
Stop
$F_{ex_{n-1}} = F_{ex_n}$
Compute standard fuel flow:
$W_{f_s} = W_{f_t} + W_f|_{T_s, M_s, H_{c_s}, \pi_s} - W_f|_{T_t, M_t, H_{c_t}, \pi_t}$
Integrate standard fuel flow
$W_s = W_o - \int_{t_o}^{t} W_{f_s} dt$
t from test climb data
$n_x = \frac{F_{ex_n}}{W_{s_n}}$
$\dot{h}_s = \frac{n_x V_{t_s}}{A_f}$
$\gamma_{D_s} = \frac{\sin^{-1} \dot{h}_s}{V_{t_s}}$
Integrate time to climb
$t = \int_{h_{s1}}^{h_s} \frac{1}{\dot{h}_s} dh$
Numerically compute:
$\frac{d\gamma_s}{dh}$
Compute: $\dot{\gamma}_s = \frac{d\gamma}{dh} \dot{h}_s$
A
$n_{z_s} = \frac{1}{g_r}(g_L \cos\gamma_{D_s} + V_t \dot{\gamma}_s - \frac{V_{t_s}^2}{r + h_s} \cos\gamma_s - 2\omega_\oplus V_{t_s} \cos\delta_{L_s} \sin\sigma_s)$
V_{t_s} taken from standard climb schedule
Transform γ_{D_s} to γ_s (reference page 17, Appendix I)

THIS PAGE LEFT BLANK FOR PRESENTATION PURPOSES

SECTION VIII

STANDARDIZATION OF PERFORMANCE PARAMETERS

SUMMARY

Once standard excess thrust has been found, the remaining calculations to compute other performance parameters of interest are relatively simple. Equations to determine the basic parameters for climbs and level accelerations have been included in this section.

TABLE OF CONTENTS

SYMBOLS USED IN THIS SECTION

Symbol	Definition	Units
A_f	acceleration factor	dimensionless
A_{fE}	acceleration factor associated with energy height	dimensionless
F_{ex}	excess thrust	lb
FU	fuel used	lb
g_L	local effective acceleration due to gravity	ft/sec^2
g_r	reference acceleration of gravity	ft/sec^2
h	geometric altitude	ft
H_c	pressure altitude	ft
H_E	energy height	ft
n_x	load factor along the x-axis	dimensionless
NAMT	nautical air miles traveled	- - -
NGMT	nautical ground miles traveled	- - -
r	local radius of the earth	ft
t	time	sec
V_t	true airspeed	ft/sec
W	airplane gross weight	lb
W_{es}	airplane gross weight at engine start	lb
W_f	fuel flow	lb/sec
γ_D	flightpath climb angle measured from the geodetic horizontal plane	rad
Subscript		
s	standard day conditions	

STANDARDIZATION OF PERFORMANCE PARAMETERS

Once excess thrust has been corrected to standard conditions an iteration procedure is used to find the parameters of concern for both climbs and level accelerations. The basic steps in the iteration procedure are shown for a climb in the section, Standardization of Excess Thrust. A similar procedure would be used for level accelerations although fewer steps are required since $v_{u_s} = 0$ and excess thrust goes into increasing kinetic energy only.

CLIMB PARAMETERS

In addition to the need for iteration procedures noted above for both climbs and accelerations, an additional complication arises when generating climb parameters. It has been accepted practice, historically, to determine climb parameters as a function of altitude, beginning at sea level. An aircraft may be at several thousand feet, however, before a pilot is able to intercept the desired climb schedule. Hence, it is not possible to collect test data through a range of altitudes immediately above sea level. Since climb performance at sea level is useful for making comparisons with other aircraft and to Standard Aircraft Characteristics Charts, it must be extrapolated to sea level, recognizing that the flight condition is impossible and that the data is fictitious.

To obtain climb performance at sea level the rate of climb is extrapolated to sea level; other parameters are then deduced from rate of climb. The steps necessary for finding standardized rate of climb might be carried out entirely in a digital computer; perhaps using a curve fit of available rate of climb data and extending it to sea level with the aid of thrust and drag data. Due to uncertainties in measured rates of climb, particularly at the lowest test altitudes, the extrapolation may not produce valid results. Hence, it may be preferable to interrupt the computer program to establish rate of climb manually and then restart the program, continuing with the standardization process.

Rate of Climb

An aircraft's climb potential is defined by

$$\frac{F_{ex}V_t}{W}$$

and represents the rate of climb which would be achieved by an airplane climbing at a constant true speed. If a climb is made at other than a constant true speed, the rate of change of kinetic energy must be accounted for to find rate of climb. This is done through the acceleration factor, A_f, and the rate of climb is, at standard conditions

$$\dot{h}_s = \frac{F_{ex_s}V_{t_s}}{A_f W_s} = \frac{n_{x_s}V_{t_s}}{A_f} \qquad (1)$$

where

$$A_f = \frac{g_L}{g_r}\left(1 + \frac{V_{t_s}}{g_r}\frac{dV_{t_s}}{dh}\right) \tag{2}$$

The acceleration factor is derived as follows. Rate of change of energy height may be stated as

$$\dot{H}_E = \dot{H}_c + \frac{V_t}{g_r}\frac{dV_t}{dh}\dot{h} \tag{3}$$

and also as

$$\dot{H}_E = \frac{F_{ex}V_t}{W} \tag{4}$$

From equation (10) of the section, Atmospheric Environment

$$\dot{h} = \frac{g_r}{g_L}\dot{H}_c \tag{5}$$

Combining equations (3), (4), and (5)

$$\dot{H}_E = \frac{g_L}{g_r}\left(1 + \frac{V_t}{g_r}\frac{dV_t}{dH_c}\right)\dot{h} \tag{6}$$

from which the acceleration factor is taken to be as defined by equation (2). This acceleration factor is useful for climbs described in the section, Standard Climb Schedules, during which altitude is monotonic increasing. For the case

where altitude is permitted to decrease, corrections are made at constant values of H_E and the acceleration factor takes the form

$$A_{fE} = \frac{g_r}{g_L}\left(1 - \frac{V_t}{g_r}\frac{dV_t}{dH_E}\right) \tag{7}$$

A_{fE} is found by defining rate of change of energy height as

$$\dot{H}_E = \dot{H}_c + \frac{V_t}{g_r}\frac{dV_t}{dH_E}\dot{H}_E \tag{8}$$

Solving for H_c

$$\dot{H}_c = \dot{H}_E\left(1 - \frac{V_t}{g_r}\frac{dV_t}{dH_E}\right) \tag{9}$$

Substituting equation (5)

$$\dot{h} = \frac{g_r}{g_L}\left(1 - \frac{V_t}{g_r}\frac{dV_t}{dH_E}\right)\dot{H}_E \tag{10}$$

or

$$\dot{h} = A_{fE}\dot{H}_E \tag{11}$$

Time to Climb

Once h_s has been established time to climb follows easily from

$$t = \int_{h_{s_1}}^{h_s} \frac{dh}{\dot{h}_s} \tag{12}$$

for continuous climbs and

$$t = \int_{H_{E_1}}^{H_E} \frac{dH_E}{\dot{H}_E} \tag{13}$$

for optimum climb schedules which use energy height as an independent variable.

Distance

Distance, conventionally shown in terms of nautical air miles traveled, is

$$NAMT = \int_{t_1}^{t} V_{t_s} \cos\gamma_s dt \tag{14}$$

The NAMT differs slightly from the distance traveled along the earth's surface, particularly for aircraft flying at extreme altitudes (e.g., about 0.4% at an altitude of 80,000 feet). The ground distance is

$$NGMT = \int_{t_1}^{t} V_{t_s} \cos\gamma_s \frac{r}{r + h_s} dt \tag{15}$$

Fuel Used and Weight

The quantity of fuel used is computed simply by integrating the standardized fuel flow:

$$FU = \int^{t} W_{f_s} dt \qquad (\ )$$

Weight during a climb is based on the aircraft gross weight at engine start and the fuel allowance for taxi, takeoff, and acceleration at sea level to the climb schedule. Standard weight during the course of a climb is, then

$$W_s = W_{es} - (\text{fuel allowance}) - FU \qquad (17)$$

LEVEL ACCELERATION PARAMETERS

The same parameters (time, distance, and fuel used) are desired in the presentation of acceleration performance. After standardized excess thrust as a function of Mach number or true speed has been established the acceleration can be found from

$$\dot{V}_{t_s} = g_r \frac{F_{ex_s}}{W_s} \qquad (18)$$

and the time to accelerate from

$$t = \int_{V_{t_{s_1}}}^{V_{t_s}} \frac{dV_{t_s}}{\dot{V}_t} \qquad (19)$$

The distance traveled is computed as for climbs. With $\gamma_s = 0$ distance over the earth is

$$NGMT = \int_{t_1}^{t} V_{t_s} \frac{r}{r + h_s} dt \tag{20}$$

Fuel used, as for climbs, is determined during the standardization process. Repeating equation (16)

$$FU = \int_{t_1}^{t} W_{f_s} dt \tag{21}$$

BIBLIOGRAPHY

1. Allen, H. Julian, and Perkins, Edward W., A Study of Effects of Viscosity on Flow Over Slender Inclined Bodies of Revolution, NACA Report 1048, Ames Aeronautical Laboratory, California, 1951.

2. Allen, Willie L., Weight, Robert H., The Use of Flightpath Accelerometers in Performance Flight Testing, Proceedings of the 13th Annual AF Science and Engineering Symposium, September 1966.

3. Anon, The American Ephemeris and Nautical Almanac, 1967, U.S. Government Printing Office, Washington, D.C. 1964.

4. Anon, U.S. Standard Atmosphere, 1962, U.S. Government Printing Office, Washington, D.C., December 1962.

5. Anon, Standard Atmosphere - Tables and Data for Altitudes to 65,800 Feet, NACA Report 1235, U.S. Government Printing Office, Washington, D.C., 1955.

6. Anon, AGARD Flight Test Manual, Vol I., Pergamon Press, 1962.

7. Anon, Strömungsmebgeräte für den Flugversuch, (Flow Measuring Apparatus for Flight Test), Technical Brochure of Donier GmbH, Friedrichshafen, Federal Republic of Germany.

8. Baker, R.M.L., Makemson, M.W., An Introduction to Astrodynamics, (Second Edition), Academic Press, New York, 1967.

9. Baker, R.M.L., Astrodynamics Applications and Advanced Topics, Academic Press, New York, 1967.

10. Beeler, D.E., et al., Flight Techniques for Determining Airplane Drag at High Mach Numbers, NACA TN 3821, NACA High Speed Flight Station, Edwards, California, 1956.

11. Berven, Lester H., Use of Flightpath Accelerometers in Performance Flight Testing: Test Techniques, Data Analysis Methods and Typical Results, AFFTC TIM 69-1001, Air Force Flight Test Center, California, July, 1969.

12. Brahinsky, H.S., Nell, C.A., Tables of Equilibrium Thermodynamic Properties of Air, Volume I, Constant Temperature, Volume II, Constant Pressure, Volume III, Constant Entropy, AEDC-TR-69-89, Volumes I, II, III, Arnold Engineering Development Center, April, 1969.

13. Caldwell, Donald M., Jr., Standard Atmospheres for Flight Test, AC-64-5, Flight Research Division Office Memo, Air Force Flight Test Center, California, September, 1964.

14. Combs, A.E., et al., Six-Degree-of-Freedom Flight Path Study Generalized Computer Program, Problem Formulation, FDL-TDR-64-1, Part I., Volume I, Air Force Flight Test Dynamics Laboratory, Wright-Patterson AFB, Ohio, October 1964.

15. Dunlap, Everett W., Porter, Milton B., Accelerations on Aircraft Induced by the Earth's Rotation, FTC-TR-66-38, Air Force Flight Test Center, California, February 1967.

16. Etkin, Bernard, Dynamics of Flight, John Wiley and Sons, Inc., New York, 1959.

17. Herrington, Russel M., et al., Flight Test Engineering Handbook, AF Technical Report No. 6273, Air Force Flight Test Center, California, revised January 1966.

18. Kaula, W.M., A Review of Geodetic Parameters, NASA-TND-1847, Goddard Space Flight Center, Maryland, May 1963.

19. King, James J., et al., Aerodynamics Handbook for Performance Flight Testing Vol I, AFFTC-TN-60-28, Air Force Flight Test Center, California, July 1960.

20. Kolacz, Paul A., Contemplation of the Official Standard Atmosphere, FTC-TIM-68-1003, Air Force Flight Test Center, California, February 1968.

21. List, R.J., Smithsonian Meteorological Tables, (Sixth Revised Edition, First Reprint), Smithsonian Institution, Washington, D.C., 1958. (Smithsonian Miscellaneous Collections, Vol 114, also Publication 4014).

22. Lush, Kenneth J., Optimum Climb Theory and Techniques of Determining Climb Schedules from Flight Test, AFFTC-TN-56-13, Air Force Flight Test Center, California, February 1956.

23. Mahoney, John J., Bennett, Donald A., A Comparative Evaluation of Three Techniques for Measurement of Level Flight Accelerations, AFFTC TN 54-2, Air Force Flight Test Center, California, 1954.

24. Makemson, M.W., Baker, R.M.L., and Westrom, G.B., "Analysis and Standardization of Astrodynamic Constants", The Journal of the Astronautical Sciences, Volume VIII, Number 1, Spring 1961.

25. Minzner, R.A., et al., The ARDC Model Atmosphere, 1959, AFCRC-TR-59-267, Air Force Cambridge Research Center, Bedford, Massachusetts, August 1959.

26. Porter, M.B., Calibrated Air Data at High Speeds, Flight Research Branch Office Memo, Air Force Flight Test Center, California, June 1969.

27. Schramm, Roland C., Scott, Maceo T., Derivative Information Recovery by a Selective Integration Technique (DIRSIT), Technical Memorandum 1040, The Army Missile Test and Evaluation Directorate, White Sands Missile Range, New Mexico, November 1962.

28. Walker, Richard C., A Comparison of Several Techniques for Determining Aircraft Test Day Climb Performance, AC-65-7, Flight Research Division Office Memo, Air Force Flight Test Center, California, June 1965.